



저작자표시-비영리-변경금지 2.0 대한민국

이용자는 아래의 조건을 따르는 경우에 한하여 자유롭게

- 이 저작물을 복제, 배포, 전송, 전시, 공연 및 방송할 수 있습니다.

다음과 같은 조건을 따라야 합니다:



저작자표시. 귀하는 원저작자를 표시하여야 합니다.



비영리. 귀하는 이 저작물을 영리 목적으로 이용할 수 없습니다.



변경금지. 귀하는 이 저작물을 개작, 변형 또는 가공할 수 없습니다.

- 귀하는, 이 저작물의 재이용이나 배포의 경우, 이 저작물에 적용된 이용허락조건을 명확하게 나타내어야 합니다.
- 저작권자로부터 별도의 허가를 받으면 이러한 조건들은 적용되지 않습니다.

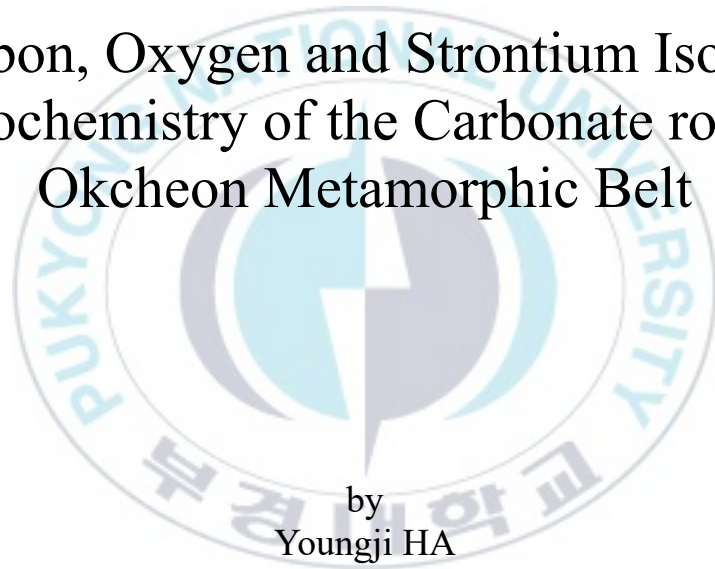
저작권법에 따른 이용자의 권리는 위의 내용에 의하여 영향을 받지 않습니다.

이것은 [이용허락규약\(Legal Code\)](#)을 이해하기 쉽게 요약한 것입니다.

[Disclaimer](#)

Thesis for Degree of Doctor of Philosophy

Carbon, Oxygen and Strontium Isotope
Geochemistry of the Carbonate rocks,
Okcheon Metamorphic Belt



by
Youngji HA

Division of Earth Environmental System Science
The Graduate School
Pukyong National University

August, 2021

Carbon, Oxygen and Strontium Isotope Geochemistry of the Carbonate rocks, Okcheon Metamorphic Belt

옥천변성대 탄산염 암석의 탄소, 산소 및 스트론튬 지구화학

Advisor: Prof. Kye-Hun PARK

by
Youngji HA

A thesis submitted in partial fulfillment of the requirements for the degree of

Doctor of Philosophy

in Division of Earth Environmental System Science
(Major of Earth & Environmental Sciences), The Graduate School
Pukyong National University

August 2021

Carbon, Oxygen, and Strontium Isotope Geochemistry of the
Carbonate rocks, Okcheon Metamorphic Belt

A dissertation
by
Youngji HA

Approved by:

Yong-Sun SONG

Kye-Hun PARK

Seung-Gu LEE

Hyeoncheol KIM

Jong-Sik Ryu

August 27, 2021

TABLE OF CONTENTS

TABLE OF CONTENTS	i
LIST OF FIGURES	v
LIST OF TABLES	viii
ABSTRACT	ix
CHAPTER 1: Thesis overview	1
1. Introduction	2
2. Method used	6
2.1 Concept of Chemostratigraphy	6
2.1.1 Carbon isotopes	7
2.1.2 Oxygen isotopes	9
2.1.3 Strontium isotope	10
2.2 Limitations and advantage of isotope stratigraphy	11
3. Analytical Methods	16
3.1 Carbon and Oxygen isotopes	16
3.1.1 Faculty of Science, Niigata University	16
3.1.2 Beta Analytic Inc.	17
3.2 Trace elements and rare earth elements (REE)	18
3.2.1 Faculty of Science, Niigata University	18

3.2.2	Korea Basic Science Institute (KBSI) ·····	19
3.3	Strontium isotope ·····	20
3.3.1	Faculty of Science, Niigata University ·····	20
3.3.2	Korea Basic Science Institute (KBSI) ·····	20
3.3.3	Korea Institute of Geoscience and Mineral Resources (KIGAM) ·····	21
4.	Study Outline ·····	23
4.1	General geology ·····	23
4.2	Geumgang Limestone: Chapter 2 ·····	30
4.3	Seochangni, Samtaesan, and Heungwolri Formations: Chapter 3 ·····	31

CHAPTER 2: Carbon and oxygen isotopes and geochemistry of Neoproterozoic cap carbonate, Geumgang Limestone, from the Okcheon Metamorphic Belt: Chemostratigraphical age and its implication ·····	34
---	----

Abstract ·····	35
1. Introduction ·····	37
2. Geological Setting ·····	40
3. Materials and Methods ·····	47
3.1 Material descriptions ·····	47
3.2 Analytical methods ·····	52
4. Results and Interpretation ·····	53
4.1 Carbon and oxygen isotope compositions ·····	53

4.2	Trace and rare earth element concentrations	58
4.3	Strontium isotope composition	64
5.	Discussion	74
5.1	Evidence from carbon isotopes for post glacial deposits: Geumgang Limestone	75
5.2	The stratigraphic implications for the occurrence of Neoproterozoic glaciogenic sedimentary successions in the Okcheon Metamorphic Belt	77
5.3	Hwanggangni and Bugnori Formations	79
5.3.1	Identicalness of Geumgang Limestone distributed in the Okcheon Metamorphic Belt	79
5.3.2	Further stratigraphic implications	81
5.4	Correlation with the Okcheon Metamorphic Belt and Chinese Cratons	84
6.	Conclusion	88

CHAPTER 3:	Carbon chemostratigraphic age constraints on the carbonate successions distributed in border between the Okcheon Metamorphic Belt and Taebaeksan Basin	89
------------	--	----

Abstract	90
1. Introduction	91
2. Geological Setting	98
3. Samples and Analytical Methods	102
4. Result and Discussion	112

4.1 Trace element and REE plus yttrium	112
4.2 Carbon isotope records from carbonate successions in the Chungju-Jecheon area	119
4.3 Regional comparison of Carbon isotope composition	124
4.4 Further tectonic implications	135
5. Conclusion	139

SUMMARY AND CONCLUDING REMARKS	142
REFERENCES	143
ABSTRACT (in Korean)	166

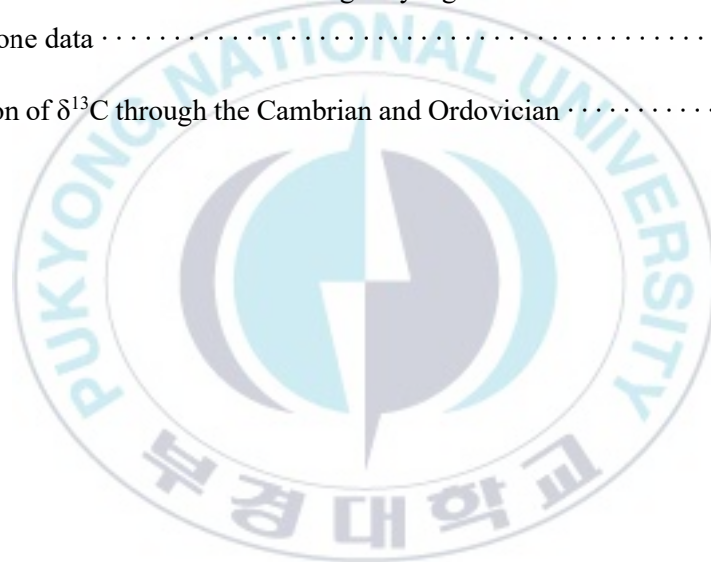


LIST OF FIGURES

1-1. Composite $\delta^{13}\text{C}$ records for the Neoproterozoic from marine carbonate rocks with Cambrian data	15
1-2. a) A map showing the Korean Peninsula with parts of the North China Craton and the South China Craton. b) A map showing the Okcheon metamorphic belt distributed over the south-central Korean Peninsula	32
2-1. Geological map of the Okcheon-Boeun area with sampling locations	45
2-2. Geological map of the northeastern Okcheon metamorphic belt and the western Taebaeksan Basin with sampling locations	46
2-3. Outcrop photographs of the Geumgang Limestone at different study areas	50
2-4. Photographs for the slab samples from the Geumgang Limestone	51
2-5. Cross-plots of the carbon and oxygen isotopic compositions of all Geumgang Limestone from the Okcheon Metamorphic Belt	55
2-6. Correlation diagrams of Y/Ho versus Zr and $\sum\text{REE}$ versus Zr of the Geumgang Limestone	61
2-7. PAAS-normalized Rare Earth Element plus Yttrium of the Geumgang Limestone from the Okcheon Metamorphic Belt	65
2-8. Covariations between $(\text{Eu}/\text{Eu}^*)_{\text{N}}$ PAAS ratio and Ba/Sm ratio in the Geumgang Limestone	66
2-9. The plot of $(\text{Pr}/\text{Pr}^*)_{\text{N}}$ PAAS ratio versus $(\text{Ce}/\text{Ce}^*)_{\text{N}}$ PAAS ratio used to show La and Ce anomalies of the Geumgang Limestone	67
2-10. Geochemical discrimination diagrams to distinguish various depositional	

environments of the Geumgang Limestone. a) Sr/Ba vs. Sr/Rb, b) Rb–Sr–Ba triangular, c) $(Ce/Ce^*)_N$ vs. $(La/Yb)_N$, and d) $(Eu/Eu^*)_N$ vs. $(Ce/Ce^*)_N$ diagrams	68
3-1. Geological map of the northeastern Okcheon metamorphic belt and the southwestern Taebaeksan Basin with sampling locations	94
3-2. Outcrop photographs of the Seochangni Formation	103
3-3. Outcrop photographs of the Samtaesan Formation	104
3-4. Outcrop photographs of the Heungwolri Formation	105
3-5. Outcrop photographs of the Joseon Supergroup	106
3-6. Photographs for the slab samples from the Seochangni Formation	107
3-7. Photographs for the slab samples from the Samtaesan Formation	108
3-8. Photographs for the slab samples from the Heungwolri Formation	110
3-9. Photographs for the slab samples from the Joseon supergroup	111
3-10. PAAS-normalized REE + Y diagrams of the Seochangni, Samtaesan, and Heungwolri Formation	114
3-11. Geochemical discrimination diagrams to distinguish various depositional environments of the carbonate rocks from the Seochangni, Samtaesan and Heungwolri Formations	115
3-12. Carbon versus oxygen cross-plot for the Seochangni, Samtaesan and Heungwolri Formations and the Joseon Supergroup	122
3-13. Carbon isotopic compositions for the regions east and north of the Geumsusan Quartzite	125
3-14. Carbon isotopic compositions for the area between Busan and Bakdallyeong gneiss complexes	127

3-15. Carbon isotopic compositions for the area between the Seochangni Formation and the Geumsusan Quartzite	129
3-16. Carbon isotopic compositions for the Samtaesan and the Heungwolri Formations in the Husan-ri area	130
3-17. Carbon isotopic compositions for the southwest periphery of the Busan gneiss complex	131
4-1. Composite a) carbon and b) strontium isotope records for the Neoproterozoic from marine carbonate rocks including Hyangsanni Dolomite and Geumgang Limestone data	140
4-2. Variation of $\delta^{13}\text{C}$ through the Cambrian and Ordovician	141



LIST OF TABLES

1-1. The methods used and institution conducting the analysis	22
2-1. Quadrangles and Stratigraphy names, with GPS coordinates for sampling localities of the Geumgang Limestone	49
2-2. Data of carbon, oxygen, and Strontium isotopic composition were obtained from the Geumgang Limestone for this study	56
2-3. Trace element concentrations in ppm and strontium isotope compositions of the Geumgang Limestone	70
2-4. Rare earth element and Yttrium concentrations and PAAS-normalized REE parameters calculated for the Geumgang Limestone	72
3-1. Quadrangles and Stratigraphy names, with GPS coordinates for sampling localities of the Seochangni, Samtaesan and Heungwolri Formations	95
3-2. Rare earth elements plus Yttrium concentrations of the Seochangni, Samtaesan, and Heungwolri Formations	117
3-3 PAAS-normalized rare earth element parameters and trace element concentrations of the Seochangni, Samtaesan, and Heungwolri Formations	118
3-4. Carbon and oxygen isotopic composition of the Seochangni, Samtaesan and Heungwolri Formations and Joseon Supergroup	132

Carbon, Oxygen and Strontium Isotope Geochemistry of the Carbonate rocks, Okcheon Metamorphic Belt

Youngji HA

Division of Earth Environmental System Science, The Graduate School,
Pukyong National University

Abstract

In the Okcheon Metamorphic Belt, carbonate rocks distributed over a wide range remain age-unknown. The reason is that there are few suitable absolute dating methods applicable to carbonate rocks. This paper tried to determine the timing of their formation more precisely by applying a chemical stratigraphic method to these unknown carbonate rocks.

Chapter 1 gives an overview of the subject of this paper. In particular, we discussed the importance and limitations of carbon isotope data for studying Neoproterozoic carbonate sediments.

Chapter 2 is a study of carbonate rocks, commonly referred to as so-called Geumgang Limestone, in the Okcheon, Boeun, and Chungju regions, and discussed whether this layer is a cover carbonate deposited after a Neoproterozoic glaciation period. In conclusion, Geumgang limestone consistently shows a low $\delta^{13}\text{C}$ value (-12.25‰~-6.05‰), which corresponds to the $\delta^{13}\text{C}$ value of a typical cover carbonate rock. Therefore, this result supports the existing hypothesis that a part of the Okcheon metamorphic zone was deposited during a Neoproterozoic glaciation event.

Chapter 3 dealt with the Seochangni Formation, the Samtaesan Formation, and the Heungwolri Formation distributed in the Chungju-Jecheon region, regarded as the lower Paleozoic strata of the Taebaeksan Basin. However, the carbon isotope analysis of these rocks shows a different result from traditional belief.

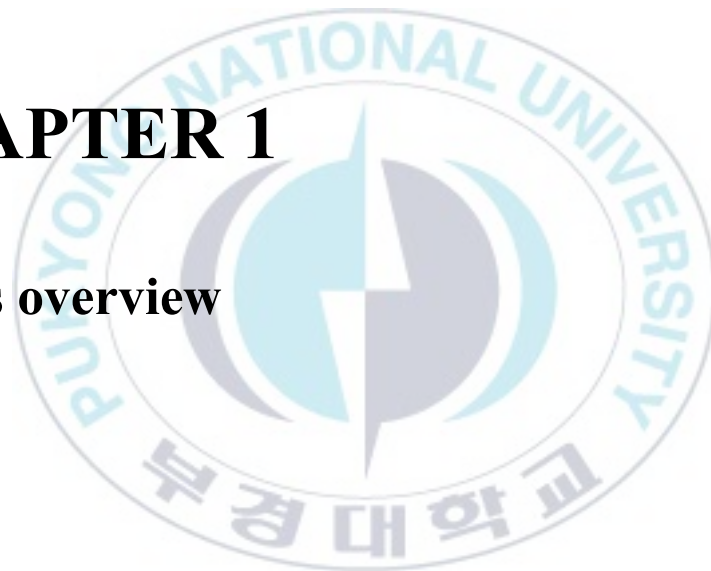
The $\delta^{13}\text{C}$ values obtained from these layers often show values greater than 1.5‰, which is greater than the average value of about 0‰ of the Cambrian-Ordovician period, which means the Early Cambrian or an older Neoproterozoic. Therefore, the presence of Neoproterozoic rocks in addition to the Paleozoic ones is apparent among these carbonate rocks.

Taken together, this study revealed that sedimentary layers related to a Neoproterozoic glaciation existed in the Okcheon Metamorphic Belt. In addition, this study clarified that most of the carbonate rocks distributed in the western part of the Geumsusan Quartzite Formation, described as the Samtaesan Formation and the Heungwolri Formation, are Neoproterozoic layers. Therefore, it is necessary to redefine the boundary between the Okcheon Metamorphic Belt and the Taebaeksan Basin.

Keywords: Late Neoproterozoic, Early Paleozoic, Okcheon Metamorphic Belt, Taebaeksan Basin, Carbonate Sequences, Chemostratigraphy

CHAPTER 1

Thesis overview



1. Introduction

During the Neoproterozoic, the Earth had an extreme climate change called snowball Earth and is an important tectonic evolutionary period during which assembly and breakup of the supercontinent Rodinia occurred (Li et al., 2013; Li et al., 1996).

Many studies related to these subjects have been conducted in various regions of the South China Craton (e.g., Li et al., 1996; Zhang et al., 2005; McFadden et al., 2008; Zhao and Cawood, 2012; Yu et al., 2017), and more recently, studies on the southern and northern margins of the North China Craton have increased (Fairchild et al., 2000; Shen et al., 2005; Shen et al., 2008, 2010; Yang et al., 2019; Zhou et al., 2020).

Studies on Neoproterozoic periods have also been reported from several parts of North Korea (Peng et al., 2011; Hu et al., 2012), which appear to have evolved in connection with North China Craton since at least Paleoproterozoic.

In the case of South Korea, Neoproterozoic ages have been reported from the western part of the Gyeonggi Massif and various regions of the Okcheon metamorphic belt (Lee et al., 1998a; Kim et al., 2006; Kee et al., 2019).

These results suggest that the traditional view of crustal evolution on the Korean Peninsula must be greatly modified in many ways. Among these, the Okcheon metamorphic belt, which has been recognized as a key part in understanding the crustal evolution of the Korean Peninsula, still needs studies to identify the timing of its formation and the tectonic environment.

The Okcheon Metamorphic Belt, located in the middle of the Korean Peninsula, is distributed between the Paleoproterozoic Gyeonggi and Yeongnam Massifs. It is

mainly composed of medium pressure type metamorphosed volcano-sedimentary rocks. The predominant lithology is pelitic and psammitic schist-phyllite and sparsely distributed carbonates, calcareous metasedimentary rocks and-amphibolites. There is still much debate about when this belt was made, the stratigraphical categorization and their structural relationships of its constituent units, and its relationship to the Gyeonggi and Yeongnam Massifs.

The traditional view is that both the Gyeonggi and Yeongnam Massifs are part of a Sino-Korean Craton connected to the North China Craton. In this case, the Okcheon metamorphic belt is also part of the Sino-Korean Craton. However, there is a suggestion that the boundary between the Gyeonggi and Yeongnam Massifs, respectively correlated to South China Craton and North China Craton, passes along the southern margin of the Okcheon Metamorphic Belt (Chough et al., 2000; Kim et al., 2017).

The Okcheon Metamorphic Belt is a key for understanding the tectonic environment during Neoproterozoic because they show the A1-type intra-plate magmatism of about 860 Ma and 760 Ma (Lee et al., 1998a; Park et al., 2005; Kim et al., 2006, 2011), possibly associated with the break-up of Neoproterozoic supercontinent Rodinia.

The consensus is that there were multiple severe glaciations in the Neoproterozoic: i.e. Sturtian (early Cryogenian), Marinoan (late Cryogenian), and suspicious Gaskiers (Ediacaran) glaciations. The Gaskeirs Glaciation is ambiguous due to a usual absence of tillites and carbon isotope data (Halverson, 2002, 2005; Myrow and Kaufman, 1999).

Several formations in the Okcheon Metamorphic Belt have been suggested for glaciogenic sequences. The Hwanggangni Formation in the Okcheon Metamorphic Belt has been claimed to be a glacial diamictite deposition (Reedman and Fletcher,

1976; Lee et al., 1998b; Choi et al., 2012), but the timing of deposition is not yet clear. Because the presence of glaciation of Neoproterozoic is not yet unequivocal in South Korea, it is important to clarify the timing of the deposition of the Hwanggangni Formation.

In most cases, direct dating of carbonates is not applicable due to wanting for proper readily dated material for conventional dating techniques. Namely, it is deficient inaccurate age dating research for carbonates.

Because of the paucity of precise geochronologic data that have been dated directly by radiometric techniques for carbonates in the Okcheon Metamorphic Belt, the stratigraphic relationship of its sedimentary successions has still been unsolved.

Reliable and available age information of the Okcheon Metamorphic Belt has been reported only from clastic sedimentary rocks. The age-unknown carbonates distributed throughout in Okcheon Metamorphic Belt have long been a pending question. The carbonate rocks in the Okcheon Metamorphic Belt are expected to have various geological ages. Thus, the age-unknown carbonate rocks could be key layers to understand the evolution of the Okcheon Metamorphic Belt.

In this context, this thesis aims to constrain the age of carbonates previously unknown by adopting chemostratigraphy to carbonate succession in the Okcheon Metamorphic Belt.

In Okcheon Metamorphic Belt, several kinds of carbonate successions have been distributed. This thesis treats two other carbonate successions as follows. One is thin carbonate layers between the pebble-bearing phyllitic rocks and phyllitic rocks. It is a so-called Geumgang Limestone and considered as the cap carbonates, the aftermath of

“Snowball Earth”. And then also discuss the possibility of deposition of the adjacent Hwanggangni Formation which is pebble-bearing phyllitic rock and underlying Geumgang limestone, during the Neoproterozoic glaciation and the implications for the evolution of the Okcheon Metamorphic Belt.

The other is distributed in the border between the Okcheon Metamorphic Belt and Taebaeksan Basin, Seocheangni, Samtaesan, and Heungwolri Formations. It would prompt reconsidering the tectonic boundary which has been putative between the Okcheon Metamorphic Belt and Taebaeksan Basin.

Given that geochemical values from carbonates distributed in the Okcheon Metamorphic Belt, previous thoughts that the Okcheon Metamorphic Belt is an extension of collision belt between North China Craton and South China Craton and the northeastern part of the Okcheon Metamorphic Belt is correlated with South China Craton are no longer valid.

2. Method used

2.1 Concept of Chemostratigraphy

Chemostratigraphy, or chemical stratigraphy, is used to determine stratigraphic relationships and climate variability when they formed using delicate chemical variations within sedimentary sequences. Especially chemostratigraphic correlation is significant practicality in Neoproterozoic Era.

The basic principle of chemostratigraphy is that isotope ratios are not a constant but systematic increase or decrease during the geographical time scales. The systematic variations of geochemical composition are considered to be secular variations (Ramkumar et al., 2015). Such an isotope secular variation has been recorded in sedimentary materials, that can be dealt with as reliable proxies for the isotopic composition of seawater (Halverson et al., 2018). Stable isotopes are often treated the powerful proxies because their signatures immutable in sediments. Commonly used in proxies for chemostratigraphy are carbon, oxygen, sulfur and strontium isotopes. Among them, carbon ($\delta^{13}\text{C}$), oxygen ($\delta^{18}\text{C}$) and strontium ($^{87}\text{Sr}/^{86}\text{Sr}$) isotope ratios are the most commonly used proxies for the Proterozoic Eon.

Studies of carbon, oxygen, and strontium isotope geochemistry for modern seawater have flourished in the early 1990s, since then isotope data have well been documented with the changes of the geological time. Whereas there was very little information for Neoproterozoic or much longer than this era. However, the number of isotope data for Neoproterozoic has soared since the early 2000s, particularly more specifically regarding the number, correlation, causes, and consequences of glaciations during the Neoproterozoic era (Halverson et al., 2002, 2005, 2007, 2011, 2018).

In the case of pelagic carbonate, it is generated from seawater. Namely, $\delta^{13}\text{C}$ and $^{87}\text{Sr}/^{86}\text{Sr}$ recorded in it could serve as a chronological index. Because ancient marine carbonates have preserved seawater composition, so secular trend in $\delta^{13}\text{C}$ and $^{87}\text{Sr}/^{86}\text{Sr}$ can demonstrate it in which they formed. The point is that the “Chemostratigraphy” using carbon and strontium of pelagic carbonate is most reliable and invaluable as geochronological determination (Weissert et al., 2008; Ramkumar et al., 2015; Rooney et al., 2015).

In this study, I am going to apply chemostratigraphy using carbon, oxygen, and Sr isotopic compositions to constrain the age of the age-unknown carbonates scattered distributed in the Okcheon Metamorphic Belt.

2.1.1 Carbon isotopes

Carbon has two stable isotopes, the abundance of ^{12}C in nature is given as 98.89%, while ^{13}C forms the remaining 1.11% (Craig, 1953). The isotopic composition is expressed in the “ δ ” value.

The difference in the $^{13}\text{C}/^{12}\text{C}$, $^{18}\text{O}/^{16}\text{O}$ either, the ratio in nature is minuscule. Furthermore, measuring these absolute isotopic ratios is rare. Instead, it might be achieved by determining relative to a standard material. “ δ ” notation is the way to express these relative differences as a rule.

$\delta^{13}\text{C}$ (pronounce delta C thirteen) is determined relative abundances of ^{13}C and ^{12}C to a standard. $\delta^{13}\text{C}$ is expressed in part per thousand or “per mil” (‰).

$\delta^{13}\text{C}$ is defined using the following equation to calculate the ratio difference (δ).

$$\delta^{13}\text{C} = \left[\frac{\left(\frac{^{13}\text{C}}{^{12}\text{C}} \right)_{\text{sample}}}{\left(\frac{^{13}\text{C}}{^{12}\text{C}} \right)_{\text{standard}}} - 1 \right] * 1000$$

The standard most widely used is the Cretaceous Belemnite carbonate from Peedee Formations (PDB) in South Carolina.

$\delta^{13}\text{C}$ values are of great use for the Neoproterozoic owing to the high-amplitude and low-frequency fluctuations (Figure 1-1a) that features this period (Halverson et al., 2007, 2010, 2018; Kaufman et al., 2009), and carbonate successions of those days have been in good preservation.

Deductive acquaintance on the secular variation of seawater and carbonate made from seawater are indispensable to the application of carbon isotope chemostratigraphy correlation of sedimentary sequences. This secular variation curve of $\delta^{13}\text{C}$ has revealed striking $\delta^{13}\text{C}$ excursions (Sial et al., 2015).

Carbon isotope records from marine carbonate successions aged 1000 to 820 Ma (Figure 1-1a). This $\delta^{13}\text{C}$ trend is usefully used in chemostratigraphy with coupled the strontium isotope evolution curve.

Though $\delta^{13}\text{C}$ values have an averagely high value ($> +5\%$) for most of the Neoproterozoic Era, however large negative $\delta^{13}\text{C}$ excursions are interrupted (Figure 1-1a). The $\delta^{13}\text{C}$ curve display distinctive aspect interlinked with the several ~~times~~ glaciations. In other words, the large scale of negative excursion seems to be interrelated with Neoproterozoic glaciations.

The carbon isotope composition of pelagic carbonate is the most reliable proxy for chemostratigraphy. Because the $\delta^{13}\text{C}$ values are relatively immune to geological

processes as metamorphism and diagenesis. (Frimmel, 2010; Higgins et al., 2018; Hood et al., 2018). Thus, the $\delta^{13}\text{C}$ value of well-preserved carbonates, even suffered metamorphism, would provide worthwhile information (Friend et al., 2008).

The modern ocean water $\delta^{13}\text{C}$ value ranges -1.5‰ (deep water) from $+2\text{‰}$ (surface water) (Kroopnick 1985). Marine organic matter has strongly depleted ^{13}C values (ca. -25‰), and it would affect surface water enriched in ^{13}C during organic matter production. Resultingly carbon isotope fractionation has happened. The pelagic carbonate is universally known that has a $\delta^{13}\text{C}$ value between 0.2‰ to $+2\text{‰}$ (Wissert et al., 2008 and references therein).

2.1.2 Oxygen isotopes

$\delta^{18}\text{O}$ (pronounce delta O eighteen) refers to the ratio of two stable isotopes: ^{18}O : ^{16}O . The most abundant is ^{16}O of 99.8%, ^{18}O constitutes most of the remaining 0.2%. It is also expressed in parts per million (‰).

For the oxygen isotopes, Standard Mean Ocean Water (SMOW) or Vienna Standard Mean Ocean Water (V-SMOW) is used as the standard.

The relationship between sample and standard is as below:

$$\delta^{18}\text{O} = \left[\frac{\left(\frac{^{18}\text{O}}{^{16}\text{O}} \right)_{\text{sample}}}{\left(\frac{^{18}\text{O}}{^{16}\text{O}} \right)_{\text{standard}}} - 1 \right] * 1000$$

The oxygen isotopes of carbonate, shell, and glaciation are usually used to indirectly determine the temperature at that time these were formed. Because $\delta^{18}\text{O}$ the

environmental changes affect the abundance of each oxygen isotope.

The $\delta^{13}\text{C}$ profiles especially are a useful tool for correlating Neoproterozoic successions without key index fossils (Knoll and Walter, 1992; MacDonald et al., 2009, 2010). However, the combination of $\delta^{13}\text{C}$ and $\delta^{18}\text{O}$ profiles might be unsuitable for the Neoproterozoic Era, because oxygen isotopes are relatively fluctuating during post-depositional alteration. Thus, the oxygen isotopic composition of carbonate could be the point of reference of depositional and lithified conditions (Kaufman and Knoll, 1995; Jacobsen and Kaufman, 1999; Veizer et al., 1999).

Veizer et al. (2000) documented the $\delta^{18}\text{O}$ evolution (including $^{87}\text{Sr}/^{86}\text{Sr}$ and $\delta^{13}\text{C}$) in the temperature of paleotropical seawater from Phanerozoic calcitic and phosphatic shells. And Veizer et al. and his research group confirmed and suggested that the oxygen isotopic composition of the Precambrian and Paleozoic oceans was considerably lower than those of the present-day ocean (Veizer et al., 1999; Shield and Veizer, 2002). In this respect, the oxygen isotopic composition of carbonates becomes progressively depleted in ^{18}O with the increasing age of the rocks (Veizer et al., 1999).

2.1.3 Strontium isotopes

Exclusive of stable isotopes used in chemostratigraphy (Figure 1-1b), strontium isotopes are the most widely used tool for correlation. Strontium has a long ocean residence time of $\sim 2.4 \times 10^6$ years (Jones and Jenkyns, 2001), it is longer than ocean water circulation time $\sim 1.0 \times 10^3$ years. Thus, the $^{87}\text{Sr}/^{86}\text{Sr}$ ratio of global ocean ratio has been regarded as isotopically homogeneous during the timescales of $< 10^6$ years. The average present-day ocean value of $^{87}\text{Sr}/^{86}\text{Sr}$ ratio is 0.70202 from the compilation of

strontium values of the Atlantic, Indian and Pacific oceans and their marginal seas (Kuznetsov et al., 2003, 2012).

Since the beginning of measurement of strontium isotopic composition in the 1970s, the strontium isotope analyses alongside development such as laser ablation combined with inductively coupled plasma mass spectrometry (LA-MC-ICPMS) have been highly advanced. Moreover, the accuracy of strontium isotope data is also enhanced, it turns out a further betterment of the resolution for strontium isotope stratigraphy.

The $^{87}\text{Sr}/^{86}\text{Sr}$ ratio has been superimposed increased over the long term. Reasons for the increase include continental weathering and hydrothermal events. Moreover, radiogenic ^{87}Sr from radioactive decay of ^{87}Rb is causative of $^{87}\text{Sr}/^{86}\text{Sr}$ ratio growth. While volcanic activity brings the $^{87}\text{Sr}/^{86}\text{Sr}$ ratio down. To sum up, the $^{87}\text{Sr}/^{86}\text{Sr}$ ratio is strongly influenced by geological processes. The continental weathering causes an increasing $^{87}\text{Sr}/^{86}\text{Sr}$ ratio, while rifting activity causes a decreasing $^{87}\text{Sr}/^{86}\text{Sr}$ ratio.

2.2 Limitations and advantage of isotope stratigraphy

The carbon isotope curves from pelagic carbonate succession have been demonstrated by numerous studies that it is reproducible in shallow-water carbonate succession and continental organic carbon records. However, it should be remembered contributory factors which play a role in the absolute value modification of carbon isotope curves. These factors can shift carbon isotopes towards lowers or vice versa.

Carbonate succession might be alterable during various metamorphic or hydrothermal processes. The carbon isotope is thought to be depleted by metamorphism. If the metamorphic temperature is higher than 650°C, it would decrease the $\delta^{13}\text{C}$ values by 3‰ (Wada and Suzuki, 1983) even $\delta^{13}\text{C}$ values can be relatively immune to metamorphism and diagenetic alteration. (Friend et al., 2008; Higgins et al., 2018; Hood et al., 2018). Diagenetic alteration of $\delta^{13}\text{C}$ values in carbonate samples can be minimal (Kaufman et al., 1991), but overprinting by marine and meteoric fluids is also possible (Higgins et al., 2018).

As stated above, oxygen and strontium isotopes are relatively more susceptible than carbon isotopes during the geological process - metamorphism, hydrothermal alteration, diagenesis and volcanism and such. $\delta^{18}\text{O}$ values toward lower with an age of rocks (McKenzie, 1981; Hudson and Anderson, 1989; Veizer et al., 1999). For this reason, the demonstration of its primary signals is often awkward in older successions. $\delta^{18}\text{O}$ values of whole-rock samples of Precambrian successions are often interpreted as reflecting diagenetic alteration (as lithification), even though exceptive instance has been known (Knauth and Kennedy, 2009; Tahata et al., 2013). And hydrothermal alteration triggers $\delta^{18}\text{O}$ value depletion. In case that the minerals in carbonates as calcite and dolomite react to hydrous fluids, CO_2 including a high ratio of ^{18}O is moved out during decarbonation reaction (Baumgartner et al., 2001; Valley 2001; Otsuji et al., 2013). Consequentially, the carbonates suffered alteration has of course depleted $\delta^{18}\text{O}$ value.

Oxygen isotopes record both temperature and ice volume, strontium isotopes record both the rate of weathering and the balance between hydrothermal and continental sources (e.g., Flament et al., 2013).

As for the alteration of strontium isotopes, several geochemical screening such as Mn/Sr and $\delta^{18}\text{O}$ have been optimized to identify depositional chemical signatures (Jacobsen and Kaufman, 1999; Melezhik et al., 2001, 2005, 2008; Otsuji et al., 2013). Thus, proper and careful screening using manifold geochemical parameters is a great help to select reliable data.

As seen in Figure 1-1, $\delta^{13}\text{C}$ and $^{87}\text{Sr}/^{86}\text{Sr}$ curves seem to be correlative roughly. In other words, when the $^{87}\text{Sr}/^{86}\text{Sr}$ ratio has a noticeable positive anomaly, the $\delta^{13}\text{C}$ value goes down distinctly. Sial et al (2015) emphasize that there is no correlation between the two, and assert the $^{87}\text{Sr}/^{86}\text{Sr}$ ratios are independent of those of $\delta^{13}\text{C}$.

$\delta^{13}\text{C}$ curves display similar values at different geologic time scales. This situation could occur rather frequently because chemostratigraphy is based on “wiggles matching” in most cases (Weissert et al., 2008). These similar values could bring disputable interpretations of the carbon isotope curves, and furthermore perverse interpretation of geochronology. However, it might not cause any problems since many other applicable geochronological methods distinguish each other such as lithological features, fossil, and geomagnetic records.

Besides, $^{87}\text{Sr}/^{86}\text{Sr}$ ratio also practical help in discriminating between repeated $\delta^{13}\text{C}$ fluctuation because $^{87}\text{Sr}/^{86}\text{Sr}$ ratio has been gradually increased throughout most of the Neoproterozoic (Shields, 2007; McArthur et al., 2012; Melezhik et al., 2001; Halverson et al., 2007, 2011, 2018). Therefore, being simultaneous utilization of the two proxies improves the reliability of the chemostratigraphical studies. The combination of these systems makes it an even more powerful tool in solving geological problems.

No reliable radiometric ages have been reported from the carbonates in the Okcheon Metamorphic Belt, but $^{87}\text{Sr}/^{86}\text{Sr}$ ages from several carbonates, e.g.,

Hyangsanni Dolomite, are mostly within the range of 760-720 Ma (Ha et al., 2021). Even if most of the carbonate sequence in the Okcheon Metamorphic Belt reveals the heterogeneous $^{87}\text{Sr}/^{86}\text{Sr}$ ratio affected by crustal strontium involvement, the available the lowest $^{87}\text{Sr}/^{86}\text{Sr}$ ratio would indicate those of seawater in which they were deposited. In addition, this study obtains the carbon isotopes from several carbonate sequences including the Hyangsanni Dolomite in the Okcheon Metamorphic Belt. Therefore, they might help establish proper chemochrons at present knowledge.



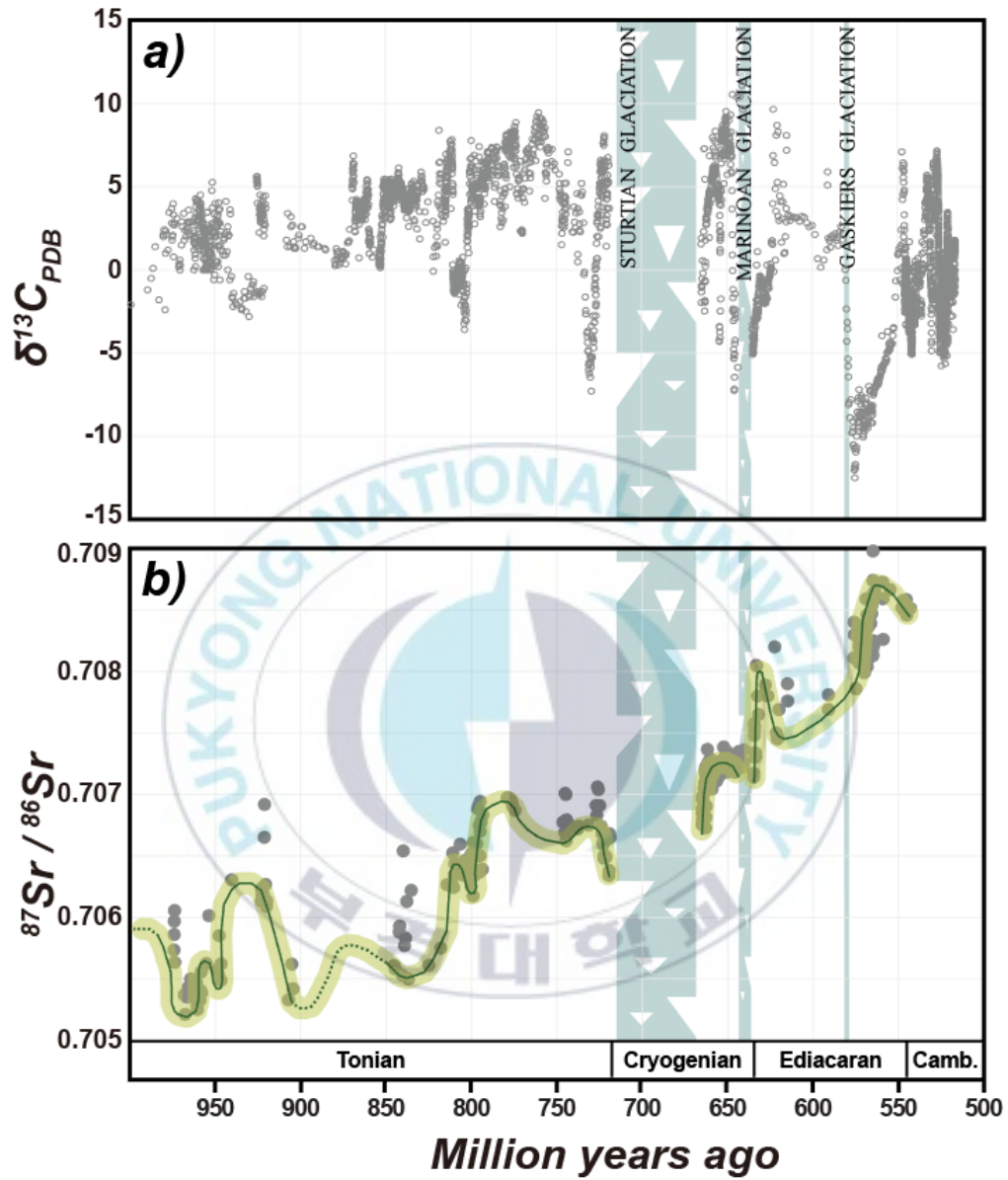


Figure 1-1. Composite $\delta^{13}C$ records for the Neoproterozoic from marine carbonate rocks with Cambrian data (modified from Zhou et al., 2020).

3. Analytical Methods

In this study, the whole-rock samples were analyzed for element concentrations including Ba, Sr, Mn, Rb, Sm and REE and Sr isotope composition.

The powdered samples prepared using knife-edge from polished slabs were analyzed, only for C-O analysis at Niigata University. In the case of the other analysis, these were carried out using the same whole-rock samples.

3.1 Carbon and Oxygen isotopes

Carbon and oxygen isotope compositions of the carbonate rocks of the study area were analyzed. Some analyses were conducted at Niigata University, Japan, and some were requested to be analyzed by Beta Analytic Inc. As for analysis conducted at Niigata University, scratched power was used for analysis (HYJ 12-1, HYJ 12-3, HYJ 13-1, HYJ 13-2, HYJ 13-7, HYJ 13-8). For the rest, bulk sample power was used for analysis at Beta Analytic Inc.

3.1.1 Faculty of Science, Niigata University

The $\delta^{13}\text{C}$ and $\delta^{18}\text{O}$ isotope data were acquired simultaneously on MAT 251 Mass Spectrometer in the Niigata University.

For sampling, staining has been done with Alizarin red-S beforehand to distinguish between calcite and dolomite. Staining of Alizarin red-S does not affect the C and O isotope ratio (Wada et al., 1983).

The sample powders for carbon and oxygen isotope analyses were taken from different portions of each slab to detect isotopic heterogeneity within the sample. Approximately, 1-mg collected by scraping knife-edge from a polished slab of the Geumgang Limestone under a binocular microscope was filled with small stainless steel cups.

These cups containing sample powder were then dropped into a reaction vessel and reacted in a common, purified concentrated H_3PO_4 bath at 110°C in a vacuum to liberate CO_2 (Wada et al., 1983). The liberated CO_2 gas was then purified cryogenically for analysis.

Machine standards calibrated to NBS-20 standard yield reproducibility of 0.03‰ and 0.05‰ for $\delta^{13}\text{C}$ and $\delta^{18}\text{O}$, respectively. The results are reported in conventional δ notation related to the V-PDB standard for carbon and V-SMOW standard for oxygen.

3.1.2 Bata Analytic Inc.

The method of carbon and oxygen isotope analysis performed at Beta Analytic Inc. was as follows.

For simultaneous measurements of $\delta^{13}\text{C}$ and $\delta^{18}\text{O}$, subsamples were taken with masses suitable to provide peaks within the operating window (50-40,000 mV) of IRMS.

Samples were placed in clean vials. Samples were then flushed with He and 5 drops of phosphoric acid (H_3PO_4) were added to the sample to stimulate CO_2 released into the headspace of the vial.

The sample was then placed in a tray, temperature-controlled at 72°C , and allowed

to equilibrate CO₂ for one hour. Helium entered the sample and a He + CO₂ mixture was injected using the ISODAT software, which synchronized the sample label with the data output. Detection of CO₂ was done via Gas Chromatography (GC) with ISODAT control. Drift correction was applied by normalizing to the values of in-house standards.

The reported values were calibrated using the international standard V-PDB. To convert a δ¹⁸O value from the SMOW to PDB -scale an equation provided by Jacques et al., (2008):

$$\delta^{18}\text{O}_{\text{SMOW}} = [(1.03086 * \delta^{18}\text{O}_{\text{PDB}}) + 30.86]$$

Consideration of the data from Beta Inc. is that it may reflect the heterogeneity due to using bulk samples. Thus, it needs to be careful that the carbon and oxygen isotope data from bulk carbonate samples cannot be simply correlatable between different samples.

3.2 Trace elements and rare earth elements (REE)

Trace elements and rare earth elements (REE) from some of the same samples for stable isotopes were measured using ICP-MS (Agilent 7500a) at the Niigata University, Japan, and some were requested to be analyzed by Korea Basic Science Institute (KBSI), Korea.

3.2.1 Faculty of Science, Niigata University

Samples were chipped using a hand press and then pulverized in an agate mortar.

After putting it in a porcelain crucible and drying it in an oven for half a day, it was secondarily crushed with an agate mortar.

Pulverized samples, approximately 50mg, suitable standards (BHVO-2, W-2a, JB-2) and several blanks were dissolved by the 35% nitric acid/ 0.5% hydrochloric acid/ 0.1% hydrofluoric acid mixture and spiked with Indium solutions as standard for measurements.

Isotope dilution methods follow the protocol described in detail by Neo et al. (2006). Trace elements including REE, Rb and Sr compositions of the samples were measured using ICP-MS (Agilent 7500a).

3.2.2 Korea Basic Science Institute (KBSI)

Approximately 0.1 g of each sample was placed in an acid-washed Teflon vessel and treated with a 4:1 mixture of HNO₃ and HClO₄ overnight and then dried. Dried samples were redissolved in a 5:3 mixture of HF and HNO₃ overnight. Then, the samples were dried and redissolved in 5ml of 6M HCl overnight. For analysis, the nearly dry residue was dissolved in 5% HNO₃.

Concentrations of trace elements were measured by inductively coupled plasma mass spectrometry (ICP-MS; X2; Thermo Scientific, Bremen, Germany) at the Korea Basic Science Institute (KBSI, Chungbuk, Korea).

The following standards were also prepared and analyzed to verify sample pretreatment and instrument analysis performance. The reproducibility of the analysis was better than $\pm 2\%$ (n = 3).

3.3 Strontium isotope

Strontium compositions of the carbonate rocks of the study area were analyzed. Some analyses were conducted by TIMS at Niigata University, Japan, and Korea Institute of Geoscience and Mineral Resources (KIGAM), Korea. The others were requested to be analyzed by Korea Basic Science Institute (KBSI), Korea. Bulk sample powers were used for all analyses.

3.3.1 Faculty of Science, Niigata University

The thermal ionization mass spectrometer (TIMS; MAT 262; Finnigan) was used for measuring Sr isotope composition, following the procedures of Miyazaki and Shuto (1998).

Extraction of Sr from sample powder used in the analysis for elements concentration had been described by Takahashi et al. (2009). This procedure uses a two-step column separation to obtain the Sr fraction.

Measured $^{87}\text{Sr}/^{86}\text{Sr}$ ratios were normalized to $^{86}\text{Sr}/^{88}\text{Sr}=0.1194$ to calibrate the instrumental mass fractionation. Repeated measurements of the Sr isotope composition for the NIST 987 standard agree well with the known values, averaging $^{87}\text{Sr}/^{86}\text{Sr}=0.710237\pm 0.000014$, 2σ , $n=20$).

3.3.2 Korea Basic Science Institute (KBSI)

The samples re-dissolved in 5% HNO_3 were dried in an acid-cleaned Teflon vessel and re-dissolved in 8M HNO_3 . Strontium was then separated from matrix elements

using Sr resin from Eichrom (Lisle, IL, USA). Strontium isotope ratios ($^{87}\text{Sr}/^{86}\text{Sr}$) were measured by multi-collector inductively coupled plasma mass spectrometry (MC-ICP-MS; Neptune; Thermo Scientific) at the KBSI.

$^{87}\text{Sr}/^{86}\text{Sr}$ ratios were normalized to $^{86}\text{Sr}/^{88}\text{Sr} = 0.1194$, and replicate analyses of NBS 987 (NIST, Gaithersburg, MD, USA) gave $^{87}\text{Sr}/^{86}\text{Sr} = 0.710247 \pm 0.000027$ (2σ , $n = 30$) with a background value of less than 0.1 ng.

3.3.3 Korea Institute of Geoscience and Mineral Resources (KIGAM)

Approximately 100mg of each sample were weighed and dissolved in a 15ml flat bottom PFA Teflon vial with concentrated HF and HClO_4 . These samples were redissolved in 0.5ml of 2.5 M HCl, and then centrifuged at 13,000 RPM for 5 minutes to separate the supernatant and residual from the sample solution. Sr fractions were separated by a two-step column chromatography, using DOWEX[®] 50WX8 (100~200 mesh) and Eichrom Technologies Inc. (100~150 μm) resin.

Rb and Sr isotopic data were measured using a TRITON Plus TIMS at KIGAM, Daejeon, Korea, following the methods mentioned in Lee (2013).

Measured $^{87}\text{Sr}/^{86}\text{Sr}$ ratios were corrected for mass fractionation by normalizing to $^{88}\text{Sr}/^{86}\text{Sr} = 8.375209$. Since ^{87}Rb overlaps with ^{87}Sr , ^{87}Rb was monitored for the interference correction. For this reason, the Sr isotope ratios were corrected for Rb interference using $^{87}\text{Rb}/^{85}\text{Rb} = 0.385700$. Replicate analyses of NBS 987 gave $^{87}\text{Sr}/^{86}\text{Sr} = 0.710262 \pm 0.000004$ ($N = 20$, 2σ standard error).

Table 1-1. The methods used and institution conducting the analysis.

	Method	Institution
$\delta^{13}\text{C}$ - $\delta^{18}\text{C}$	Isotope Ratio Mass Spectrometry (IRMS)	Faculty of Science, Niigata University Beta Analytic Inc.
$^{87}\text{Sr}/^{86}\text{Sr}$	Thermal Ionization Mass Spectrometry (TIMS) Multicollector Inductively Coupled Plasma Mass Spectrometry (MC-ICP-MS)	Faculty of Science, Niigata University KIGAM KBSI
Trace elements	Inductively Coupled Plasma Mass Spectrometry (ICP-MS)	Faculty of Science, Niigata University KBSI
		Korea Institute of Geoscience and Mineral Resources, KIGAM Korea Basic Science Institute, KBSI

4. Study Outline

This study was conducted on the central-western (Boeun-Okcheon area, Figure 2-1) and northeastern (Chungju-Jecheon area, Figure 2-2) Okcheon Metamorphic Belt bordering the Taebaeksan Basin to the east (Figure 1-2).

4.1 General geology

The Korean Peninsula consists of three parts of Precambrian basements and two fold-and-thrust belts in between from north to south: the Namgrim Massif, Imjingang Belt, Gyeonggi Massif, Okcheon Belt, and Yeongnam Massif (Figure 1a).

The basements exposed over a wide area in Korean Peninsula are mainly composed of early to middle Paleoproterozoic (2.0-1.8 Ga) high-grade gneiss complex (Kim, 2012; Oh et al., 2019; Zhao et al., 2006), with much older late Archean to early Paleoproterozoic (~2.5 Ga) rock in the Nangrim Massif (Zhao et al., 2006) and western Gyeonggi Massif (Cho et al., 2008).

Between the Nangrim and Gyeonggi Massifs, there are two sedimentary basins; called Pyeongnam Basin, and E-W trending Imjingang Belt. The Pyeongnam Basin is composed of Mesoproterozoic to Paleozoic sedimentary rocks overlying the Nangrim Massif (Hu et al., 2012; Zhai et al., 2019). The sedimentary characteristics of the Pyeongnam Basin are analogous to those of the Taebaeksan Basin of the Okcheon Belt.

Lower to south, there is an orogenic belt, Imjingang Belt, dominated by Devonian sedimentary rocks with fossils (Ree et al., 1996; Kwon et al., 2009; Kim et al., 2020). Whether this belt exists in Korean Peninsula has still been the subject of debate as well.

The Okcheon Belt is a representative Phanerozoic mobile belt alongside Imjingang Belt. Both belts are well worth considering the tectonic evolution of East Asia as well as the Korean Peninsula because either one or both would be possible candidates for the eastern continuation of the Qinling-Dabie-Sulu collision belt. (Cluzel et al., 1990; Yin and Nie 1993; Ernst and Liou, 1995; Cheong et al., 2006; Cho et al., 2017) (Figure 1).

The northern part of the Korean Peninsula is known to have evolved with the adjoining North China Craton, at least since the Paleoproterozoic (Zhai et al., 2019). However, various contrasting hypotheses have been proposed regarding the structural evolution of the southern part of the Korean Peninsula.

For the last three decades, one of the most important issues in debate for the tectonic evolution of the Korean Peninsula is whether the collisional belt between North China Craton and South China Craton continues to Korean Peninsula in the east or not (Liu, 1993; Ree et al. 1996; Cho et al., 2013). It has long been controversial that the location of the collision zone on the Korean Peninsula is either the Imjingang Belt (Ree et al., 1996) or the belt joining Hongseong and Odaesan in the Gyeonggi Massif (Oh et al., 2006, 2007). According to these discussions, it has gained increasing cogency that Taebaeksan Basin, Yeongnam Massif, and some part of Gyeonggi Massif of South Korea with Pyeongnan Basin of North Korea correlate to North China Craton, other Gyeonggi Massif and Okcheon Metamorphic Belt correlate to South China Craton (Figure 1). This contention, however, has been challenged in recent years. For instance, at least portions of the Gyeonggi Massif and Okcheon Metamorphic Belt proposed a correlation with South China Craton is suggested to be correlated with North China Craton based on recently reported detrital zircon age data.

The northeastern part of the Okcheon Metamorphic Belt is in contact with the

Cambro-Ordovician sediments of the Taebaeksan Basin. Different opinions have been proposed for this boundary as conformity, unconformity, or fault contact according to scholars (Kihm et al., 1996, 1999; Chough et al., 2000, 2006; Kim et al., 2017). In particular, Chough et al. (2000) proposed this boundary as an accretion or collision boundary between continental blocks with different evolutionary histories and named it the South Korean Tectonic Line (SKTL).

The so-called South Korean Tectonic Line (SKTL) was especially proposed as the borderline as the southerly Yeongnam Massif should correlate with the North China Craton, when following the indentation model (Chough et al., 2000). The SKTL was bounded along the western side of the Yeongnam Massif and along the Taebaeksan Basin, along the boundary with the Okcheon Metamorphic Belt. Cho et al. (2013) The Okcheon Metamorphic Belt was divided into a part that correlates with the South China Craton (SCC-like) and a part that correlates with the North China Craton (NCC-like), and SKTL was established between them (Figure 1b). According to this, the Okcheon Metamorphic Belt and the Gyeonggi Massif in the west of SKTL were correlated to the South China Craton, and the Taebaeksan Basin, and the underlying Yeongnam Massif in the east were correlated to the North China Craton. This distinction is due to the interpretation of the Okcheon Belt as a complex tectonic unit where two tectonic units with different geological characteristics united.

Although the Korean Peninsula has a strong interrelationship with China Cratons, it has not reached a convincing decision due to the scarceness of data from North Korea.

By the way, much data for the geology of North Korea has been reported in the past decade (Hu et al., 2012; Wu et al., 2007a, 2007b; Zhao et al., 2006). It has been very helpful to understand the Northeast Asian geotectonic evolution. Studies on the

Archean to Paleoproterozoic basement, previously mostly limited to some regions of the North China Craton, eastern and western blocks, and Trans-North China Orogen in between them (e.g., Liu et al., 2012; Zhao et al., 2003) have been extended to more eastern regions covering Jiao-Liao-Ji Belt in China and Nangrim Massif in North Korea (Meng et al., 2014; Tam et al., 2012; Zhai et al., 2019).

The occurrence of Neoproterozoic rocks and the geochronological data play a vital role in such a tectonic comparison between the Korean Peninsula and China Cratons. Such as late Paleoproterozoic to Mesoproterozoic detrital zircon age distribution from the Neoproterozoic rocks in the southern margin of North China Craton and southern part of North Korea put forward evidence to support the correlation between the two regions (Hu et al., 2012).

The Okcheon Belt is located between the Gyeonggi Massif in the north and Yeongnam Massif in the south, most of which consist of the Paleoproterozoic gneiss complex (Figure 1a). And it is exposed in the northeast-southwest direction with a beltlike shape. The Okcheon Belt also represents the Phanerozoic mobile belt alongside Imjingang Belt. Both belts are well worth considering the tectonic evolution of East Asia as well as the Korean Peninsula because either one or both of them would be possible candidates for the eastern continuation of the Qinling-Dabie-Sulu collision belt. (Cluzel et al., 1990; Yin and Nie 1993; Ernst and Liou, 1995; Cheong et al., 2006) (Figure 1a).

The Okcheon Belt has ordinarily divided into the Taebaeksan Basin in the northeast and Okcheon Metamorphic Belt in the southwest. These are sedimentary basins but distinct in their origin, tectonic setting, and geochronology.

The Taebaeksan Basin is composed of fossiliferous sedimentary rocks from the

early Paleozoic to early Mesozoic and exhibits low- to medium-grade metamorphism (Lee and Chough 2006; Choi et al., 2019; Kwon et al., 2019). Most of the Okcheon Metamorphic Belt remains with disputable ages because it has experienced multiple deformations and metamorphisms (Min and Cho, 1998; Cheong et al., 2003) ranging from greenschist facies to amphibolite facies, which brought poorly fossiliferous and observational difficulties of sedimentary textures. It finally led to forbidding proper interpretation of geochronology of the Okcheon Metamorphic Belt.

Accordingly, the evolution of the Okcheon Metamorphic Belt including specific depositional timing, and stratigraphic relationship, is not yet fully understood.

The Okcheon Metamorphic Belt, fold- and thrust- belt, is composed of several types of metasedimentary and metavolcanic rocks from Neoproterozoic (Lee et al., 1998; Kim et al., 2020; Lee et al., 1998a) to Permian (Lim et al., 2005) periods. And different formation names are assigned according to the main constituent rock types. The geological ages, stratigraphical categorization, and their structural relationships of constituents of the Okcheon Metamorphic Belt have been outstanding matters last few decades. Numerous studies have been actively proceeded with the advance in SHRIMP and MC-ICPMS, in respect of unsolved matters for the depositional time of the Okcheon Metamorphic Belt. In accordance with that, detailed geochronology data from metasedimentary successions in the Okcheon Metamorphic Belt has been recognized.

The Okcheon Metamorphic Belt has been suggested to divide into two regions characterized by narrow and long based on their zircon age patterns (Cho et al., 2013). They are compatible with North China Craton and South China Craton, and are called NCC-like and SCC-like, respectively. The SCC-like zone, the northwestern band of the Okcheon Metamorphic Belt, reveals the wide range of detrital zircon ages, the oldest

are some of the Paleoproterozoic and the youngest include the Paleozoic era. Lim et al. (2005, 2006, 2007) discovered that Carboniferous to Permian plant fossils in Northwestern Okcheon Metamorphic Belt which area contains the SCC-like area. On the other hand, in the NCC-like area, the detrital zircon ages of the Paleoproterozoic era are prominent, with about 750 Ma of the youngest age (Cho et al., 2013; Kim et al., 2020; Kim et al., 2021). However, the Daehyangsan Quartzite (ca. 420 Ma, Park et al., 2011) belonged to the NCC-like area seems to be the northeast extension of the SCC-like unit.

The northeastern region of the Okcheon Metamorphic Belt (Figure 1b) is supposed to have a North China Craton affinity. The felsic metavolcanics were reported in the Gyemyeongsan Formation and the Munjuri Formation in the north, and have zircon U-Pb ages of about 860 Ma (Kim et al., 2006; Kim et al., 2011) and 750 Ma (Lee et al., 1998; Cho et al., 2004; Kim et al., 2006) indicating their eruptions, respectively. The Munjuri Formation has a metavolcanic age of about 750 Ma, which is commonplace in South China Craton, hence, Cho et al. (2013) categorized the Munjuri Formation as an SCC-like constituent. But, this age is not a feature often seen in NCC-like regions, but surrounded by other constituents having NCC-affinities. Thus, it is more pertinent to categorize the Munjuri Formation as an NCC-like constituent.

Despite the U-Pb age determinations for detrital zircons (Cho et al., 2013; Kim et al., 2020), the precise depositional time of the remaining sedimentary formations is still uncertain. In the case of carbonate rocks, in particular, that do not have detrital zircon, it is more difficult to limit the depositional time because proper dating means are limited. However, a recent chemostratigraphy study based on carbon and strontium isotopic composition suggested that the Hyangsanni Dolomite was deposited in

Neoproterozoic (Ha et al., 2021).

The Taebaeksan Basin is another one that makes up the Okcheon Belt and developed on the Yeongnam Massif in the central-eastern Korean Peninsula (Figure 1). The early Cambrian - Middle Ordovician Joseon Supergroup and the late Carboniferous – Early Triassic Pyeongan Supergroup were deposited in the Taebaeksan Basin, which is compatible with the Paleozoic strata of the Pyeongnam Basin in North Korea (Chough et al., 2000). Unlike Okcheon Metamorphic Belt, the stratigraphy of the Joseon and Pyeongan Supergroups is well established due to the fossiliferous environment and well-preserved sedimentary structures (Chough et al., 2000). The Joseon Supergroup of the Taebaeksan Basin is restricted to the east of SKTL (Figure 1b).

The Joseon Supergroup, lower Paleozoic sedimentary strata in South Korea, is composed mainly of mixed carbonates and siliciclastics. Kobayashi, Yosimura, Iwaya, and Hukasawa (1942) firstly differentiated the Joseon Supergroup of the Taebaeksan Basin into five types of sequences: namely, the Duwibong-, Yeongweol-, Jeongseon-, Pyeongchang-, and Mungyeong-type sequences (see also Kobayashi, 1966). However, it is divided into the Taebaek, Yeongweol, Yongtan, Pyeongchang, and Mungyeong groups according to lithologies and stratigraphic characteristics since then (Choi, 1998; Chough et al., 2000; Choi et al., 2004; Choi and Chough, 2005; Kwon et al., 2006; Choi and Park, 2017).

While the Pyeongan Supergroup is primarily constituted by sandstones and shales, with intercalated limestone layers. The Pyeongan Supergroup is first proposed by Cheong (1969) who divided the Pyeongan Supergroup into seven lithographic units, the Manhang, Geumcheon, Jangseong, Hambaeksan, Dosagok, Gohan, and Donggo

Formations in ascending order (Kim et al., 2018).

This thesis demonstrates geochronology for carbonates which has been age debatable in the Okcheon Metamorphic Belt in the ensuing chapters, by adopting chemostratigraphy. The outline of each chapter is as follows.

4.2 Geumgang Limestone: Chapter 2

Extensive glaciations were a rare event in Earth's history and glaciogenic sequence is finitely occurrence. Korean peninsula and Chinese Cratons record remarkable series of significant geological events related to the Rodinia supercontinent such as Neoproterozoic glaciations and continental rifting. It should be noted that although Neoproterozoic diamictites are widespread, the glacial affinity in the Korean peninsula has been doubtful. The existence of the glaciogenic sequence may enable constraint on the age of the Okcheon Metamorphic Belt by deducing stratigraphic relationship with adjacent strata.

That is why rare evidence of glaciation in the Okcheon Metamorphic Belt would be the important key to understand the link between the Korean peninsula and Chinese Cratons. Furthermore, it could provide clear advantage insights into the tectonic evolution of East Asia.

Chapter 2 discusses the thin carbonate layer deeming a post-glacial cap carbonate which are intercalated between pebble-bearing phyllitic and phyllitic metasedimentary rocks. These carbonates are recognized from the Chungju-Jecheon area to the Okcheon-

Boeun area.

4.3 Seochangni, Samtaesan, and Heungwolri Formations: Chapter 3

In terms of tectonic unit division, the northeastern Okcheon Metamorphic Belt is tectonically highly important because this area is contiguous with the western margin of the Taebaeksan Basin and consists of various lithofacies including metavolcanics and carbonates.

The Seochangni Formation has been an age-unknown stratum in Okcheon Metamorphic Belt and the Samtaesan and Heungwolri Formation have considering as early Paleozoic (Cambro-Ordovician) strata in Taebaeksan Basin. The Samtaesan and Heungwolri Formations are also named at the Okcheon Metamorphic Belt based on the lithostratigraphic similarity with those in the Taebaeksan Basin. This study for these formations makes reconsider South Korea Tectonic Line (SKTL) suggested boundary between the Okcheon Metamorphic Belt and Taebaeksan Basin.

We do not attempt to differentiate the Joseon Supergroup into the lower stratigraphic units, as it displays the lithologic succession somewhat different from those of the known groups of the Joseon Supergroup.

Chapter 3 deals with several carbonates distributed in the Chungju-Jecheon area; Seochangni, Samtaesan, and Heungwolri Formations.

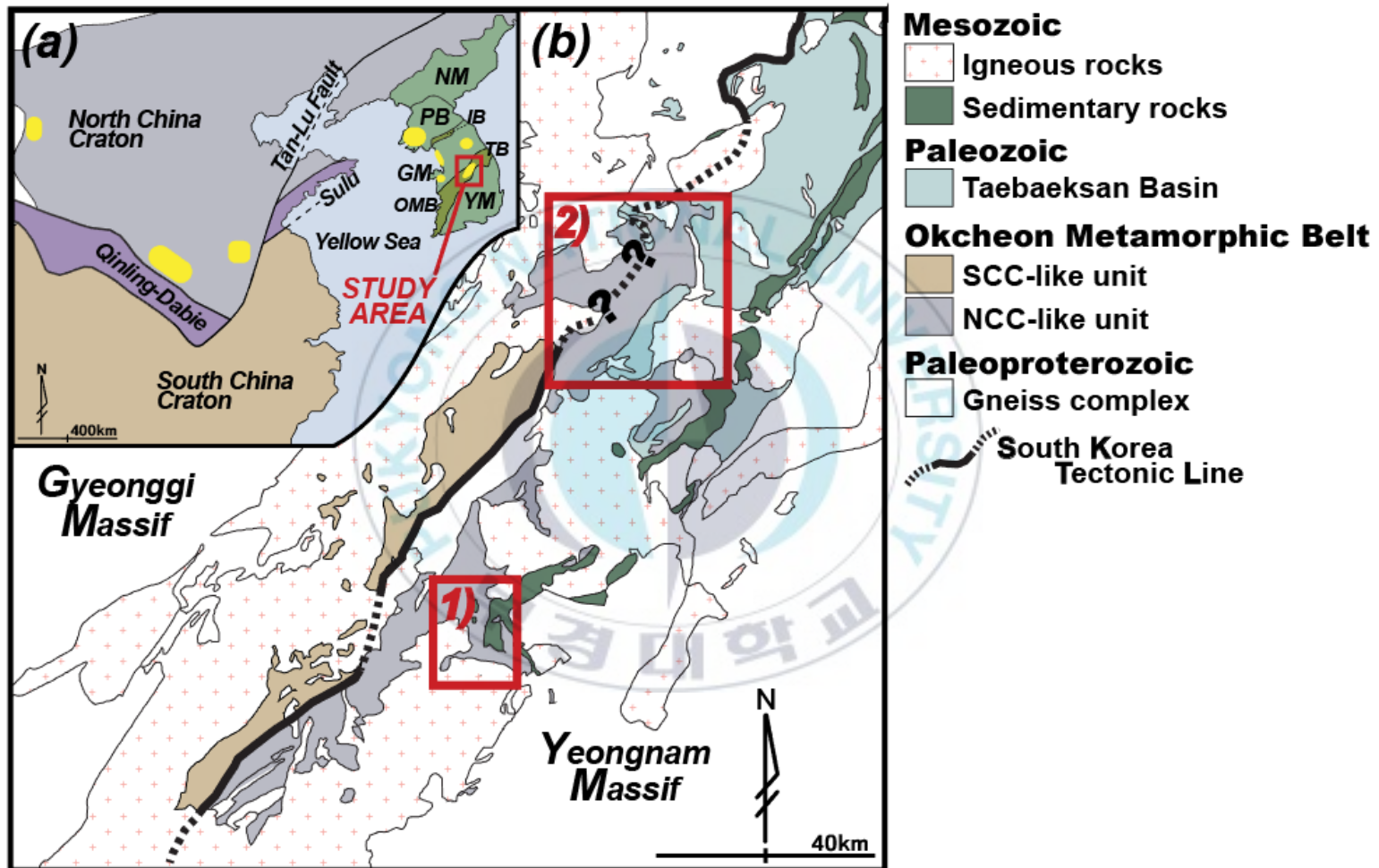
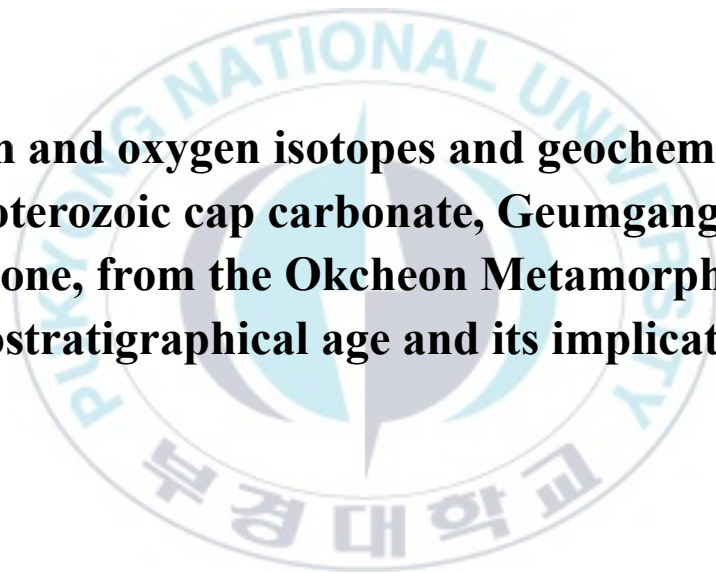


Figure 1-2. a) A map showing the Korean Peninsula with parts of the North China Craton and the South China Craton. The continental collision belts of the Dabie and Sulu regions are also shown. The areas marked in yellow are rough representations of areas where Neoproterozoic sedimentary formations are distributed in South Korea, North Korea, and North China Craton. From left, western (Zhengmuguan Formation; Yang et al., 2019), southern (Luoquan Formation; Le Heron et al., 2018; 2019; 2020), and southeastern (Huaibei Group; Zhou et al., 2020) North China Craton; southwestern (Pirangdong Formation; Kim et al., 2016) North Korea; western (Kim et al., 2019), southwestern (Kee et al., 2019; Oh et al., 2009), and northeastern Gyeonggi Massif (Lee et al., 2020); and northeastern Okcheon metamorphic belt (Kim et al., 2006, 2020). The tectonic units of the Korean Peninsula are marked with abbreviations. NM: Nangrim Massif, PB: Pyongnam Basin, IB: Imjingang belt, GM: Gyeonggi Massif, OMB: Okcheon metamorphic belt, TB: Taebaeksan Basin, and YM: Yeongnam Massif. b) A map showing the Okcheon metamorphic belt distributed over the south-central Korean Peninsula. The Okcheon metamorphic belt was divided into two, NCC (North China Craton)-like and SCC (South China Craton)-like, modified after Cho et al. (2013). Red boxes indicate the study areas. 1) Okcheon-Boeun area (Figure 2-1). 2) Chungju-Jecheon area (Figure 2-2).

CHAPTER 2

Carbon and oxygen isotopes and geochemistry of Neoproterozoic cap carbonate, Geumgang Limestone, from the Okcheon Metamorphic Belt: Chemostratigraphical age and its implication



Abstract

The age-unknown limestone distributed throughout the Okcheon Metamorphic Belt has been a longstanding conundrum. Among the rest, the Geumgang Limestone is suggested as a cap carbonate based on the occurrence sharply overlies Hwangganni Formation considered as Neoproterozoic diamictite (Choi et al., 2012). However, as of yet, it is a controversial issue since no distinct glacial sedimentological feature has been founded in both formations.

In the case that the Okcheon Metamorphic Belt had experienced glaciation in Neoproterozoic Era, some age-unknown limestone including Geumgang Limestone should have recorded its signal.

To verify the imprinted evidence of a glaciation event in the Okcheon Metamorphic Belt, we carried out a series of geochemical analyses for the Geumgang Limestone formation that occurred in the Okcheon, Chungju and Jecheon area.

Most $\delta^{13}\text{C}$ and $\delta^{18}\text{O}$ values of samples show more depleted general cap carbonates. Besides, $^{87}\text{Sr}/^{86}\text{Sr}$ ratios also display more radiogenic values than that of the Neoproterozoic Era.

It is difficult to a simple and direct comparison between being well-preserved cap carbonates and the Geumgang Limestone because the Okcheon Metamorphic Belt had undergone greenschist to amphibolite facies metamorphism. In this sense, the isotopic data cannot dovetail those of general cap carbonates. Thus, these exceptional isotopic values can be interpreted by alteration during metamorphism.

Nevertheless, it possibly corresponding to the glaciation events in Neoproterozoic based on a comparison of negative carbon isotope composition with the global trend.

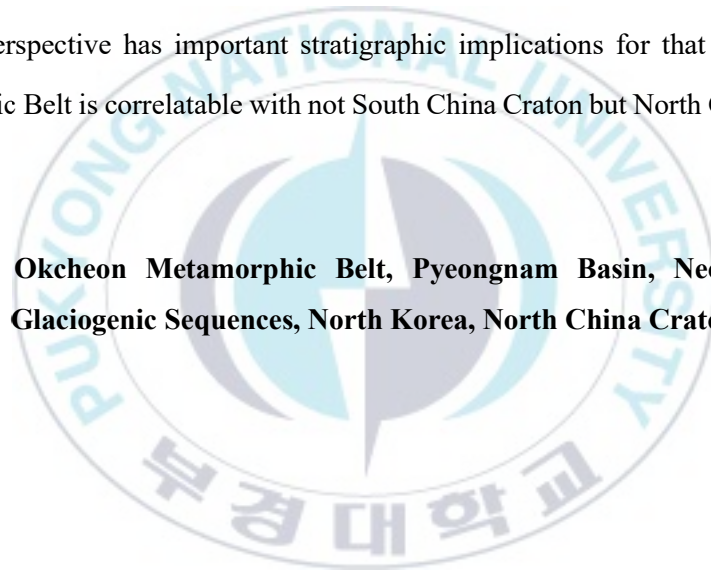
Cap carbonates define the pronounced notable negative excursions in

Neoproterozoic successions. The negative carbon isotope excursion of Geumgang Limestone is analogous to that of Neoproterozoic cap carbonates ~~in~~ worldwide though it has a more depleted $\delta^{13}\text{C}$ value.

Here, we focus Provide new insights for the formation of the Okcheon Metamorphic Belt. Integrating our data and previous studies for adjacent formations, we suggest the Geumgang Limestone was deposited after the Neoproterozoic glaciation even though we cannot pinpoint when.

This perspective has important stratigraphic implications for that the Okcheon Metamorphic Belt is correlatable with not South China Craton but North China Craton.

Keywords: Okcheon Metamorphic Belt, Pyeongnam Basin, Neoproterozoic, Glaciogenic Sequences, North Korea, North China Craton



1. Introduction

The Okcheon Metamorphic Belt (also called the Chungcheong Basin) has been hypothesized that it was an eastward extension of the Nanhua Basin of South China Craton following the break-up of the Rodinia supercontinent in early Neoproterozoic (Choi et al., 2012; Du et al., 2020). As previously stated, the Earth had an extreme climate change called Snowball Earth event during the Neoproterozoic (Hoffman et al., 1998; Kennedy et al., 2001; Halverson et al., 2002; Sansjofre et al., 2011; Cox et al., 2016).

Recent zircon U-Pb age determinations show that regional sedimentation, arc-related magmatism and intracratonic rifting have occurred in the central Korea Peninsula during the Neoproterozoic. (Kim et al., 2020 and references therein). Furthermore, it is an important tectonic evolutionary period during which assembly and disruption of the Rodinia supercontinent.

Currently available geochronological data allow that the Neoproterozoic Era, especially the Cryogenian Period (ca. 720-635 Ma) experienced at least two major glacial events: the older Sturtian Glaciation (early Cryogenian), and the younger Marinoan Glaciation (late Cryogenian) (Font et al., 2006; Macdonald et al., 2010; Halverson et al., 2004; Hoffman et al., 2017; 2019). The Sturtian Glaciation may have been the most severe glacial event globally. At this time, the huge area to the paleo-Equator has been covered with ice, as suggested by the Snowball Earth hypothesis (Kirschvink, 1992; Hoffman et al., 1998; Schrag et al., 2002; Meert et al., 2004; Wang et al., 2020).

It is assumed that the ice covering the tremendous continents has melted quickly after the end of the ice age. Most Neoproterozoic glaciogenic deposits are shrouded in carbonate deposits known as "cap carbonates" (Kennedy, 1996, 2011; James et al., 2001;

Corsetti et al., 2005, 2006, 2007; Shields et al., 2005; Pokrovsky et al., 2020; Hohl et al., 2017; Yang et al., 2019). the mechanism of its formation remains unsolved, with competing hypotheses such as the gas hydrate destabilization, plumeworld, and calcareous loess models (Wang et al., 2020 and references therein)

In the case that the Okcheon Metamorphic Belt had experienced glaciation in Neoproterozoic Era, some age-unknown carbonate including the Geumgang Limestone should have recorded its signal.

The Geumgang Limestone is exposed between the pebble-bearing phyllitic rocks and phyllitic rocks, with only about 10 m in width and about 100 km in length. It has a possibility of post-glaciogenic cap carbonates. In this context, the underlying pebble-bearing phyllitic rock, Hwanggangri Formation, has been interpreted as glaciogenic diamictite (Reedman and Fletcher, 1976; Lee et al., 1998; Choi et al., 2012). Therefore, the Geumgang Limestone is a key stratum helpful in understanding the Neoproterozoic Snowball Earth event in the Korean peninsula (Reedman and Fletcher, 1976; Lee et al., 1998; Choi et al., 2012; Ryu and Ahn, 2016) and establishing the stratigraphy of the Okcheon Metamorphic Belt. Because the post-glacial cap carbonates can help to limit its geological time.

In this chapter, I discuss the possibilities and implications of the Geumgang Limestone as post-glacial cap carbonates, preponderantly using carbon isotope composition including additional analytical data. Together with that, I try to reassess the role of the Geumgang Limestone in the Okcheon Metamorphic Belt and its stratigraphic implication.

I have carried out a series of geochemical analyses to verifying the imprinted evidence of a glaciation event in the Okcheon Metamorphic Belt for the Geumgang Limestone formation that occurred in the Okcheon and Chungju area.

In general, post-glacial cap carbonates are characterized by very low carbon isotope values (as low as $\sim -5\%$; Kaufman et al., 1993; Kennedy et al., 1998; Jiang et al. 2003; Yang et al., 2019). Most $\delta^{13}\text{C}$ and $\delta^{18}\text{O}$ values of samples show more depleted than general cap carbonates. Besides, the $^{87}\text{Sr}/^{86}\text{Sr}$ ratio also displays more radiogenic value than that of the Neoproterozoic Era.

It is difficult to a simple and direct comparison between being well-preserved cap carbonates and the Geumgang Limestone because the Okcheon Metamorphic Belt had undergone greenschist to amphibolite facies metamorphism. In this sense, the isotopic data cannot dovetail those of general cap carbonates. Thus, these exceptional isotopic values can be interpreted by alteration during metamorphism.

Nevertheless, it possibly corresponding to the glaciation events in Neoproterozoic based on a comparison of negative carbon isotope composition with the global trend. Cap carbonates define the pronounced notable negative excursions in Neoproterozoic successions. The negative carbon isotope excursion of the Geumgang Limestone is analogous to that of Neoproterozoic cap carbonates worldwide though it has a more depleted $\delta^{13}\text{C}$ value.

Ryu and Ahn (2017) discussed the possibility of the Geumgang Limestone being post-glacial cap carbonates through carbon and oxygen stable isotope analysis but could not draw a clear conclusion. However, they raised the possibility that some Geumgang Limestones with low carbon isotope values were made by hydrothermal alteration after their formation.

Combining our data with previous studies of the adjacent strata suggests that the Geumgang Limestone was deposited after the Neozoic Ice Age, although we do not know exactly when.

2. Geological Setting

The Okcheon Metamorphic Belt is composed of several types of metasedimentary and metavolcanic rocks, and different formation names are assigned according to the main constituent rock types. First, felsic metavolcanics were reported in the Gyemyeongsan Formation and the Munjuri Formation in the north, and have zircon U-Pb ages of about 860 Ma (Kim et al., 2006; Kim et al., 2011) and 750 Ma (Lee et al., 1998; Cho et al., 2004; Kim et al., 2006) respectively. Unlike this Neoproterozoic metavolcanics, the depositional time of the metasedimentary layers of the Okcheon Metamorphic Belt is not yet known precisely. Recent studies have suggested that some of these have a Neoproterozoic, the youngest detrital zircon age of about 750 Ma from the Seochangni Formation, (Kim et al., 2021) and some have a Carboniferous-Permian sedimentation period on the evidence of a fossil plant (Lim et al., 2005, 2006, 2007) from so-called Okcheon Supergroup (refer to Choi et al., 2012 for a summary).

Despite the U-Pb age determinations for detrital zircons (Cho et al., 2013; Kim et al., 2020), the precise depositional time of the remaining sedimentary formations is still uncertain. In particular, in the case of carbonate rocks that do not have detrital zircon, it is more difficult to limit the depositional time because proper dating means are limited. However, a recent chemostratigraphy study based on carbon and strontium isotopic composition suggested that the Hyangsanni Dolomite was deposited in Neoproterozoic (Ha et al., 2021).

Among the layers constituting the Okcheon Metamorphic Belt, the Hwanggangni Formation and the Bugnori Formation represent pebble-bearing phyllite as the main constituent rocks taking up an area of 60% Okcheon Metamorphic Belt.

The Hwanggangni Formation and the Bugnori Formation were first named in the 1:50,000-scale Hwanggangni quadrangle (Lee and Park, 1965). The Hwanggangni

Formation is distributed over a wide area in the mid-southern part of the Okcheon Metamorphic Belt. This formation is also recognized close to the left of the South Korean Tectonic Line in northeastern Okcheon Metamorphic Belt, but on the other, it is mapped as the Bugnori Formation by Lee and Park (1965).

In the northeastern Okcheon Metamorphic Belt, these two formations do not come into direct contact, and the Myeongori Formation, mainly composed of phyllite, exists between the two. According to the Hwanggangni quadrangle (Lee and Park, 1965), the Chungju area, there is a relatively thin, continuous carbonate layer with a thickness of about 15-20 meters between the Myeongori Formation and the Bugnori Formation.

There is also a suggestion that these two formations are identical formations that are repeated by folding (Choi et al., 2012). However, Lee and Park (1965) denied this relationship because a thin carbonate layer that exists between the Myeongori Formation and the Bugnori Formation must also exist between the Myeongori Formation and the Hwanggangni Formation in order for repetition by folding to be established. Lee and Park (1965) also argued that the Bugnori Formation and the Hwanggangni Formation mentioned the differences in lithologies between them as another basis for distinct sedimentary layers. They also described that the Hwanggangni Formation has a calcareous matrix and pebbles often have a diameter of more than 15 cm, whereas the Bugnori Formation has a primarily sandy matrix with pebbles of much smaller and uniform size. However, the pebbles of the Bugnori Formation do not show a distinct difference in size compared to the Hwanggangni Formation.

The Hwanggangni Formation is considered as a glacial deposit together with Bugnori Formation. These pebble-bearing phyllites of the Okcheon Metamorphic Belt are also called tillites or diamictites and have been proposed several times as glacial sediments (Reedman and Fletcher, 1976; Lee et al., 1998; Choi et al., 2012). Hwanggangni and Bugnori Formations, however, have been constantly questioned

regarding depositional timing, their origins, and the resultant identicalness of both formations.

Lee et al. (1998b) suggested the sedimentation time of the Hwanggangni Formation as Late Paleozoic for the following reasons. First, Lee et al. (1989) claimed the discovery of Cambro-Ordovician conodont fossils from limestone clasts of the Hwanggangni Formation. However, the discovery of conodonts from the Hwanggangni Formation has not been confirmed since then and needs to be verified. Second, the CHIME age of granite clasts from the Hwanggangni Formation was determined to be 367 Ma (Cho et al., 1996). Research published later (Suzuki et al., 2006) suggested that Paleoproterozoic granitic gneiss clasts in the Hwanggangni Formation had xenotime grains with a metamorphic rim of about 370 Ma, suggesting that sedimentation of the Hwanggangni Formation was thereafter. In contrast, Choi et al. (2012) suggest that this formation is glaciogenic diamictite deposited during the Neoproterozoic Snowball Earth event based on correlation with the stratigraphy of the Nanhua Basin in South China Craton, but did not provide definitive evidence. The detrital zircons of the Hwanggangni Formation characterize age groups of about 750 Ma and about 1870 Ma, which means their deposition is later than 750 Ma (Cho et al., 2013; Kim et al., 2020).

Phyllitic rocks are distributed over a wide area of the Okcheon Metamorphic Belt together with the pebble-bearing phyllitic rocks in addition to Chungju and nearby areas in the northeast. These phyllitic rocks and pebble-bearing phyllitic rocks, having thin carbonate layers, have been written in different names depending on the quadrangles. It may classify them under two large groups. One is the Hwanggangni quadrangle (Lee and Park, 1965) covering the northern region of the Okcheon metamorphic Belt, and others are the Okcheon (Kim et al., 1978) and Boeun (Kim et al., 1977) quadrangles covering the southern region of the Okcheon Metamorphic Belt. The quadrangles are all 1:50,000 scales.

The Hwanggangni quadrangle (Lee and Park, 1965) divides the pebble-bearing phyllitic rocks into the Hwanggangni Formation and Bugnori Formation. The thin carbonate layer is exposed in contact with only Bugnori Formation. In the 1:50,000-scale quadrangles for the Okcheon (Kim et al., 1978) and Boeun (Kim et al., 1977), on the other hand, these rocks are collectively called Hwanggangni Formation.

Meanwhile, the formation which has similar lithologies with Hwanggangni Formation in the Chungju area, has been denominated by the Iwonni Formation. This formation is distributed in some areas of 1:50,000-scale Yongyuri (Yoo and Hong, 1973) and Miweon (Lee et al., 1980) quadrangles. Such pebble-bearing phyllitic layers are also characterized by the development of a narrow carbonate layer of about 10 meters between adjacent phyllitic layers called Changni Formation.

The pelitic rocks are classified into the Seochangni, Myeongori, and Munjuri formations in the Hwanggangni quadrangle (Lee and Park, 1965). These formations are sedimentary layers composed mainly of pelitic rocks such as phyllite, slate, or shale distributed in the northeastern part of the Okcheon Metamorphic Belt. The Myeongori Formation is only in contact with the carbonate layer.

However, in the 1:50,000-scale of the Okcheon (Kim et al., 1978) and Boeun (Kim et al., 1977) quadrangles, such pelitic rocks are rather simply treated. The sedimentary layers distributed in the southern region of the Okcheon Metamorphic Belt are largely composed of pelitic rocks. Such pelitic rocks that were investigated and named later than these, are typically Munjuri Formation and Changni Formation. During geological surveys in the Boeun and Okcheon areas for the preparation of 1:50,000 scale quadrangle, sedimentary layers composed of mostly green phyllitic rocks were classified as Munjuri Formation, and those composed of dark gray phyllitic rocks were named as the Changni Formation (Kim et al., 1977, 1978).

The lithologies of the Changni Formation are similar to the Seochangni Formation

or the Myeongori Formation, which are distributed in the northeastern part of the Okcheon metamorphic belt but do not come into direct contact with them, and there is no definite evidence for correlation, so different formation names are maintained. There is no significant difference between the Munjuri Formation and the Changni Formation except for the general color, and even this may be difficult to distinguish in some outcrops. In the Munjuri Formation distributed in the Chungju area, characteristic A-1 type metavolcanics were widely distributed, and its zircon U-Pb age was found to be about 750 Ma (Lee et al., 1998; Cho et al., 2004; Kim et al., 2006). However, such A-1 type metavolcanics are unknown in the Munjuri Formation, which is distributed in the southern part of the Okcheon metamorphic belt. However, so far, such A-1 type metavolcanics have not been known in the Munjuri Formation, which is distributed in the southern part of the Okcheon metamorphic belt, suggesting the possibility of being a sedimentary layer that is not correlated with the Munjuri Formation in the Chungju area.

In this study, formation names are used as follows to avoid confusion. The carbonates which are developed between pebble-bearing phyllitic rocks and pelitic rocks and surmised by post-glaciogenic cap carbonate, are denominated as “Geumgang Limestone”. And the pebble-bearing phyllitic rocks are treated as a single formation, named “Hwanggangni Formation” based on the affinity with thin carbonate layer. In addition, it deems a diamictite.

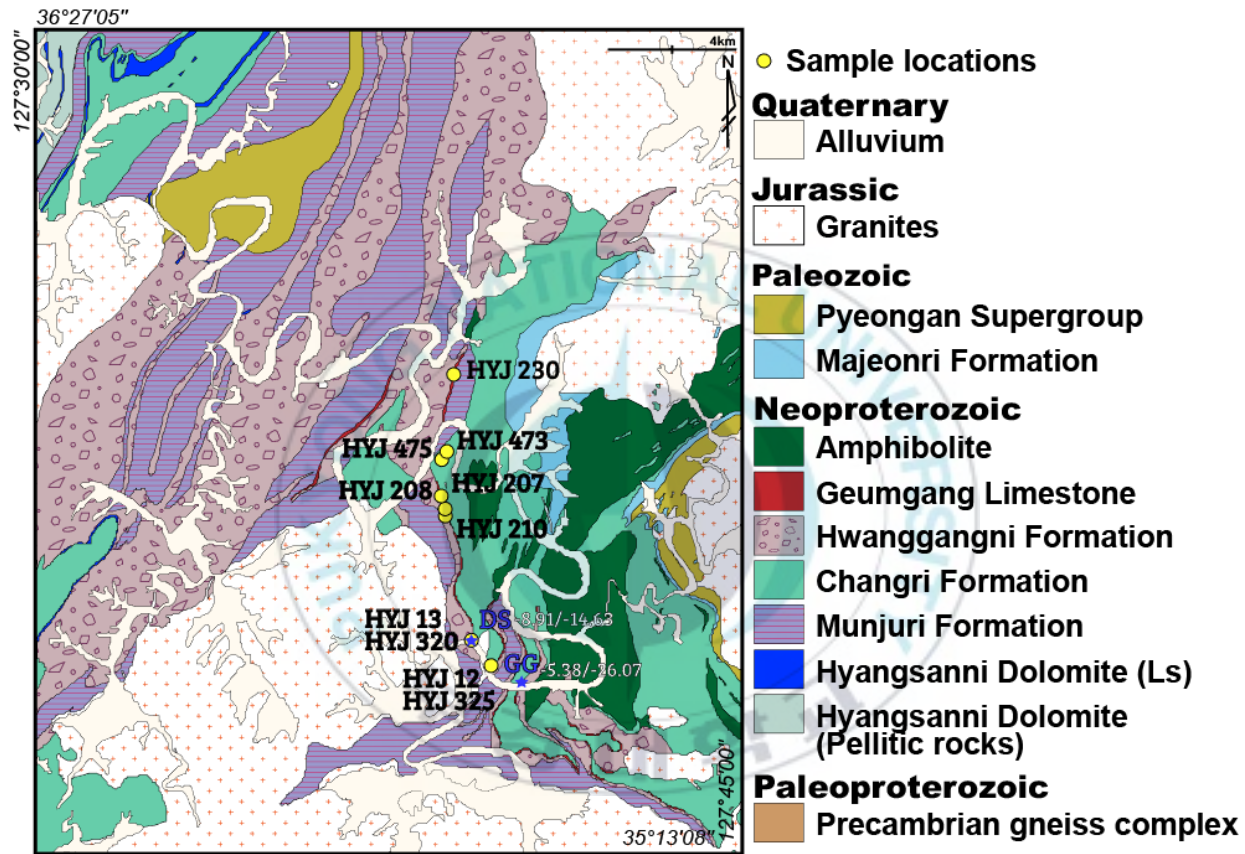


Figure 2-1. Geological map of the Okcheon-Boeun area, modified after Kim et al. (1978) and Kim et al. (1977). Sampling locations of the Geumgang Limestone are shown with outcrop numbers. Blue asterisks with data (DS and GG) are from the previous study (Ryu and Ahn, 2016).

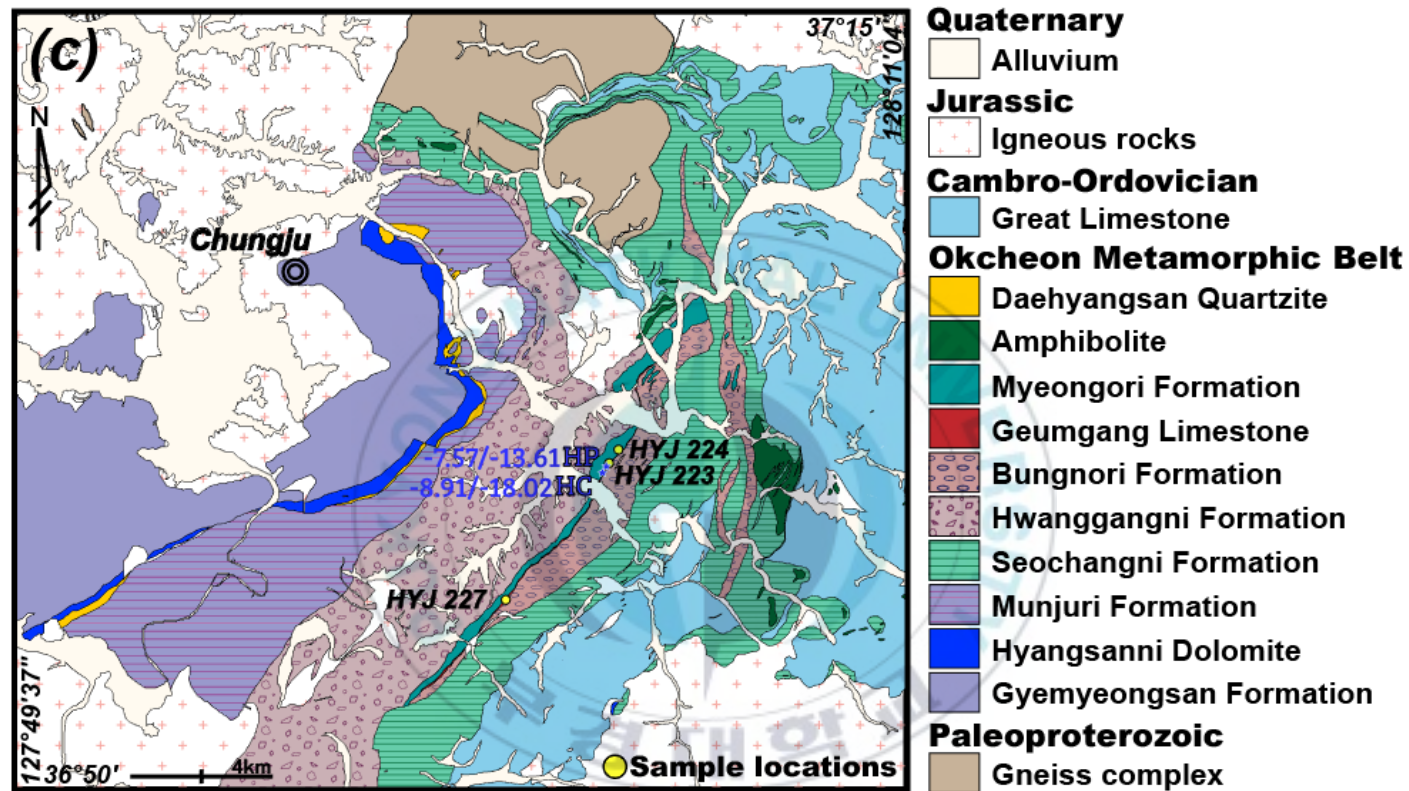


Figure 2-2. Geological map of the northeastern Okcheon metamorphic belt and the western Taebaeksan Basin modified after Kim et al., (1967), Lee et al., (1965), Geological Society of Korea (1962) and Won et al. (1967). Sampling locations of the Geumgang Limestone are shown along with outcrop numbers. Blue asterisks with data are from the previous study (Ryu and Ahn, 2016).

3. Materials and Methods

3.1 Material descriptions

The Geumgang Limestone samples were collected from the carbonates proposed as cap carbonates by Choi et al. (2012) and intercalated carbonates in between metasedimentary layers (Figure. 2-3 and Figure. 2-4). In the case of Geumgang Limestone samples, these are named differently on quadrangles. Their stratigraphic names, exposed quadrangles and GPS coordinates are summarized in Table 1.

Okcheon quadrangle:

HYJ 12 (HYJ 325), HYJ 13 (HYJ 320), HYJ 207, HYJ 208, and HYJ 210

Except for HYJ 210 sample, the others are Limestone, named Geumgang Limestone. These limestone samples were collected from the Okcheon area in the Okcheon quadrangle (Kim et al., 1978). Limestone occurs along with the contact between the phyllitic rocks, Changni Formation, and the pebble-bearing phyllitic rocks, Hwanggangni Formation. The Changni Formation is composed of dark grey to black slate to phyllite, and the Hwanggangni Formation has diverse pebbles and a dark-colored matrix. The site, especially collected HYJ 13 sample, is characterized by ‘Granite Boulder’ supposed to diamictite by Choi et al. (2012). HYJ 207 and HYJ 208 samples, that were collected from about 5km extended northwest of HYJ 13 outcrop. HYJ 210 is a limestone pebble of the Hwanggangni Formation.

Boeun quadrangle: HYJ 230, HYJ 473, and HYJ 475

The samples are pebbles of the Hwanggangni Formation collected from the

Okcheon area in the Boeun quadrangle (Kim et al., 1977). On Boeun quadrangle, limestone named the Hyangsanni Formation occurs boundary between the Hwanggangni Formation and Munjuri Formation whose constituent rock of the Munjuri Formation is various; metavolcanic rocks and metasedimentary rocks. However, we could not examine the limestone outcrop at fieldwork. HYJ 230 sample is a pebble of the Hwanggangni Formation and looks somewhat similar to HYJ 473 sample. HYJ 473 and HYJ 475 samples are also considered as limestone in direct contact with the Changni Formation, pelitic rocks.

Hwanggangni quadrangle: HYJ 223, HYJ 224, and HYJ 227

The limestone samples (HYJ 223 and HYJ 224) were collected from the Jecheon area in the Hwanggangni quadrangle (Lee and Park, 1965). It occurs with about 20m widths between the Myeongori Formation and Bugnori Formation. This limestone is named the Bugnori Formation even comprising white limestone. The Myeongori Formation consists of dark grey to black slate and phyllite. HYJ 227 sample was collected from about 5km extended southwest of HYJ 223 and HYJ 224 outcrops.

Table 2-1. Quadrangles and Stratigraphy names, with GPS coordinates for sampling localities of the Geumgang Limestone.

Sample #	Quadrangle	Stratigraphy name	GPS coordinate
HYJ 12		Geumgang Limestone	N36 17.063 E127 39.483
HYJ 325			N36 17.055 E127 39.490
HYJ 13		Geumgang Limestone	N36 17.496 E127 39.095
HYJ 320	Okcheon		N36 17.481 E127 39.096
HYJ 207		Geumgang Limestone	N36 19.887 E127 38.479
HYJ 208		Geumgang Limestone	N36 19.698 E127 38.556
HYJ 210		Hwanggangni Formation Limestone pebble	N36 19.621 E127 38.561
HYJ 230		Hwanggangni Formation Limestone pebble	N36 22.045 E127 38.790
HYJ 473	Boeun	Limestone intercalated in Changni Formation	N36 20.498 E127 38.439
HYJ 475		Limestone intercalated in Changni Formation	N36 20.486 E127 38.437
HYJ 223		Bugnori Formation Limestone	N36 56.372 E128 03.762
HYJ 224	Hwanggangni	Bugnori Formation Limestone	N36 56.444 E128 03.835
HYJ 227		Bugnori Formation	N36 53.884 E128 01.360



Figure 2-3. Outcrop photographs of the Geumgang Limestone at different study areas. The granitoid rock marked with dashed line in HYJ 320 was suspected to be a drop stone (Choi et al., 2012).



Figure 2-4. Photographs for cross-section of studied sample, Geumgang Limestone.

3.2 Analytical methods

In this study, the whole-rock samples were analyzed for element concentrations including Ba, Sr, Mn, Rb, Sm and REE and Sr isotope composition.

In the case of carbon and oxygen isotope compositions, some analyses were conducted at Niigata University, Japan, and some were requested to be analyzed by Beta Analytic Inc. The samples analyzed carbon and oxygen isotopes at Niigata University were also conducted trace element analysis at Niigata University. While those samples analyzed at Beta Analytic Inc were dealt with trace element analysis at KBSI.

The scratched powder samples (HYJ 12-1, HYJ 12-3, HYJ 13-1, HYJ 13-2, HYJ 13-7, HYJ 13-8) prepared using knife-edge from polished slabs were analyzed, only for C-O analysis at Niigata University. In the case of the other analysis, these were carried out using the same whole-rock samples.

$^{87}\text{Sr}/^{86}\text{Sr}$ ratio from TIMS is measured at KIGAM, while those from MC-ICP-MS are measured at KBSI.

4. Results and Interpretation

4.1 Carbon and oxygen isotope compositions

The results of the analysis were reported in conventional delta (δ) notation using the V-PDB standard for carbon and the V-PDB standard for oxygen and are presented in Table 2-2. As for data from Niigata University, the $\delta^{18}\text{O}$ -VPDB and $\delta^{18}\text{O}$ -VSMOW values were acquired simultaneously. While Beta analytical Inc gives only $\delta^{18}\text{O}$ -VPDB, thus I calculated the $\delta^{18}\text{O}$ -VPDB to $\delta^{18}\text{O}$ -VSMOW when compiling the graph.

The conversion equation $\delta^{18}\text{O}$ of the values of V-PDB to V-SMOW is:

$$\delta^{18}\text{O}_{\text{SMOW}} = \delta^{18}\text{O}_{\text{PDB}} * 1.03086 + 30.86$$

A total of 40 carbon and oxygen isotope compositions were measured for a total of 33 Geumgang Limestone samples.

The $\delta^{13}\text{C}$ (PDB) value ranges between -12.25 ‰ and -6.05 ‰ and the corresponding $\delta^{18}\text{O}$ (PDB) value varies from -30.45 ‰ to -11.8 ‰, as shown in Table 2-2 and Figure 2-5. The $\delta^{13}\text{C}$ values are more depleted to other typical cap carbonates worldwide, as low as -6‰ (Kaufman et al., 1997; Kennedy et al., 1998; Halverson et al., 2005; Jiang et al., 2007; Hohl et al., 2017).

Previous studies have shown that carbon and oxygen isotopic values have a negative association with the degree of metamorphism (Baker and Fallick, 1989a, b; Melezhik et al., 2001a, b, 2005). And the positive association of that can be an indicator for diagenetic overprint (Hohl et al., 2017 and references therein).

The relationship between $\delta^{13}\text{C}$ and $\delta^{18}\text{O}$ is not covariant and sporadically plotted in a binary diagram (Fig. 2-5), indicating that isotopic signals are little altered. However, the depleted $\delta^{18}\text{O}$ display an interesting interpretational problem.

The -10 ‰ of $\delta^{18}\text{O}$ value is used to be interpreted as criteria of unaltered value (Nogueira et al., 2003, 2007). Meanwhile, some researchers suggest a tolerant $\delta^{18}\text{O}$ threshold of 18‰ - 20‰ (Tang et al., 2013 and references therein; Aharon, 2005; Melezhik et al., 2005).

All samples from the Geumgang Limestone have distinctly lesser $\delta^{18}\text{O}$ than -10 ‰. These values conflict with interpretation for $\delta^{13}\text{C}$ versus the $\delta^{18}\text{O}$ binary diagram. In general, however, the $\delta^{13}\text{C}$ values are rather insensitive to geological processes such as metamorphism and diagenesis, while $\delta^{18}\text{O}$ values more sensitive thus can be over susceptible (Kaufman and Knoll, 1995; Jacobsen and Kaufman, 1999).

Diagenesis generally causes a negative $\delta^{13}\text{C}$ excursion instead of a positive $\delta^{13}\text{C}$ excursion in altered samples (Jiang, 2007). Compared with other cap carbonate successions previously published $\delta^{13}\text{C}$ records, the record from the Guemgang Limestone would be the most complete available record available in Korea.

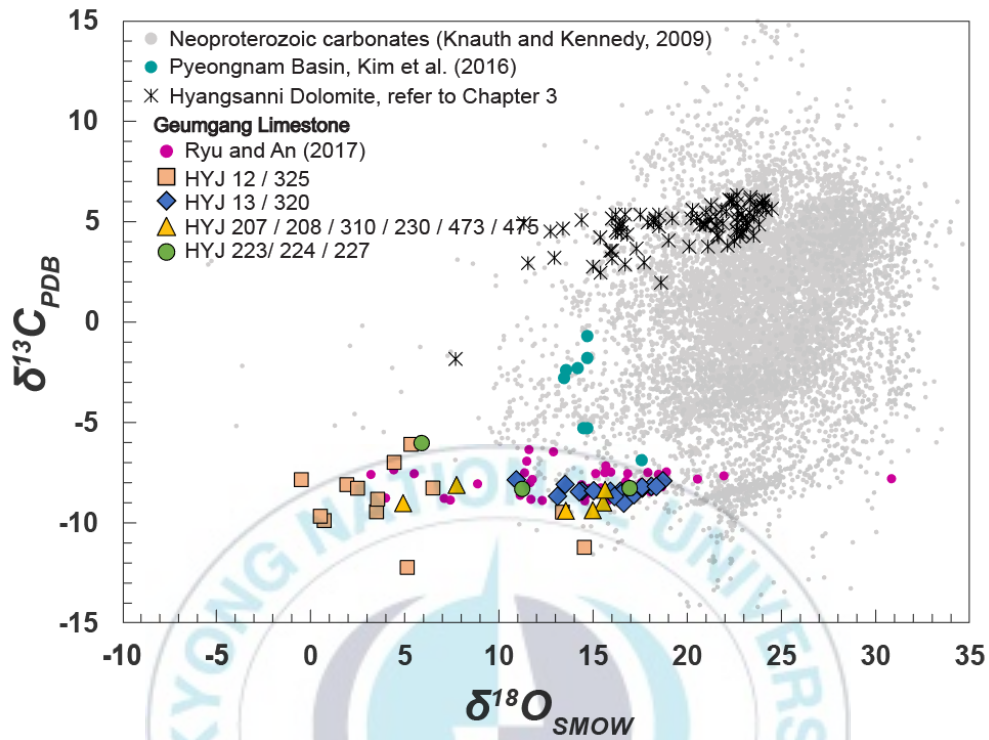


Figure 2-5. Cross-plots of the carbon and oxygen isotopic compositions of all Geumgang Limestone from the Okcheon Metamorphic Belt. Gray symbols are from Neoproterozoic carbonates (Knauth and Kennedy, 2009). Bluish greens are from the Pyeongnam Basin, North Korea (Kim et al., 2016). Asterisks are from carbonates from the Hyangsanni Dolomite, which are thought to be formed during Neoproterozoic Era (this study). The others are from Geumgang Limestone for this study. The units of data are per mil (‰).

Table 2-2. Data of carbon, oxygen, and Strontium isotopic composition were obtained from the Geumgang Limestone for this study.

Sample #	$\delta^{13}\text{C}$ (‰,PDB)	$\delta^{18}\text{O}$ (‰,PDB)	$\delta^{18}\text{O}$ (‰,SMOW)	Remark for C-O	$^{87}\text{Sr}/^{86}\text{Sr}$ (TIMS)	$^{87}\text{Sr}/^{86}\text{Sr}$ (MC- ICP-MS)
HYJ 12-1	-6.11	-24.79	6.57	NU	0.720767	
	-7.02	-25.66	5.68	NU		
HYJ 12-3-1	-9.50	-16.98	13.36	BETA		0.715484
HYJ 12-3-2	-8.13	-28.10	3.17	NU		0.717200
	-9.48	-26.57	3.47	BETA		
HYJ 12-5	-8.30	-27.55	2.46	BETA		0.717857
HYJ 12-6	-9.92	-29.27	0.69	BETA		0.727606
HYJ 325-L1	-12.25	-24.98	5.11	BETA		
HYJ 325-L2	-9.70	-29.47	0.48	BETA		
HYJ 325-L3	-11.25	-15.85	14.52	BETA		
HYJ 325-L4	-8.85	-26.51	3.53	BETA		
HYJ 325-L5	-7.88	-30.45	-0.53	BETA		
HYJ 325-L6	-8.29	-23.66	6.47	BETA		
HYJ 13-1	-8.45	-14.00	17.70	NU	0.712510	
	-8.60	-13.53	18.18	NU		
HYJ 13-2	-8.44	-15.96	14.41	BETA		0.713963
	-8.62	-13.29	18.43	NU		
HYJ 13-3	-8.48	-16.10	14.26	BETA		0.714029
	-8.45	-14.51	15.90	BETA		0.713582
HYJ 13-4	-7.93	-11.80	18.70	BETA		0.712289
HYJ 13-5	-8.21	-12.40	18.08	BETA		0.711760
HYJ 13-6	-8.30	-12.86	17.60	BETA		0.717355
HYJ 13-7	-8.58	-13.96	17.74	NU		
	-8.24	-12.87	17.59	BETA		0.712481
HYJ 13-8	-9.05	-13.81	17.89	NU		
	-8.42	-15.37	15.02	BETA		0.715580
HYJ 320-1	-7.88	-19.36	10.90	BETA		
HYJ 320-2	-8.11	-16.84	13.50	BETA		
HYJ 320-3	-8.21	-12.14	18.35	BETA		
HYJ 320-4	-8.71	-14.30	16.12	BETA		
HYJ 320-5	-8.70	-17.23	13.10	BETA		

Table 2-2. (Continued)

Sample #	$\delta^{13}\text{C}$ (‰,PDB)	$\delta^{18}\text{O}$ (‰,PDB)	$\delta^{18}\text{O}$ (‰,SMOW)	Remark for C-O	$^{87}\text{Sr}/^{86}\text{Sr}$ (TIMS)	$^{87}\text{Sr}/^{86}\text{Sr}$ (MC- ICP-MS)
HYJ 207	-8.14	-22.44	7.73	BETA		
HYJ 208	-9.01	-14.88	15.52	BETA		
HYJ 210	-9.40	-15.42	14.96	BETA		
HYJ 230	-9.05	-25.20	4.88	BETA		
HYJ 473	-9.42	-16.81	13.53	BETA		
HYJ 475	-8.38	-14.78	15.62	BETA		
HYJ 223	-8.34	-19.05	11.22	BETA		
HYJ 224	-8.30	-13.51	16.93	BETA		
HYJ 227	-6.05	-24.24	5.87	BETA		



4.2 Trace and rare earth element concentrations

The concentrations of trace and rare earth elements in the Geumgang Limestone are presented in Table 2-3 and 2-4.

For the rare earth elements data, anomalies were calculated as below:

$$(Ce/Ce^*)_N = 2 * Ce_N / (La_N + Pr_N) \quad : \quad \text{Bau and Dulski (1996)}$$

$$(Eu/Eu^*)_N = 2 * Eu_N / (Sm_N + Gd_N) \quad : \quad \text{Kamber and Webb (2001)}$$

$$(Pr/Pr^*)_N = 2 * Pr_N / (Ce_N + Nd_N) \quad : \quad \text{Bau and Dulski (1996)}$$

The concentration of each element was normalized to its concentration in Post-Archean Australian Shale (PAAS) (McLennan, 1989), as indicated by the subscript “N”.

Geumgang Limestone has variable REEs concentrations, from 4.68 to 234.56. These values lack consistency in even the same sample location.

The rare earth elements (REE) in carbonate rocks are easily contaminated by continental inputs because terrestrial silicate materials have commonly much higher REE contents than carbonate minerals. The terrestrial materials are the one of primary factors that affect REE compositions in carbonate rocks. Fortunately, Zr is an effectual proxy of the detrital input (Yang et al., 2019 and references therein)

Yttrium (Y) and Holmium (Ho) have similar ionic radii and charge; thus, these freely substitute for each other. Ho is removed apace than Y from seawater because they are different in surface complexation behavior (Bau et al., 1999; Filho et al., 2018).

The Y/Ho ratios in seawater are easily shifting (Yang et al., 2019) and it is also one of the useful parameters for estimating the purity of carbonates. Therefore, the fluctuations in the Y/Ho ratio seen in cap carbonates may reflect the main effects of different water masses (Meyer et al., 2012). Modern seawater has a substantially higher

Y/Ho ratio (44-77, Nozaki et al., 1997; 60–90, Lawrence et al., 2006a, 2006b) than the upper continental crust (~26; Kamber et al., 2005).

The Y/Ho ratios for Geumgang Limestone range from 22.4 to 38.8. Excepting 2 samples ($Y/Ho \leq 24$), others are mostly between modern seawater Y/Ho values (27-57, Hohl et al., 2017). However, the values are substantially lower than the range of typical modern seawater (>44), rather than very close to those of upper continental crust (27.5, Kamber et al., 2005; 25-28 chondritic value, Bolhar, 2007) and freshwater carbonates (Bolhar and Van kranedonk, 2007).

Y/Ho ratios in the cap carbonates are always lower than modern seawater values, which is interpreted to reflect dilution of the seawater signal by glacial meltwater influx during deglaciation (Lawrence and Kamber, 2006; Hohl et al., 2017).

Therefore, ignoring data with Y/Ho below 44 may limit the proper interpretation of mixing between seawater and glacial meltwater. All measured geochemical signatures are considerably ambiguous because it is not accordance with typical values from other cap carbonates.

We see no significant covariation between Zr versus Y/Ho and Zr versus total REE contents in the Geumgang Limestone (Figure. 2-6). These trends suggest limited detrital influences in our samples, Geumgang Limestone.

Marine carbonate REE+Y may represent the seawater conditions when it was deposited. And thus, the REE+Y of the marine carbonate could be used to track the redox state of seawater during cap carbonate depositions (Huang et al. 2009; Yang et al., 2019).

REE+Y patterns generally display flat patterns with no distinctive positive La anomaly, negative Ce anomaly and positive Y anomaly, and non or slight depleted LREE (Elderfield and Greaves, 1982). While the REE+Y pattern shows the notable Eu

anomaly in some samples as seen in Figure 2-7. Therefore, it is assumed that marine sediments with positive Eu anomalies usually evidence an effect derived by hydrothermal fluids (Ling et al., 2013).

REE abundances are controlled primarily by iron oxyhydroxide scavenging (Sherrell et al., 1999), and ancient iron formations associated with submarine hydrothermal activities often show positive Eu anomalies (Ling et al., 2013; Slack et al., 2007). On the other hand, in terms of genetic indicators, positive Eu anomalies in marine sediments are regarded as an influence of hydrothermal fluids (Derry and Jacobsen, 1990).

Although the Geumgang Limestone contains no iron formation, some samples (HYJ 12-6, HYJ 325-L2, HYJ 210, HYJ 230 and HYJ 227) have elevated iron contents (Fe(%) > 1) compared to the others.

The iron in samples associated with high Al and Ti contents (proxies for terrestrial input) could be derived from a chemical weathering pulse, comparative enrichment in Al and Ti are observed in these samples. Therefore, the positive Eu anomalies are generally interpreted to be of terrestrial input origin.

Considering Zr versus REE relationship, however, such interpretation for positive Eu anomaly is contradictory. The cap carbonates display either no or positive Eu anomalies, with values ranging from 0.95 to 2.43 (Hohl et al., 2017).

However, Eu concentration measurements by ICP-MS are affected by the problem of Ba interference, and inaccurate corrections can cause noticeable anomalies. Accordingly, the Eu anomalies must be careful in dealing with it (Jiang et al., 2007; Hohl et al., 2017).

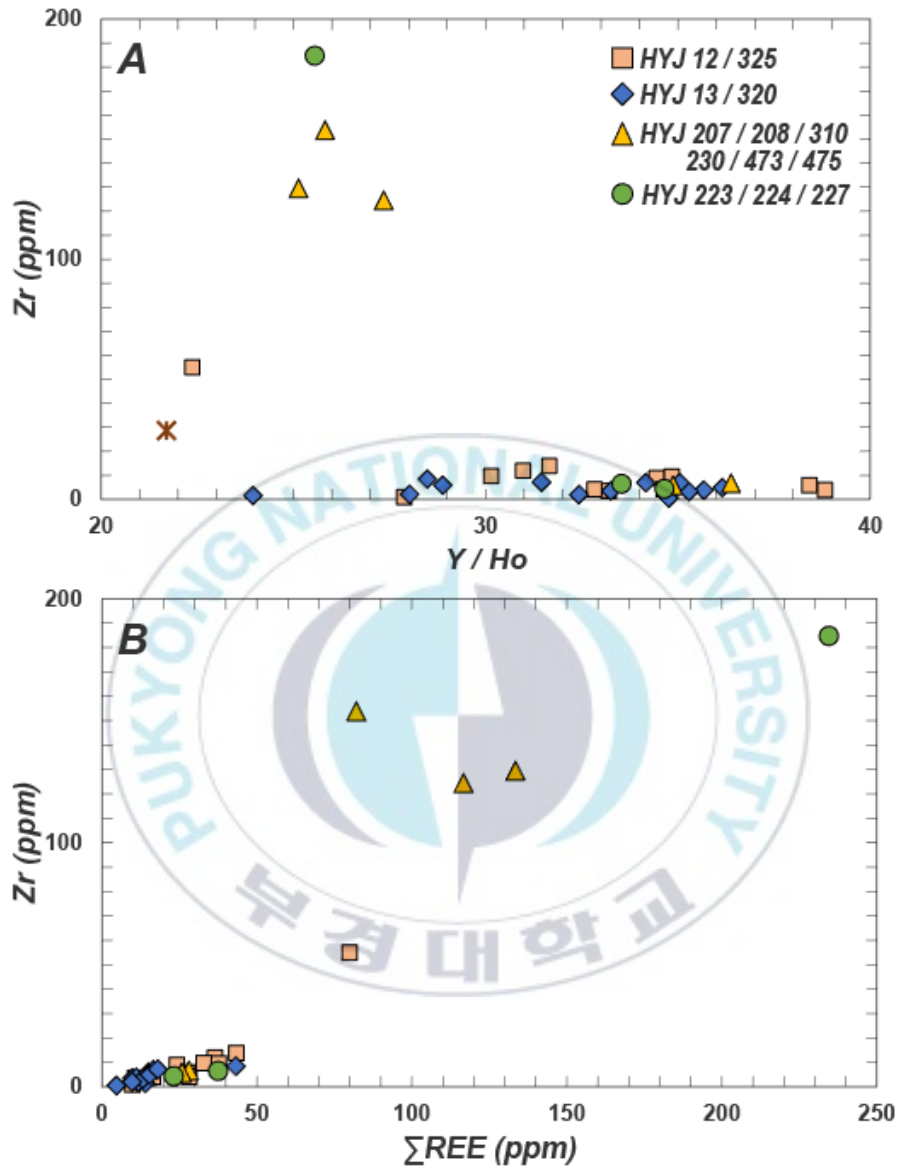


Figure 2-6. Correlation diagrams of Y/Ho versus Zr and Σ REE versus Zr of the Geumgang Limestone.

The apparent negative Eu anomaly may reflect a possible overcorrection of Eu because the sample is rich in Ba (ppm). We can see scattered but moderate positive covariation between Ba/Sm and Eu/Eu* ratio. It would imply the possibility which the positive Eu anomalies can be caused by Ba interference during ICP-MS measurement (Jiang et al., 2007) (Figure 2-8).

The Geumgang Limestone is characterized by moderately positive La anomalies, falling in the transition between freshwater carbonates and modern seawater in the diagram $(Ce/Ce^*)_N$ vs. $(Pr/Pr^*)_N$ (Figure 2-9, Bolhar and Vankrnedonk, 2007), and this is similar to the value of the Pocatello cap carbonates in Idaho, which was previously caused by the upwelling of seawater mixed with hydrothermal fluids (Meyer et al., 2012).

The variation in La from slightly negative anomalies to moderately positive anomalies seem to reflect the transition from freshwater to hydrothermally overprinted seawater.

Such an REE+Y pattern from the Geumgang Limestone is more similar to that of river/estuaries than typical seawater (Huang et al., 2009). It, hence, could be interpreted that it was meltwater dominated the depositional environment in shallow water during deglaciation since enormous meltwater crowded into the surface ocean after Snowball Earth (Huang et al., 2009).

Mn/Sr ratios are commonly used to assess the influence of diagenetic overprinting on carbonates rocks with Y/Ho, Fe/Sr and $\delta^{18}O$ values. High Mn contents together with $Mn/Sr > 2$ are generally considered as a parameter for diagenetic alteration of carbonates. On all occasions, geochemical parameters and their threshold values are empirical. In the same vein, a concurrence of Mn/Sr ratio as diagenetic alteration criteria also has not reached yet. (e.g., 1 to 3 (Kaufman et al., 1993; Brasier et al., 1996; Kennedy et al., 1998; Jacobsen and Kaufman, 1999) and 10 (Kaufman and Knoll,

1995)).

In this study, most samples in the Geumgang Limestone have a low Mn/Sr ratio (<1), ranging from 0.3 to 24.9; only 5 values over 2. To interpret liberally, our data is within unaltered range. The samples having an Mn/Sr ratio of more than 2 have the highest Σ REE (82-235 ppm).

With a low Mn/Sr ratio, below 50 of Fe/Sr value also indicates pristine seawater value (Fölling and Frimmel, 2002). Most of our data have much a lower 30 of Fe/Sr value, despite a few conspicuous high values (>100).

Unfortunately, it is not clear, based on available data from this study, whether our geochemical data from the Geumgang Limestones are primary or metamorphosed. But it seems to be fairly pristine, low Mn/Sr, Fe/Sr ratio and high Sr content (300 ppm) and weak correlation between two stable isotopes identified in the Geumgang Limestone reinforce this interpretation.

The Geochemical signals of continental input suggest that the Geumgang Limestone. As seen in Figures 2-10a and 2-10b, the Geumgang Limestone samples have relatively low Sr/Ba and Sr/Rb ratios. In both $(Ce/Ce^*)_N$ vs $(La/Yb)_N$ (Figure 2-10c) and $(Ce/Ce^*)_N$ vs $(Eu/Eu^*)_N$ (Figure 2-10d) diagrams, most of the Geumgang Limestone samples are plotted in the passive margins (Figure 2-10c) and inland plus margins (Figure 2-10d) field rather than the open ocean field. These tendencies indicate the influence of terrigenous materials. Generally, cap carbonate sequences have greatly been affected by glacial meltwater with terrigenous input originated by continental weathering along the continental margin (Yang et al., 2019). Therefore, we can interpret the depositional setting of the Geumgang Limestone as the those of the cap carbonate sequence. However, the uncertainties of our interpretations are somewhat high, therefore further in-depth and additional geochemical studies are required necessity to ensure data reliability.

4.3 Strontium isotope composition

The currently available $^{87}\text{Sr}/^{86}\text{Sr}$ ratios of most cap carbonate sequences are definitely high compared to generally recognized values of the Neoproterozoic seawater (e.g. Jacobsen & Kaufman 1999; Halverson et al. 2005; 2007; 2018). However, and Sr concentrations and radiogenic $^{87}\text{Sr}/^{86}\text{Sr}$ ratios vary according to region and time (Hohl et al., 2017).

Nonetheless, the $^{87}\text{Sr}/^{86}\text{Sr}$ ratio generally reflects the nature of lithologies without any fractionation by biological and physiochemical processes, its ratio has been used for tracing the age or origin of the rocks (Shin et al., 2018).

There are $^{87}\text{Sr}/^{86}\text{Sr}$ values only on HYJ 12 and HYJ 13. The Geumgang Limestone is characterized by relatively low Sr content, mostly lower than 350 ppm, and a high radiogenic $^{87}\text{Sr}/^{86}\text{Sr}$ ratio, over 0.7117 (Table 2-2). With these values, other geochemical parameters such as Ba/Sm, Fe/Sr, and Mn/Sr which assess post-depositional alteration of strontium isotopes indicate post-depositional alteration of the Geumgang Limestone. In addition, the large fluctuation between 0.71176 to 0.72076 from the Geumgang Limestone suggests the influence of the terrigenous inputs with freshwater while this carbonate sequence deposition (Sawaki et al., 2010; Guacaneme et al., 2017, Hohl et al., 2017).

Taken together, therefore, it seems to be a plausible inference that a weak correlation among $\delta^{18}\text{O}$, $^{87}\text{Sr}/^{86}\text{Sr}$ and $\delta^{13}\text{C}$ implies little diagenetic or metamorphic effects on Geumgang Limestone.

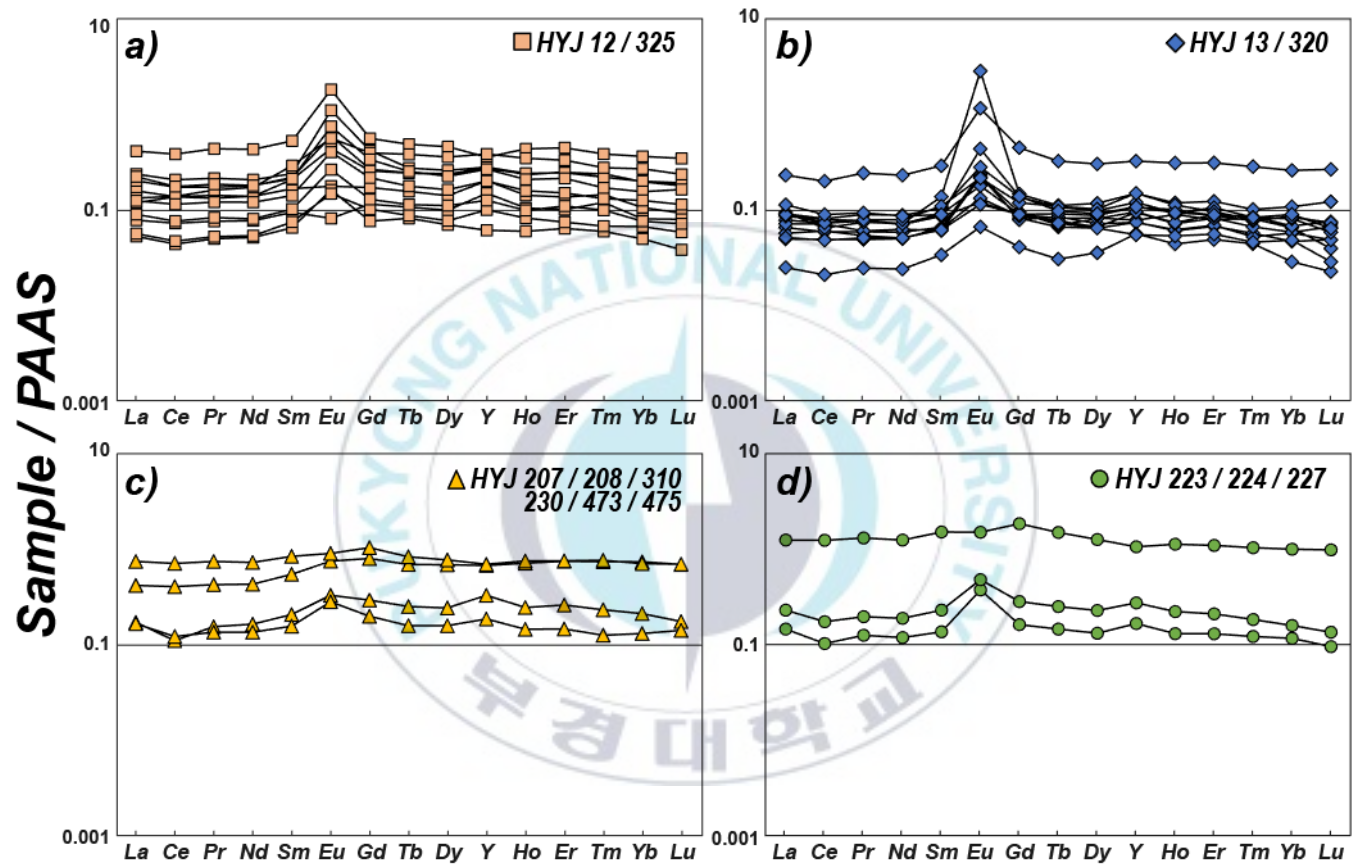


Figure 2-7. PAAS-normalized Rare Earth Element plus Yttrium of the Geumgang Limestone from the Okcheon Metamorphic Belt, PAAS data is from McLennan, (1989).

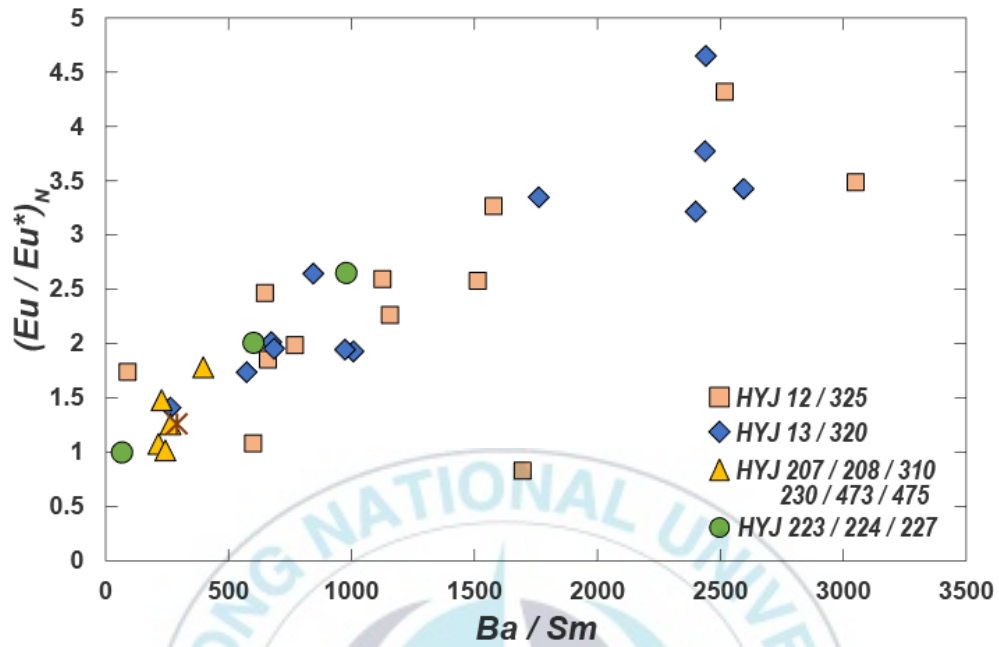


Figure 2-8. Covariations between $[Eu/Eu^*]_{PAAS}$ ratio and Ba/Sm ratio in the Geumgang Limestone.

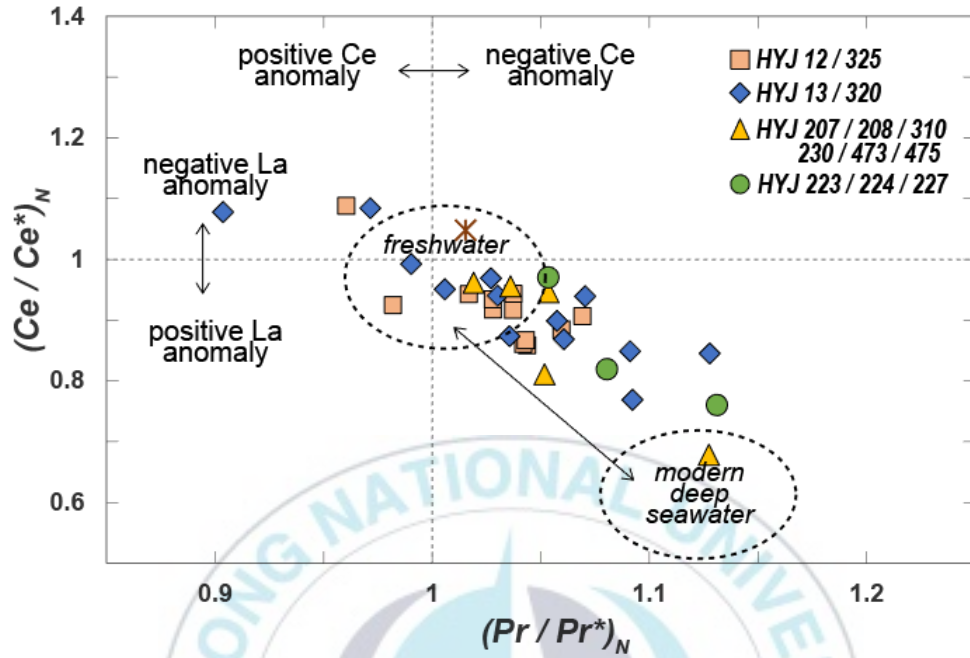


Figure 2-9. The plot of $(Pr/Pr^*)_N$ PAAS ratio versus $(Ce/Ce^*)_N$ PAAS ratio used to show La and Ce anomalies of the Geumgang Limestone (after Bau and Dulski, 1996) adapted from Yang et al. (2019).

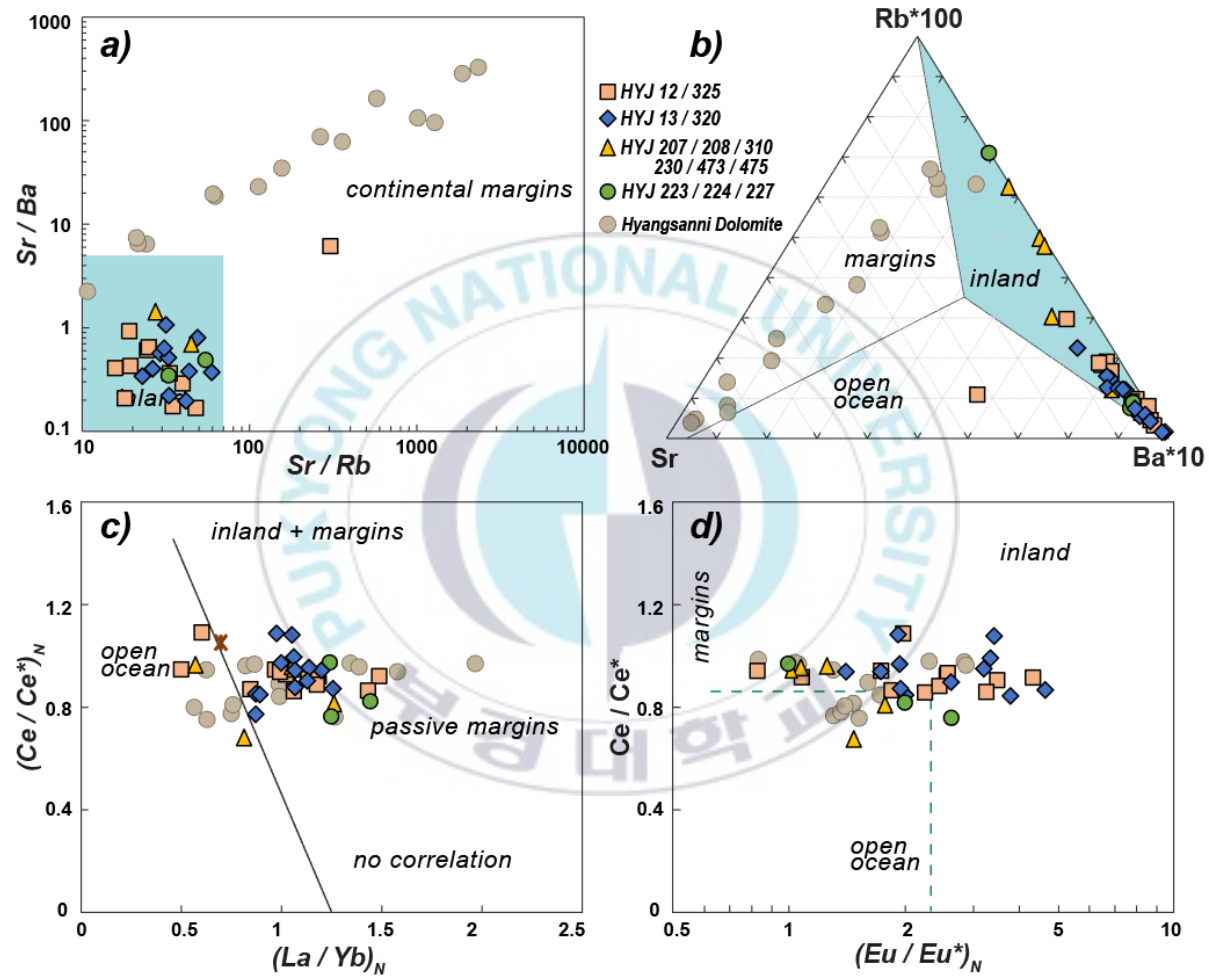


Figure 2-10. Geochemical discrimination diagrams to distinguish various depositional environments of the Geumgang Limestone. a) Sr/Ba vs. Sr/Rb, b) Rb–Sr–Ba triangular, c) $(Ce/Ce^*)_N$ vs. $(La/Yb)_N$ and d) $(Eu/Eu^*)_N$ vs. $(Ce/Ce^*)_N$ diagrams. Rare earth element abundances were normalized to PAAS (McLennan, 1989) and the Eu and Ce anomalies were calculated, following the equation proposed by Bau and Dulski (1996) and Kamber and Webb (2001), respectively. Samples with symbols are described in the figure, and Hyangsanni Dolomite data is from Ha et al., (2021).



Table 2-3. Trace element concentrations in ppm and strontium isotope compositions of the Geumgang Limestone.

Sample #	Al (%)	Ti (%)	Fe (%)	Zr	Mn	Rb	Sr	Ba	Sm	Ba /Sm	Fe /Sr	Mn /Sr	⁸⁷ Sr/ ⁸⁶ Sr (measured)	2σ	Remark
HYJ 12-1				5.9	219	13.53	332.3	576	0.96	600		0.7	0.720767	0.000016	NU
HYJ 12-3				3.9	189	6.39	255.5	933	0.55	1696		0.7			
HYJ 12-3-1	0.53	0.02	0.48	4.2	215	9.5	318.1	923	1.20	770	15.1	0.7	0.715484	0.000027	KBSI
HYJ 12-3-2	0.93	0.04	0.59	12.0	217	20.8	375.8	1907	1.26	1514	15.8	0.6	0.717200	0.000021	KBSI
HYJ 12-5	0.33	0.01	0.21	0.9	169	10.7	169.7	439	0.38	1156	12.3	1.0	0.717857	0.000017	KBSI
HYJ 12-6	3.35	0.23	1.96	55.0	223	79.0	263.7	9152	3.00	3051	74.4	0.8	0.727606	0.000026	KBSI
HYJ 325-L1	0.81	0.05	0.60	13.9	441	16.3	570.9	3450	1.37	2518	10.5	0.8			
HYJ 325-L2	0.91	0.04	3.06	9.7	1404	2.9	867.8	149	1.67	89	35.2	1.6			
HYJ 325-L3	0.42	0.03	0.39	9.6	257	6.4	306.2	1925	1.22	1578	12.6	0.8			
HYJ 325-L4	0.61	0.03	0.42	8.9	232	19.1	374.6	923	0.82	1126	11.1	0.6			
HYJ 325-L5	0.33	0.02	0.28	3.6	311	13.2	254.9	291	0.44	661	11.0	1.2			
HYJ 325-L6	0.23	0.01	0.31	4.2	178	9.3	234.3	382	0.59	648	13.1	0.8			
HYJ 13-1	0.29	0.01	0.27	3.5	124	5.3	233.5	652	0.37	1762	11.6	0.5	0.712510	0.000016	NU
HYJ 13-2	0.38	0.01	0.29	1.6	114	4.0	128.1	127	0.48	264	22.4	0.9	0.714029	0.000028	KBSI
HYJ 13-3	0.31	0.01	0.25	1.9	111	5.6	185.9	888	0.37	2400	13.2	0.6	0.713582	0.000026	KBSI
HYJ 13-4	0.13	0.01	0.15	0.5	81	2.3	68.6	128	0.19	674	22.1	1.2	0.712289	0.000028	KBSI

Table 2-3. (Continued)

Sample #	Al (%)	Ti (%)	Fe (%)	Zr	Mn	Rb	Sr	Ba	Sm	Ba /Sm	Fe /Sr	Mn /Sr	⁸⁷ Sr/ ⁸⁶ Sr (measured)	2σ	Remark for ⁸⁷ Sr/ ⁸⁶ Sr
HYJ 13-5	0.35	0.02	0.24	3.8	103	5.4	176.5	363	0.36	1008	13.7	0.6	0.711760	0.000017	KBSI
HYJ 13-6	0.41	0.02	0.22	3.3	88	12.4	285.0	882	0.34	2595	7.8	0.3	0.717355	0.000029	KBSI
HYJ 13-7	0.43	0.02	0.24	5.9	88	7.1	188.6	496	0.51	973	12.5	0.5	0.712481	0.000023	KBSI
HYJ 13-8	1.65	0.02	0.22	7.0	74	26.4	259.9	17125	0.77	22241	8.6	0.3	0.715580	0.000027	KBSI
HYJ 320-1	0.34	0.02	0.35	6.9	211	9.4	293.8	490	0.58	845	12.0	0.7			
HYJ 320-2	0.22	0.01	0.19	2.1	260	3.1	151.8	201	0.35	573	12.8	1.7			
HYJ 320-3	0.27	0.01	0.26	4.9	133	2.5	147.3	418	0.61	685	17.8	0.9			
HYJ 320-4	0.35	0.02	0.31	7.2	120	5.4	227.0	1221	0.50	2441	13.4	0.5			
HYJ 320-5	0.47	0.03	0.54	8.4	156	5.9	304.5	3900	1.60	2438	17.7	0.5			
HYJ 207	0.26	0.02	0.42	6.7	178	12.7	351.7	260	1.14	228	12.0	0.5			
HYJ 208	0.24	0.02	0.23	5.9	142	5.0	225.6	342	0.86	397	10.1	0.6			
HYJ 210	6.17	0.44	3.95	153.8	4374	132.9	175.9	786	2.98	264	224.8	24.9			
HYJ 230	5.35	0.37	4.03	129.5	559	98.1	193.1	977	4.56	214	208.9	2.9			
HYJ 223	0.46	0.02	0.35	4.4	249	6.4	352.7	764	0.78	979	9.9	0.7			
HYJ 224	0.26	0.02	0.25	6.5	190	7.8	258.3	789	1.31	602	9.8	0.7			
HYJ 227	6.50	0.55	4.29	184.7	611	137.8	97.7	560	8.42	67	439.4	6.3			

Table 2-4. Rare earth element and Yttrium concentrations and PAAS-normalized REE parameters calculated for the Geumgang Limestone. The data are presented in parts per million (ppm).

Sample #	Y	La	Ce	Pr	Nd	Sm	Eu	Gd	Tb	Dy	Ho	Er	Tm	Yb	Lu	ΣREE	(Ce/ Ce*) _N	(Pr/ Pr*) _N	(Eu/ Eu*) _N	Y /Ho
HYJ 12-1	5.64	6.28	11.40	1.31	4.89	0.96	0.198	0.83	0.13	0.69	0.147	0.40	0.061	0.31	0.042	27.65	0.92	1.03	1.08	38.4
HYJ 12-3	4.20	3.12	6.06	0.70	2.74	0.55	0.092	0.56	0.09	0.49	0.108	0.30	0.050	0.24	0.036	15.12	0.94	1.02	0.83	38.8
HYJ 12-3-1	7.85	4.74	11.35	1.22	4.91	1.20	0.488	1.23	0.19	1.14	0.239	0.74	0.092	0.58	0.083	28.20	1.09	0.96	1.99	32.8
HYJ 12-3-2	7.54	7.98	14.29	1.58	6.30	1.26	0.655	1.28	0.20	1.16	0.243	0.73	0.100	0.58	0.080	36.44	0.92	0.98	2.58	31.0
HYJ 12-5	1.74	2.12	3.69	0.46	1.84	0.38	0.181	0.37	0.07	0.34	0.062	0.19	0.025	0.15	0.017	9.90	0.86	1.04	2.26	27.9
HYJ 12-6	9.90	16.17	31.43	3.95	15.00	3.00	1.981	2.67	0.39	2.20	0.442	1.31	0.160	1.05	0.154	79.91	0.91	1.07	3.49	22.4
HYJ 325-L1	7.81	9.35	17.04	1.96	7.26	1.37	1.211	2.00	0.22	1.26	0.247	0.72	0.092	0.58	0.086	43.40	0.92	1.04	4.32	31.7
HYJ 325-L2	10.68	5.29	11.49	1.48	6.05	1.67	0.622	1.89	0.30	1.72	0.354	0.97	0.116	0.78	0.105	32.86	0.94	1.04	1.74	30.1
HYJ 325-L3	7.44	8.82	14.50	1.70	6.34	1.22	0.823	1.61	0.20	1.09	0.213	0.63	0.072	0.45	0.074	37.74	0.86	1.04	3.27	34.8
HYJ 325-L4	5.62	4.95	9.50	1.11	4.25	0.82	0.447	1.04	0.14	0.79	0.163	0.45	0.055	0.37	0.051	24.14	0.93	1.03	2.60	34.4
HYJ 325-L5	2.83	2.26	3.95	0.49	1.91	0.44	0.166	0.49	0.07	0.38	0.085	0.22	0.029	0.20	0.027	10.72	0.87	1.04	1.85	33.2
HYJ 325-L6	3.54	3.58	6.36	0.77	2.86	0.59	0.295	0.62	0.09	0.54	0.102	0.33	0.042	0.22	0.033	16.45	0.88	1.06	2.47	34.6
HYJ 13-1	2.02	1.93	3.95	0.44	1.72	0.37	0.240	0.39	0.05	0.30	0.061	0.19	0.023	0.13	0.021	9.81	0.99	0.99	3.35	33.3
HYJ 13-2	2.13	3.01	5.84	0.68	2.41	0.48	0.130	0.42	0.06	0.39	0.089	0.23	0.033	0.19	0.017	13.99	0.94	1.07	1.41	24.0
HYJ 13-3	2.02	2.52	4.75	0.53	2.00	0.37	0.253	0.37	0.07	0.34	0.062	0.20	0.021	0.16	0.021	11.67	0.95	1.01	3.22	32.4
HYJ 13-4	1.54	0.97	1.71	0.22	0.83	0.19	0.073	0.19	0.02	0.17	0.044	0.14	0.018	0.08	0.010	4.68	0.85	1.09	2.02	34.8

Table 2-4. (Continued)

Sample #	Y	La	Ce	Pr	Nd	Sm	Eu	Gd	Tb	Dy	Ho	Er	Tm	Yb	Lu	ΣREE	(Ce/ Ce*) _N	(Pr/ Pr*) _N	(Eu/ Eu*) _N	Y /Ho
HYJ 13-5	2.56	2.20	4.84	0.48	1.74	0.36	0.144	0.41	0.06	0.31	0.072	0.23	0.027	0.17	0.029	11.07	1.08	0.97	1.93	35.7
HYJ 13-6	2.59	2.76	5.71	0.54	2.14	0.34	0.238	0.45	0.05	0.38	0.074	0.26	0.035	0.19	0.033	13.20	1.08	0.90	3.42	35.3
HYJ 13-7	2.90	3.30	6.35	0.69	2.45	0.51	0.192	0.42	0.07	0.41	0.100	0.25	0.031	0.24	0.031	15.06	0.97	1.03	1.95	28.9
HYJ 13-8	4.02	3.61	5.19	0.66	2.45	0.77	2.962	0.69	0.09	0.55	0.118	0.35	0.041	0.31	0.053	17.83	0.77	1.09	21.25	34.2
HYJ 320-1	3.25	3.50	6.50	0.80	3.01	0.58	0.301	0.64	0.08	0.46	0.093	0.30	0.034	0.23	0.026	16.56	0.90	1.06	2.65	35.0
HYJ 320-2	1.50	1.99	3.88	0.46	1.75	0.35	0.124	0.42	0.06	0.30	0.054	0.16	0.019	0.14	0.013	9.72	0.94	1.03	1.74	28.0
HYJ 320-3	4.04	3.42	5.88	0.70	2.70	0.61	0.232	0.56	0.08	0.48	0.112	0.28	0.032	0.24	0.032	15.35	0.87	1.04	1.95	36.2
HYJ 320-4	2.92	4.34	7.16	0.83	2.94	0.50	0.466	0.65	0.08	0.43	0.093	0.25	0.034	0.25	0.028	18.05	0.87	1.06	4.65	31.5
HYJ 320-5	8.68	8.79	15.87	2.14	7.78	1.60	1.220	2.06	0.25	1.41	0.305	0.88	0.114	0.73	0.114	43.25	0.85	1.13	3.77	28.5
HYJ 207	8.77	6.52	8.77	1.36	5.53	1.14	0.351	1.35	0.19	1.12	0.241	0.73	0.093	0.59	0.075	28.08	0.68	1.13	1.48	36.4
HYJ 208	5.00	6.31	9.68	1.19	4.57	0.86	0.301	0.92	0.12	0.74	0.143	0.42	0.051	0.37	0.061	25.74	0.81	1.05	1.78	34.9
HYJ 210	17.87	15.73	31.80	3.70	14.35	2.98	0.793	3.64	0.52	3.15	0.692	2.09	0.294	2.04	0.294	82.06	0.96	1.02	1.26	25.8
HYJ 230	18.38	27.78	55.34	6.43	24.08	4.56	0.953	4.71	0.63	3.53	0.731	2.11	0.303	1.95	0.295	133.40	0.96	1.04	1.08	25.1
HYJ 223	4.62	5.74	8.46	1.14	4.16	0.78	0.412	0.78	0.12	0.64	0.133	0.38	0.051	0.34	0.043	23.17	0.76	1.13	2.65	34.6
HYJ 224	7.57	9.01	14.25	1.78	6.57	1.31	0.526	1.35	0.20	1.09	0.226	0.62	0.076	0.46	0.060	37.52	0.82	1.08	2.01	33.5
HYJ 227	28.75	47.74	99.04	11.61	42.45	8.42	1.629	8.61	1.16	5.93	1.125	3.14	0.423	2.84	0.429	234.56	0.97	1.05	1.00	25.6

5. Discussion

Most of the metasedimentary rocks of the Okcheon Metamorphic Belt are still unclear about their sedimentation times. In some of these, Paleozoic sedimentation seems to be apparent, with the discovery of Carboniferous and Permian fossils and the identification of Devonian to Carboniferous detrital zircons.

The Okcheon Metamorphic Belt is distributed in a long band in the northeast-southwest direction from the vicinity of Chungju in the northeast to the Ganggyeong in the southwest.

Based on the U-Pb age distribution pattern of the detrital zircons, Cho et al. (2013) divide it into northwest and southeast bands and refer to them as SCC-like and NCC-like, respectively. Paleozoic sedimentary rocks of the Okcheon Metamorphic Belt are distributed in the northwestern band of the Okcheon Metamorphic Belt, which Cho et al. (2013) have identified as SCC-like. However, no Phanerozoic detrital zircons have been found in the metasedimentary rocks in the NCC-like band of Cho et al. (2013). The youngest detrital zircon U-Pb age in these NCC-like bands is approximately 750 Ma, limiting the maximum sedimentation age.

Amphibolites of about 750 Ma in the Boeun and Okcheon areas intruded only the Changni Formation among several metasedimentary formations of the Okcheon Metamorphic Belt. Thus, Changni Formation was deposited earlier than about 750 Ma, and may be older than other metasedimentary formations of the Okcheon Metamorphic Belt in the region.

In the vicinity of Chungju, amphibolite intruded only the Seochangni Formation. There is no precise dating of amphibolites near Chungju, but if the amphibolites are the

same age as in the Boeun-Okcheon area, Seochangni Formation is also a sedimentary rock before about 750 Ma.

Most carbonate rocks distributed between the Seochangni Formation and Geumsusan Quartzite were classified as Samtaesan and Heungwolri formations. However, the carbon isotope values reported in the carbonate rocks of the Samtaesan Formation in the region are consistently higher ($>4\text{‰}$) than those of the Cambro-Ordovician ($<1.5\text{‰}$), and it is more appropriate to interpret them as Neoproterozoic rocks rather than constituent rocks of the Joseon Supergroup.

Taken together, the evidence suggests that most of the metasedimentary rocks of the Okcheon Metamorphic Belt near Chungju were produced in Neoproterozoic.

The study has been executed for the area where the cap carbonates are exposed, part of northwestern the Okcheon Metamorphic Belt in central Korea (Fig. 2-1 and 2-2). The thin layer carbonates deeming post-glacial cap carbonates are locally recognized. And it has a thickness of about 10 meters and extends from the Chungju to Boeun-Okcheon area. It is uncommonly intercalated between the pebble bearing phyllitic and phyllitic metasedimentary rocks.

5.1 Evidence from Carbon isotopes for post glacial deposits: Geumgang Limestone

As previously stated, the carbon isotope ratios analyzed in the Geumgang Limestone are consistently low, similar to post-glacial successions, and are unlikely to

be lowered by other causes. The Geumgang Limestone has minimum value of -12.25, it is indeed lower than general cap carbonates (as low as -6‰, Kaufman et al., 1997; Kennedy et al., 1998; Halverson et al., 2005; Jiang et al., 2007; Hohl et al., 2017).

The cause of the $\delta^{13}\text{C}$ noticeable negative excursion, down to -12‰, is still a matter of debate. Nonetheless, the most reasonable interpretation of such distinctively negative $\delta^{13}\text{C}$ is cap carbonates.

For such a peculiar low value, we merit consideration as follows:

(1) The negative excursion is supposed to be corresponding to the Shuram negative excursion. Which is reaching -12‰ and also enigmatic features of Ediacaran $\delta^{13}\text{C}$ chemostratigraphy (Riccomini et al., 2007; Grotzinger et al., 2011). If the Geumgang Limestone carbon isotopes are equivalent of the Shuram excursion, the age of Geumgang Limestone has been limited to middle Ediacaran at ~551 Ma (Zhou et al., 2017 and referenced therein).

(2) The carbon isotope is thought to be depleted by metamorphism. If the metamorphic temperature is higher than 650°C, it would decrease the $\delta^{13}\text{C}$ values by 3‰ (Wada and Suzuki, 1983) even $\delta^{13}\text{C}$ values can be relatively immune to metamorphism and diagenetic alteration. (Higgins et al., 2018; Hood et al., 2018).

The Okcheon Metamorphic Belt generally underwent greenschist to amphibolite facies metamorphism, as well as extensive hydrothermal alteration, which must have caused a great decrease in $\delta^{18}\text{O}$. The isotope signatures of the Geumgang Limestone seem to undergo metamorphic and diagenetic overprints. Since the grade of metamorphism of the Okcheon Metamorphic Belt is only up to greenschist or amphibolite facies, the extent of $\delta^{18}\text{O}$ depletion in the Geumgang Limestone thus

cannot be interpreted by solely considering metamorphic-diagenetic alteration, and the impact of hydrothermal alteration must also be taken into account.

The site, especially collected HYJ 13 and HYJ 320 samples, had been characterized by the occurrence of 'glaciogenic dropstone' (Lee et al., 1998; Choi et al., 2012). It was evident that the Geumgang Limestone preserved glacial events during Neoproterozoic.

However, it has been recently turned out to be a part of the 'Jurassic Granite Boulder' (Cheong et al., 2016). This precludes any further discussion for evidence of diamictite, and also makes it difficult to interpret the depositional setting of the Hwanggangni formation and peripheral formations.

Analysis of $\delta^{13}\text{C}$ and $\delta^{18}\text{O}$ for the Geumgang Limestone overlying the Hwanggangni Formation being propounded to be diamictite reveal negative $\delta^{13}\text{C}$ excursions approximate the cap carbonates elsewhere.

5.2 The stratigraphic implications for the occurrence of Neoproterozoic glaciogenic sedimentary successions in Okcheon Metamorphic Belt

Neoproterozoic sediments have not been seen in the southern part of the Korean Peninsula. However, recent reported U-Pb zircon age data from metasedimentary rocks, plutonic rocks, and metavolcanic rocks from the central Korean Peninsula, establishes the scattered distribution of Neoproterozoic sediments there.

The Hwanggangni Formation and Geumgang Limestone have been considered as

diamictite-cap carbonate couplets, nonetheless these formations have been insufficiently studied.

Multiple Neoproterozoic glaciation events are well known by extensive research since Kirschvink (1992) proposed the ‘Snowball Earth hypotheses (e.g., Fairchild and Kennedy, 2007). Thus, the occurrence of glaciogenic sedimentary successions in the Okcheon Metamorphic Belt may lay the foundation of perceiving age-unknown strata in the Okcheon Metamorphic Belt as Neoproterozoic. In other words, age-unknown strata in the Okcheon Metamorphic Belt can be limited age to an equivalent Neoproterozoic glaciation event.

Notwithstanding Geumgang Limestone is atypical for preserving classic glacial signatures, the interpretation of the Geumgang Limestone as Neoproterozoic post-glacial cap carbonates is consistent with other evidence indicating that other metasedimentary rocks of the Okcheon Metamorphic Belt are Neoproterozoic.

Similar glacial carbon isotopic signatures are witnessed in North Korea, the middle Korean Peninsula, which suggests that the connection to Neoproterozoic glaciation is not fortuitous in Korean Peninsula.

In Yongtan Group of Pyeongnam Basin in North Korea, Gaskiers glaciations related glaciogenic sequence was reported (Kim et al., 2016). The Yongtan Group is made up of the Pirangdong Formation and Rungri Formation from bottom up and is considered as tillite and cap carbonates, respectively based on carbon isotope composition. It also suggests that Okcheon Metamorphic Belt may correlate to Neoproterozoic strata in the Pyeongnam Basin, North Korea.

Because this region has suffered intermediate pressure type regional

metamorphism and ductile deformation, it used to have much poor knowledge than Taebaeksan Basin for Paleozoic strata. Recent several studies for central to the southwestern part of the Okcheon Metamorphic Belt have identified the existence of upper Paleozoic strata throughout that region (Lim et al., 2005,2006,2007; Kim et al., 2016; Kim et al., 2018).

Furthermore, it suggests that the Okcheon Metamorphic Belt and Taebaeksan Basin may be one sedimentary basin with continuous sedimentary sequence from Neoproterozoic to Early Paleozoic correlated to the Pyeongnam Basin in North Korea. Such interpretation contrast with the conventional perspective that geotectonically correlates southwestern Okcheon Metamorphic Belt with South China Craton.

In this case, the South Korean Tectonic Line (SKTL), which is set to pass between the Okcheon Metamorphic Belt and Taebaeksan Basin, may pass between the NCC-like and SCC-like bands that divide the Okcheon Metamorphic Belt, or may be located further west. It is not possible to rule out the possibility that the eastern extension of China's Early Triassic continental collision belt did not pass through the Korean peninsula.

5.3 Hwanggangni and Bugnori Formations

5.3.1 Identicalness of Geumgang Limestone distributed in the Okcheon Metamorphic Belt

In geological maps of the Boeun-Okcheon region, Boeun (Kim et al., 1978) and Okcheon (Kim et al., 1978) quadrangles, the pebble-bearing phyllitic layers and the

adjacent phyllitic layers were named the Hwanggangni Formation and Changni Formation, respectively. Hwanggangni Formation is named after sediments with similar lithologies in Chungju.

In order to unify the formation names in the Boeun-Okcheon area with those in the Chungju area, in this study, the pebble bearing phyllitic layer bordering this layer is called the Bugnori Formation and the phyllitic metasedimentary layer of the Myeongori Formation.

If the Geumgang Limestone in the Chungju and Boeun-Okcheon areas are the same cap carbonate layer, the Hwanggangni Formation and Changni Formation in Boeun-Okcheon area are distributed on both sides should be correlated to Bugnori Formation and Myeongori Formation in Chungju area, respectively. However, it is necessary to verify whether they are the same sedimentary formation with the same depositional period as the Hwanggangni Formation in the Chungju area. Currently, it cannot be ruled out that some or all of these may be layers correlated with the Bugnori Formation rather than the Hwanggangni Formation.

It is important to know when Hwanggangni Formation, a tillite deposit in the vicinity, is formed to determine whether the Geumgang Limestone is a post-glacial cover carbonate of Neoproterozoic. Some studies suggest Hwanggangni Formation as Paleozoic, but it is not based on solid evidence. Recently, U-Pb zircon age determination attempts have been made for various metasedimentary formations of the Okcheon Metamorphic Belt (Cho et al., 2013). A couple of studies reported that granite pebbles in the Hwanggangni Formation had an age of about 400 million years.

Ryu and Ahn (2016) interpreted that some of the analyzes had quite high carbon isotope values due to hydrothermal alteration. Rather, however, it seems more

reasonable to interpret them as different layers of different origin, since these values are distinct from cap carbonates and carbonate rocks of other origins with similar values exist around them. For example, the Hyangsanni Dolomite and the limestones of the Seochangni Formation have carbon isotope values of around +4 and appear to be deposited in the Neoproterozoic glacial period.

Some of the carbonate rock samples (GS and HS) reported by Ryu and Ahn (2016) show relatively higher carbon isotope values than characteristic post-glacial cap carbonates. The reason is that they may have been altered to have different values from the original, or they may not have been cap carbonates from the start.

The two samples with high carbon isotope values of Ryu and Ahn (2017) also have different characteristics that distinguish them from other Geumgang Limestones. These samples are distinguished from other Geumgang Limestones with low MgO values by having a high MgO content of up to about 20%.

One of the two samples above was taken from the carbonate rock layer that exists inside the Myeongori Formation, not the boundary between the Myeongori Formation and Bugnori Formation, and whose extension is not traced far. The other is from carbonate rocks that appear between the Hwaggangni Formation and Munjuri Formation in the Goesan Region but do not extend far. Therefore, it is not appropriate to include them in the Geumgang Limestone, which extends to very long distances along the boundary between the Bugnori Formation and Myeongori Formation.

5.3.2 Further stratigraphic implications

In the Hwaggangni geological map, a thin but continuous limestone layer is

developed between the Bugnori Formation and Myeongori Formation.

Some later geologic maps in the south also show similar limestone layers between the pebble-bearing phyllitic bed and the phyllitic bed.

This limestone layer was named the Geumgang Limestone in the Okcheon quadrangle (Kim et al., 1978), and most agree to apply this name similarly to limestone in other areas of the Okcheon Metamorphic Belt that appear between the pebble-bearing phyllitic bed and the phyllitic bed.

However, the pebble-bearing phyllitic bed and phyllitic bed, which are divided by the Geumgang Limestone, are confusingly named differently according to quadrangles. The possibility that these two formations are separate glacial deposits cannot be excluded. The contentious definition of the Hwanggangni Formation whether it is diamictite or not makes it tough to interpret the tectonic evolution of the Okcheon Metamorphic Belt.

The sedimentary formation, named Changni Formation, is distributed only in the Boeun-Okcheon area and, like Myeongori Formation, consists mainly of black slate or phyllite.

Diamictite layers distributed over a large area of the Okcheon Metamorphic Belt often have relatively narrow white limestone layers with a width of several meters to several tens of meters at the boundary of the layer. These diamictite deposits are often in contact with pelitic metasedimentary rocks on both sides, but no limestone layer appears at both boundaries.

If the limestone layer is post-glacial cover carbonates, it should of course be placed stratigraphically above the glacial deposit diamictite. Conversely, the pelitic

metasedimentary layer in contact with the diamictite deposits in the absence of the development of the limestone layer is stratigraphically the lower layer.

However, the existence of glaciogenic deposits or not is a debatable issue-because glacial features such as dropstones, striated clasts, tepee-like structures and etc are lacking. Nevertheless, there is imperative to consider the particular characteristics of the Okcheon Metamorphic Belt which has undergone greenschist – amphibolite facies metamorphism. Because the glacial features might be overprinted or misidentified with structures caused by deformation and metamorphic reaction (e.g. confusion striations with slickenlines, Monhanty et al., 2015).

The pebble-bearing pelitic metasedimentary rocks distributed in the Okcheon Metamorphic Belt are named with three different formation names: Hwanggangni, Bugnori, and Iwonni formations. It is uncertain, however, whether these layers are all the same diamictite deposits produced by the glaciation of the same age.

Among the diamictite layers distributed in the Chungju area, the limestone layer developed in contact with the Bugnori Formation, but not in the Hwanggangni Formation. If the strata are not overturned, the Hwanggangni Formation in Chungju, stratigraphically higher than the cap carbonates, is interpreted as a separate glacial deposit after the Bugnori Formation. Thus, the possibility that these two layers are glacial deposits at different times cannot be ruled out. This means that these different layers do not represent discrete glaciations.

In the Miwon-Yongyuri region, limestone layers are developed adjacent to Iwonni Formation, but not in the case of the Hwanggangni Formation. Iwonni Formation can correlate to the Bugnori Formation if these limestone layers are the same post-glacial cover carbonates in Chungju. And matrixes of these two formations are psammitic

while those of the Hwanggangni Formations are pelitic matrix.

In the Boeun and Okcheon geological maps, all of the pebble-bearing pelitic deposits are named the Hwanggangni Formation, some of which have a limestone layer developed at the boundary, and others do not. In this area, it would be better to distinguish between the diamictites with a limestone layer at the boundary and diamictites without by different names.

For consistency of naming, I suggest that the diamictite deposit with the limestone layer developed at the boundary is called the Bugnori Formation, otherwise it is called the Hwanggangni Formation.

About a decade ago, a series of studies (Lim et al., 2005, 2006, 2007) proposed new classifications of sedimentary deposits, geological ages, and stratigraphy for several regions of the Okcheon Metamorphic Belt, based on the fossils they found and the zircon U-Pb dating they performed.

5.4 Correlation with the Okcheon Metamorphic Belt and Chinese Cratons

One of the most important issues that came to the fore in understanding the tectonic evolution of the Korean Peninsula is a correlation with north and south China Cratons. Accordingly, various tectonic models have been proposed, and Okcheon Metamorphic Belt has often been regarded as continues of the Qinling-Dabie-Sulu Belt situated between the North and South China Craton consisting of current China.

Since Yin and Nie (1993) has proposed, the Korea Peninsula has divided into three major Precambrian Massifs, i.e., Nangrim, Gyeonggi and Yeongnam Massif, the hypothesis that the Nangrim and Yeongnam Massif have correlated with North China Craton and Gyeonggi Massif has correlated with South China Craton, respectively, has been supported by the majority.

The Mesoproterozoic and Neoproterozoic rocks pertaining to amalgamation and disruption of the Columbia and Rodinia supercontinent respectively, in the Korean peninsula are relatively rare reported than North China Craton and South China Craton.

The Mesoproterozoic age especially sparse throughout the world, and also the Neoproterozoic glacial event is highly characteristic, it may provide key to understanding the tectonic evolution of the Korean Peninsula.

With reference to glaciogenic sediments, much of the previous research has long been focused on the affinity to South China Craton because of the insufficiency of data from the North China Craton. However, a new perspective on the tectonic correspondence between Korean Peninsula and North China Craton is needed as much information has been newly published for North China Craton. Evidence has also been reported for the glaciation of Neoproterozoic in the western margin (Yang et al., 2019 and references therein) and southern margin of the North China Block (Le Heron et al., 2018; Li et al., 2018; Chen et al., 2020) and Neoproterozoic to Early Paleozoic Pyeongnam Basin of North Korea (Kim et al., 2016) as well.

The glacial events have occurred following the amalgamation of supercontinents (Young, 2013). Therefore, the presence of glaciogenic strata(sediments) in the central Korean Peninsula (Okcheon Metamorphic Belt), southern North Korea (Pyeongnam Basin) and southern to the western margin of North China Craton implies that they have

geological linkage, even though the glacial affinity of the Korean peninsula is still uncertain. Due to this, understanding of glaciogenic sediments would provide a clue for reconstructing East Asian tectonics during Neoproterozoic.

Even if a portion of the Okcheon Metamorphic Belt was deposited during the Neoproterozoic glaciation period, the proposal to extend it to the South China Block (Choi et al., 2012, Wang et al., 2017) needs to be reconsidered.

The detrital zircons of the Neoproterozoic Seochangni Formation distributed northeast of the Okcheon Metamorphic Belt show a characteristic late Paleoproterozoic to Mesoproterozoic U-Pb age distribution pattern.

Neoproterozoic sedimentary formations with very similar characteristics appear in the southern margins of North Korea and the North China Block, which are unconformably underlain beneath adjacent Early Paleozoic sedimentary basins.

The rift-related Neoproterozoic plutonic rocks and volcanic rocks have been recently investigated throughout Korean Peninsula, the southern margin of the Nangrim Massif (Peng et al., 2011), various regions of the Okcheon Metamorphic Belt (Lee et al., 1998; Oh et al., 2009; Kim et al., 2009; Kim et al., 2011; Kee et al., 2019), northern and southwestern Gyeonggi Massif (Kim et al., 2008; Kim et al., 2013a, 2013b; Lee et al., 2020) and the Hongseong-Imjingang Belt (Oh et al., 2007; Kim et al., 2008, 2018; Park et al., 2017; Kee et al., 2019).

The Neoproterozoic magmatism events have been reported from both North China Craton and South China Craton; the Qingbaikou system in the southern margin of the North China Craton and the marginal part of Yangtze Block in South China Craton.

Given that tectonic setting, it can be accounted for as. The southern Nangrim

Massif, Imjingang Belt, northern Gyeonggi Massif and central-southern part of the Okcheon Metamorphic Belt are correlated to the North China Craton. Whereas southwestern Gyeonggi Massif including the Hongseong area can be correlated to the South China Craton.

Further, upper Paleozoic strata, namely Pyeongan Supergroup, is identified over a wide Okcheon Metamorphic belt as well as the Taebaeksan Basin. Most previous research has been focused on that of in the Taebaeksan Basin relatively immune to (barely affected by) metamorphism and deformation. Such a recent finding lends weight to the possibility that Okcheon Metamorphic Belt would correlate to North China Craton (Lim et al., 2005, 2006, 2007; Choi et al., 2015; Kim et al., 2017; 2018).

Thus, the relationship between the lower Paleozoic Taebaeksan Basin and the Seochangni Formation adjacent to it is more likely to be an unconformity relationship, as in the southern margins of the North Korea and North China Craton, rather than the discrete blocks being contacted by fault boundary.

Some researchers argued that there is a large-scale fault called the South Korean Tectonic Line (SKTL) between the Okcheon Metamorphic Belt in the west correlate to the South China Craton and the Taebaeksan Basin in the east correlate to the North China Craton.

However, if sedimentary formations associated with the Neoproterozoic glaciation of the Okcheon Metamorphic Belt correlate with those in the southern margin of the North China Craton, the existence of the South Korean Tectonic Line (SKTL) is unfounded.

6. Conclusion

Available geochronological data require age-unknown carbonates as the geochronology only for the siliciclastic rocks has demonstrably been known. The $\delta^{13}\text{C}$ values of this cap carbonate, Geumgang Limestone, are quite valuable. By correlation, the Hwanggangni, Bugnori and Geumgang Limestone may include glaciogenic strata, thus these units could also be interpreted as Neoproterozoic in age.

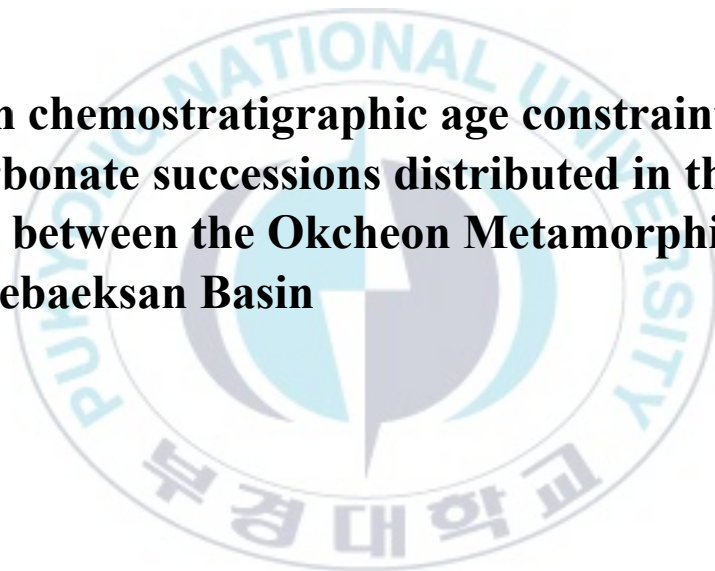
Negative $\delta^{13}\text{C}$ values down to -12‰ typify the cap carbonates, and it is particularly to Paleozoic carbonate. Integrating our geochemical data and stratigraphic correlation among periphery strata and based on a comparison of the carbon isotope variations with a global trend, it verifies that the Geumgang Limestone has a strong correlation with the post-glacial environment.

Although thus no reliable age is available at present, the pebble bearing phyllitic rocks, Hwangganni Formation, Bugnori Formation, and Iwonni Formation, have been suggested to be correlated with the diamictite of the global snowball Earth event.

Therefore, the inference that the Geumgang Limestone is cap carbonate is perfectly obvious. The finding of the Neoproterozoic glaciation related the Geumgang Limestone from the Okcheon Metamorphic Belt will untangle obscure tectonic linkage between North and South China Craton and Korean Peninsula.

CHAPTER 3

Carbon chemostratigraphic age constraints on the carbonate successions distributed in the border between the Okcheon Metamorphic Belt and Taebaeksan Basin



Abstract

Although the nature and tectonic significance of the Okcheon Metamorphic Belt remain contentious. The Chungju-Jecheon areas are located at the juncture of the Okcheon Metamorphic Belt and Taebaeksan Basin. Many petrological, structural, and stratigraphical studies have been reported in recent years, but most are focused on metasedimentary sequences in the Chungju area. For the constraints of unrevealed carbonates, several geochemical analyses for the Seochangni, Samtaesan, and Heungwolri Formation were conducted in the study area. In this chapter, we are trying to constrain the ages for the Seochangni, Samtaesan, and Heungwolri Formations in the Chungju-Jecheon area based on chemostratigraphy evidence.

In general, a high $\delta^{13}\text{C}$ value ($>1.5\%$) is referring to Neoproterozoic while Cambro-Ordovician carbonates have a $\delta^{13}\text{C}$ mean value of about 0% . In the case of the Chungju-Jecheon area, stimulating $\delta^{13}\text{C}$ values have been yielded. Some parts of the Samtaesan and Heungwolri Formation regarded in Ordovician have significantly higher $\delta^{13}\text{C}$ values implying Neoproterozoic. Besides, the Seochangni Formation recently recognized as Neoproterozoic has lower $\delta^{13}\text{C}$ values than generally conceded Neoproterozoic $\delta^{13}\text{C}$ value.

In summary, Precambrian strata and Phanerozoic strata have been mixed in the Chungju-Jecheon area. Therefore, reconsideration for the tectonic boundary between the Okcheon Metamorphic Belt and Taebaeksan Basin and harmonizing the nomenclature based on $\delta^{13}\text{C}$ are needed.

Keywords: Okcheon Metamorphic Belt, Taebaeksan Basin, Pyeongnam Basin, Late Neoproterozoic, Early Paleozoic, North Korea, North China Craton

1. Introduction

The northeast-trending Okcheon Belt distributed between the Gyeonggi Massif and Yeongnam Massif in the middle of the Korean Peninsula has been divided between the northeast Taebaeksan Basin and southwest the Okcheon Metamorphic Belt. However, researchers differ in opinion as to the basis of subdivision and position of the tectonic line (e.g. Kim et al., 1986; Cluzel et al., 1990, 1991, 1992; Kang, 1994a; Chough et al., 2000).

The northeastern the Okcheon Metamorphic Belt is one of the important regions to unravel the tectonic evolution history of the Okcheon Metamorphic Belt since not only covering age unknown limestone and other various types of rocks but locating near the Taebaeksan Basin.

The study area is around Lake Chungju located in the Chungju-si and Jecheon-si area in Chungcheongbuk-do Province, where the contact between the northeast Okcheon Metamorphic Belt and the southwest Taebaeksan Basin by the so-called South Korean Tectonic Line (SKTL) border. Although the nature and tectonic significance of the Okcheon Metamorphic Belt, its stratigraphy and depositional timing remain contentious.

Researchers have conducted a number of petrological, structural, and stratigraphical studies on the Okcheon Metamorphic Belt. Nonetheless, the consensus has not been reached yet between two conflicting suggestions for timing of the Okcheon Metamorphic Belt, Precambrian (Kim, 1968; Kim, 1971; Reedman and Fletcher, 1976; Choi et al., 2012) and Paleozoic (Lee et al., 1998; Yi et al., 2000; Suzuki et al., 2006; Kim et al., 2009).

Insufficiency of reliable geochronological information forbids proper interpretation. However, recent geochemical and geochronological studies for several formations comprising Okcheon Metamorphic Belt lend weight to the idea that it is formed in Neoproterozoic.

In the past, unfortunately, the latest meaningful studies have focused on the Chungju area, comprising Gyeomeyongsan Formation, Hyangsanni Dolomite, Daehyangsan Quartzite, and Munjuri Formation in ascending order. While studies for the Jecheon area in direct contact with the Taebaeksan Basin have been still inadequate.

In this chapter, we are going to discuss the timing of sedimentation for carbonate rocks from the Chungju-Jecheon area (Samtaesan, Heungweolri, and Seochangni Formations) based on chemostratigraphy using the carbon and strontium isotopic composition.

The Samtaesan and Heungwolri Formations commonly referred to as the upper part of the lower Paleozoic Joseon Supergroup is widely distributed in covered Jecheon (Kim et al., 1967), Yeongchun (GICTR, 1962), and Hwanggangni (Lee and Park, 1965) quadrangles.

The same stratigraphic classification has been adopted for carbonates in the Jecheon quadrangle (1:50,000-scale, Kim et al., 1967)) due to the similarity of the lithology of adjoining three quadrangles. Therefore, the depositional age has been generally regarded as early Paleozoic for carbonates in the Jecheon area.

Stable isotope analysis of two formations manifests different results from conventional thought. In consideration of the high carbon isotopic composition suggesting Neoproterozoic, some parts of the Samtaesan Formation and Heungwolri

Formation in the Jecheon area could not be regarded as Paleozoic strata.

As for the Seochangri Formation, it has revealed distinguished carbon isotopic composition indicating Paleozoic and Neoproterozoic. The Neoproterozoic geochronological information is identified by strontium isotopic composition and zircon U-Pb data from alternated pelitic rocks.

Taken together, the study area, the Chungju-Jecheon area, seems to be composed mainly of mixed Precambrian strata and Phanerozoic strata. It implies the necessity for reconsidering the tectonic boundary which has been putative between the Okcheon Metamorphic Belt and Taebaeksan Basin.

Additionally, we put forward defining new stratigraphic classification on a basis of carbon isotopic composition. In other words, stratigraphic units having $\delta^{13}\text{C}$ values over 1.5 ‰ should be given the Seochangri Formation or a new name.

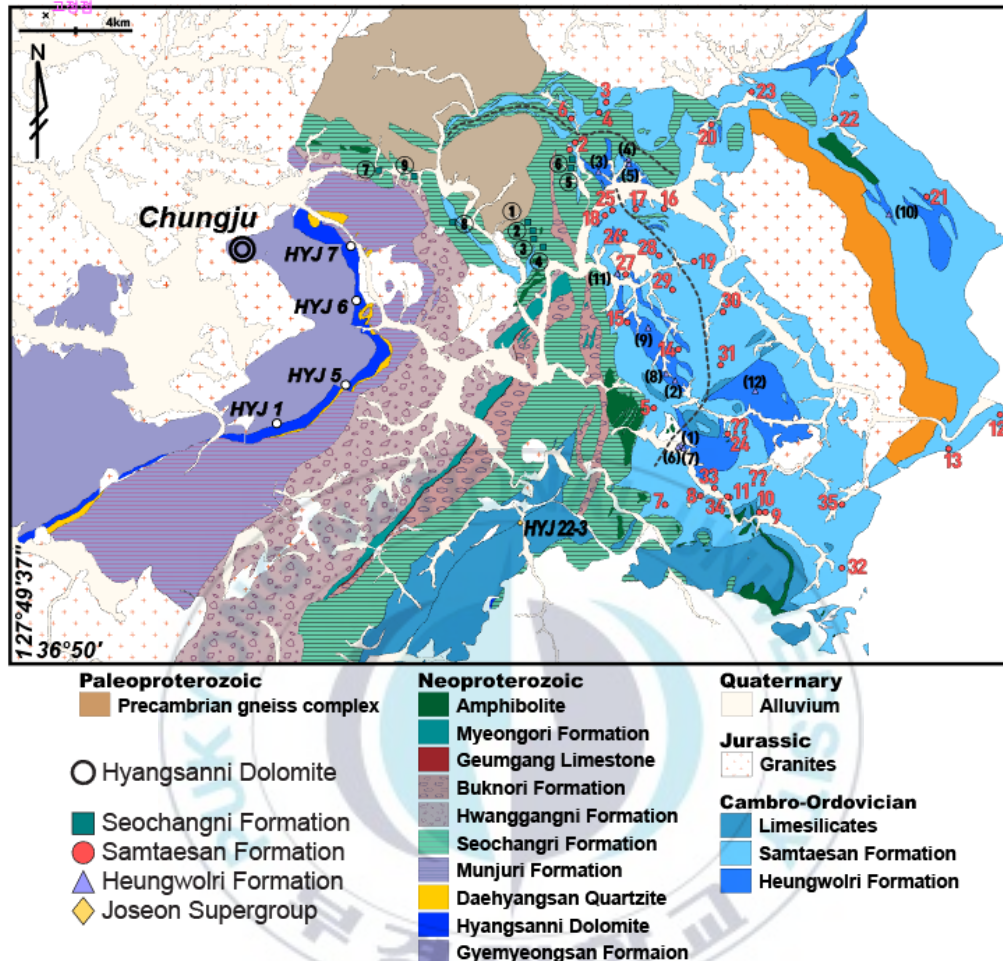


Figure 3-1. Geological map of the northeastern Okcheon metamorphic belt and the southwestern Taebaeksan Basin (Kim and Lee, 1965; Lee and Park, 1965; Kim et al., 1967; Park and Yeo, 1971). Sampling locations are shown along with outcrop numbers and symbols. The circled numbers with green square symbols: Seochangni Formation. The red numbers with red circle symbols: Samtaesan Formation. The numbers in parenthesis with purple upright triangle symbols: Heungwolri Formation. Yellow diamond symbol: Joseon Supergroup. Open circles: Hyangsanni Dolomite (Ha et al., 2021).

Table 3-1. Quadrangles and Stratigraphy names, with GPS coordinates for sampling localities of the Seochangni, Samtaesan and Heungwolri Formations. The numbers in the first column are matched those seen in the geological map (Figure 3-1).

Number on the map	Sample #	Quadrangle	GPS coordinate
Seochangni Fm.			
①	HYJ 106-1		N37 00.652 E128 04.836
②	HYJ 109-1	Jecheon	N37 00.463 E128 04.974
③	HYJ 110		N37 00.335 E128 04.992
④	HYJ 112-2	Hwanggnagni	N37 00.132 E128 05.244
⑤	HYJ 120-1		N37 02.003 E128 06.153
⑥	HYJ 122		N37 02.119 E128 06.215
⑦	HYJ 410	Jecheon	N37 01.887 E128 00.434
⑧	HYJ 414		N37 00.665 E128 02.616
⑨	HYJ 415		N37 01.756 E128 01.453
Samtaesan Fm.			
1	HYJ 124		N37 02.376 E128 06.132
2	HYJ 126-1		N37 02.568 E128 06.238
3	HYJ 151	Jecheon	N37 03.522 E128 07.142
4	HYJ 153-2		N37 03.323 E128 06.875
5	HYJ 160	Hwanggnagni	N36 56.304 E128 08.528
	HYJ 174 -1		
6	HYJ 174- 2	Jecheon	N37 03.134 E128 06.108
	HYJ 174- 3		
7	HYJ 303		N36 53.965 E128 08.892
8	HYJ 304		N36 54.209 E128 09.921
9	HYJ 305	Hwanggnagni	N36 53.809 E128 11.840
10	HYJ 306		N36 53.799 E128 11.656
11	HYJ 308		N36 54.169 E128 10.740

Table 3-1. (Continued)

Number on the map	Sample #	Quadrangle	GPS coordinate
12	HYJ 400		N36 56.121 E128 18.783
	HYJ 401-1		N36 55.306 E128 17.293
13	HYJ 401-2	Danyang	N36 55.263 E128 17.225
	HYJ 401-3		
14	HYJ 403		N36 57.667 E128 09.299
15	HYJ 405	Hwanggnagni	N36 58.344 E128 07.749
16	HYJ 406		N37 01.009 E128 08.831
17	HYJ 407-1	Jecheon	N37 01.027 E128 07.961
18	HYJ 408		N37 00.880 E128 07.081
	HYJ 409-1		
19	HYJ 409-2	Hwanggnagni	N36 59.734 E128 09.675
20	HYJ 419	Jecheon	N37 02.972 E128 10.248
21	HYJ 421	Yeongchun	N37 01.262 E128 16.596
22	HYJ 426		N37 03.119 E128 13.878
23	HYJ 428	Jecheon	N37 03.771 E128 11.345
24	HYJ 508		N36 55.655 E128 10.696
25	HYJ 517		N37 00.995 E128 07.325
26	HYJ 519		N37 00.404 E128 07.612
27	HYJ 523		N36 59.458 E128 07.652
28	HYJ 524		N36 59.890 E128 08.690
29	HYJ 527		N36 59.076 E128 09.111
30	HYJ 530	Hwanggnagni	N36 58.615 E128 10.542
31	HYJ 532		N36 57.309 E128 10.516
32	HYJ 535		N36 52.521 E128 14.146
33	HYJ 538		N36 54.388 E128 10.329
34	HYJ 539		N36 53.842 E128 14.103
	HYJ 541w		N36 54.023 E128 14.077
35	HYJ 541b		

Table 3-1. (Continued)

Number on the map	Sample #	Quadrangle	GPS coordinate
	Heungwolri Fm.		
(1)	HYJ 23		N36 55.405 E128 09.242
	HYJ 24-1		
(2)	HYJ 24-2	Hwanggnagni	N36 56.978 E128 09.124
	HYJ 24-3		
(3)	HYJ 131-2		N37 01.893 E128 06.892
(4)	HYJ 136	Jecheon	N37 02.120 E128 07.796
(5)	HYJ 137-5		N37 02.037 E128 07.769
(6)	HYJ 162		N36 55.404 E128 09.235
(7)	HYJ 309		N36 55.334 E128 09.389
(8)	HYJ 402	Hwanggnagni	N36 57.096 E128 08.938
(9)	HYJ 404a		N36 58.197 E128 08.374
(10)	HYJ 423	Yeongchun	N37 00.827 E128 15.521
(11)	HYJ 520-1		N36 59.462 E128 07.465
(12)	HYJ 533	Hwanggnagni	N36 56.697 E128 11.507
	Lime-silicate rock		
	HYJ 22-3	Hwanggangni	N36 53.616 E128 04.614
	Pungchon Ls.		
	HYJ 31-1	Changdong	N37 30.334 E128 24.940
	HYJ 37-1		
	HYJ 37-2	Dangyang	N36 59.440 E128 26.213
	Jeongseon Ls.		
	HYJ 32-1	Changdong	N37 30.320 E128 25.067
	Machari Fm.		
	HYJ 33-1	Yeongwol	N37 17.134 E128 25.029
	Yeongheung Fm.		
	HYJ 34	Yeongwol	N37 12.676 E128 24.920

2. Geological Setting

Lithologies in the Lake Chungju area can be subdivided into four major groups: they are the Paleoproterozoic metamorphic rocks, Neoproterozoic Okcheon Supergroup, lower Paleozoic Joseon Supergroup, and Mesozoic granitoids (Choi et al., 2012).

As mentioned, several times, the Okcheon Belt consists of the Okcheon Metamorphic Belt which is composed of the Neoproterozoic metavolcanic successions and age-debatable metasedimentary successions and the Taebaeksan Basin constituted by Paleozoic sedimentary successions (Figure 3-1).

The Okcheon Metamorphic Belt and Taebaeksan Basin have been correlated with South China Craton and North China Craton, respectively, based on the correlation of fossil components, lithologies, and zircon age distribution patterns (Chough et al., 2013; Cho et al., 2013; and references therein). Besides, the Taebaeksan Basin is also correlative with the Pyeongnam Basin in North Korea. The relationship between the Okcheon Metamorphic Belt and Taebaeksan Basin is as important as a stratigraphical relationship for the constituent of the Okcheon Metamorphic Belt. However, it is also lingering outstanding issues whether their relationship is conformity, unconformity, or structural junction.

The Taebaeksan Basin comprises the lower Paleozoic Joseon Supergroup and upper Paleozoic Pyeongan Supergroup, and there is about 140 Ma of long hiatus between them. The early Cambrian to the middle Ordovician Joseon Supergroup has been divided into five groups, depending on each of their distinctive sequences of lithology in different regions: which are the Taebaek, Yeongwol, Yongtan, Pyeongchang, and Mungyeong groups (Kobayashi, 1966; Choi, 1998). It could also be

roughly divided into the Taebaek, Yeongwol, and Mungyeong groups (Choi, 2014; Choi et al., 2016). Among them, the Yeongwol group is regionally extensive with the Taebaek group. The Taebaeksan Basin part which takes up most of the study area is confined to the Yeongwol unit of the Joseon Supergroup.

The Yeongwol Group is located in the western part of the Taebaeksan Basin and suggested that it is adjoined the Okcheon Metamorphic Belt by the South Korean Tectonic Line (Chough et al., 2013) or Central Okcheon Thrust (Ree et al., 2001). The Yeongwol Group is composed of the Sambangsan, Machari, Wagok, Mungok, and Yeongheung Formations, in ascending order (Yosimura, 1940; Kobayashi, 1966; Choi, 1998). The lowest Sanbansan Formation is made up of siliciclastic sequences, while the other upper four layers are principally composed of carbonate rocks. (Choi et al., 2018).

The stratigraphy of the Yeongwol group, developed in the Yeongwol-Jecheon area, has been known to well understand due to fertile fossil occurrences such as conodonts and trilobites (Son et al., 2008). The Yeongwol group is fault-bounded, the Pyeongchang Fault, on the west Jecheon and east Yeongwol area, and research has mostly been conducted on the Yeongwol area which is the eastern part of the Pyeongchang Fault.

The Yeongwol group in the Jecheon area, which is distributed in the west of the Pyeongchang Fault, is distinctly different from those in the Yeongwol area, in the lithologies and constituents (Kwon et al., 2019 and references therein).

The eastern part of the Pyeongchang thrust fault is actively studied (Yoshimura, 1940; Kobayashi, 1966; Kim et al., 1973; Park et al., 1994; Lee, 1995; Choi, 1998; Kim and Choi, 2000), while there is a dearth of the stratigraphical research for western part (Lee, 1983; Son et al., 2001, 2008). Some authors (GICTR, 1962; Kim et al., 1973)

suggested Wagok and Mungok Formations in the eastern are stratigraphically equivalent to the Heungwolri and Samtaesan Formations in the western, respectively.

In the study area, at the boundary of the Okcheon Metamorphic Belt and the Taebaeksan Basin, there are carbonate rocks classified into several different sedimentary layers. The carbonate rocks, which are widely distributed between the west of The Geumsusan Quartzite and the Seochangni Formation, are classified as the Samtaesan Formation and Heungwolri Formation of the Cambro-Ordovician Joseon Supergroup (Figure 3-1). However, in this area, Cambro-Ordovician fossils were found only in one location (Chough et al., 2006). The rest are regarded as belonging to the Joseon Supergroup only by the similarity of lithologies. In addition, relatively thin layers of carbonate rocks exist in several places within the Seochangni Formation.

The carbonates in the study area, Hyangsanni Dolomite and Seochangni Formation are distributed in the western part, and the Samtaesan and Heungwolri Formations by the Bonghwajae-Wolaksan border.

The Seochangni Formation overlay the Heungwolri and Samtaesan Formations and its distribution is very large in the west of the Jecheon quadrangle (Kim et al., 1967), but toward the east, it becomes gradually smaller. This formation is largely consisted of chlorite schist and phyllite interbed by quartzite, limestone, and black slate. For this study, we collected limestone samples from the Seochangni Formation.

The east of the Jecheon quadrangle (Kim et al., 1967) mainly consisted of the Heungwolri Formation at the lower part and Samtaesan Formation at the upper. The Heungwolri Formation in the area crops along the crest of anticline as a banded shape. In some parts, Samtaesan Formation is recrystallized into lime-silicate and hornfels by granite intrusions. Some parts of the Heungwolri Formation are fine to medium in grain, but the major part is massive. The Samtaesan Formation is platy or massive and its

color is light grey or dark grey, their strikes are extremely disturbed.

Although the Seochangni Formation is distributed in a wide area, this formation nearly phyllitic rocks, thus good calcareous outcrop exposures are rather poor. Though the outcrop exposure of the Heungwolri and Samtaesan Formations is extensive, it is not easy to identify the stratigraphic boundaries among the formations.

The study area is around the administrative area of the Geumseong Myeon, Cheongpung Myeon, and Susan Myeon, where the northeast Okcheon Metamorphic Belt meta occupied by metaclastic rocks and southwest carbonate dominated Taebaeksan Basin are juxtaposed. Here comprise mainly Precambrian basement, Cambro-Ordovician Samtaesan Formation and Heungwolri Formation, and age-unknown Seochangni Formation (Figure 3-1).

As previously stated, however, the Yeongwol group displays lateral variations such as lithologies, depositional condition, and depositional timing between east and west sections of the Yeongwol group based on the Pyeongchang Fault. Therefore, the Yeongwol Group should be stratigraphically separated by the Yeongwol sequence and Jecheon sequence based on the Pyeongchang thrust fault. In other words, the Samtaesan and Heungwolri Formations in the Jecheon area have traditionally been considered as Cambro-Ordovician deposits belonging to the Joseon Supergroup, but they need to be studied in more detail through subsequent research.

3. Samples and Analytical Methods

The whole-rock samples were analyzed for element concentrations including Ba, Sr, Mn, Rb and, REE and Sr isotope composition. The analysis for Carbon and Oxygen was carried out using the same whole-rock samples at Beta Analytic Inc.

For a stable isotope study, samples were collected from the Seochangni (Figure 3-2), Samtaesan (Figure 3-3), and Heungwolri Formations (Figure 3-4) encompassing Jecheon (Kim et al., 1967), Hwanggangni (Lee and Park, 1965), Danyang (Won and Lee, 1967), and Yeongchun (GICTR, 1962) quadrangles. In addition, carbonates of Pungchon Limestone, Jeongseon Limestone, Machari Formation, and Yeongheung Formation are also collected from further northeast than Jecheon area.

The Samtaesan and Heungwolri Formations are carbonate sequences representing the Yeongwol Group of the Taebaeksan Basin. In this study, limestone and dolomite named in the Hwanggangni quadrangle (Lee and Park, 1965) are collectively referred to as the Samtaesan and Heungwolri Formations.

For geochemical analysis, an aliquot of 0.2g of the powdered sample was dissolved in only 1M acetic acid for 90 minutes. After dissolution, it was centrifuged and then the supernatant was separated and dried. The solution was diluted to 2000 times for trace and rare earth elements measurement. Trace elements of the carbonate were analyzed by ICP-MS (iCapTQ model, Thermo Fisher Scientific, Bremen, Germany) at Core Research Facilities, Pusan National University, Korea.

The carbon and Oxygen isotopic values were analyzed by the whole rock sample. Isotopic analysis was conducted using IRMS at Beta Analytic Inc.



Figure 3-2. Outcrop photographs of the Seochangni Formation.





Figure 3-3. Outcrop photographs of the Samtaesan Formation.

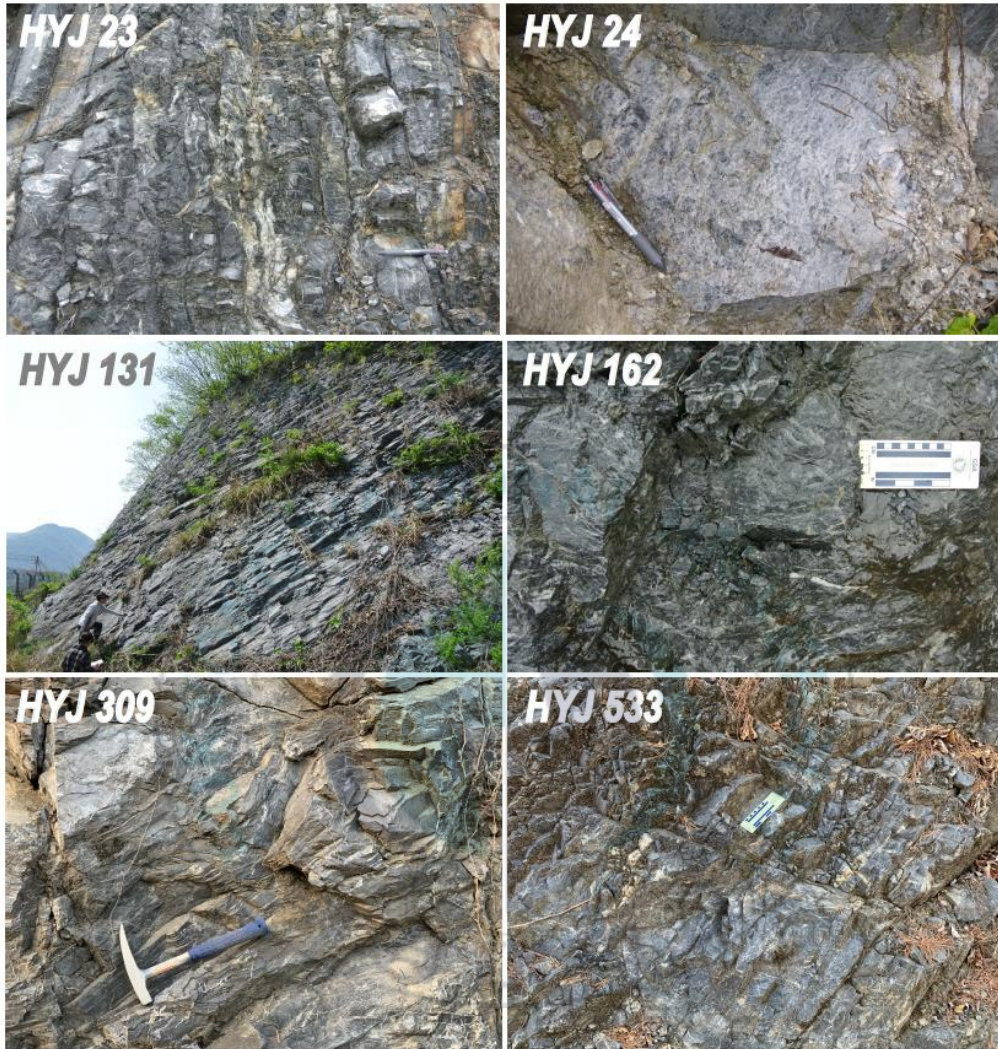


Figure 3-4. Outcrop photographs of the Heungwolri Formation.



Figure 3-5. Outcrop photographs of the Joseon Supergroup.

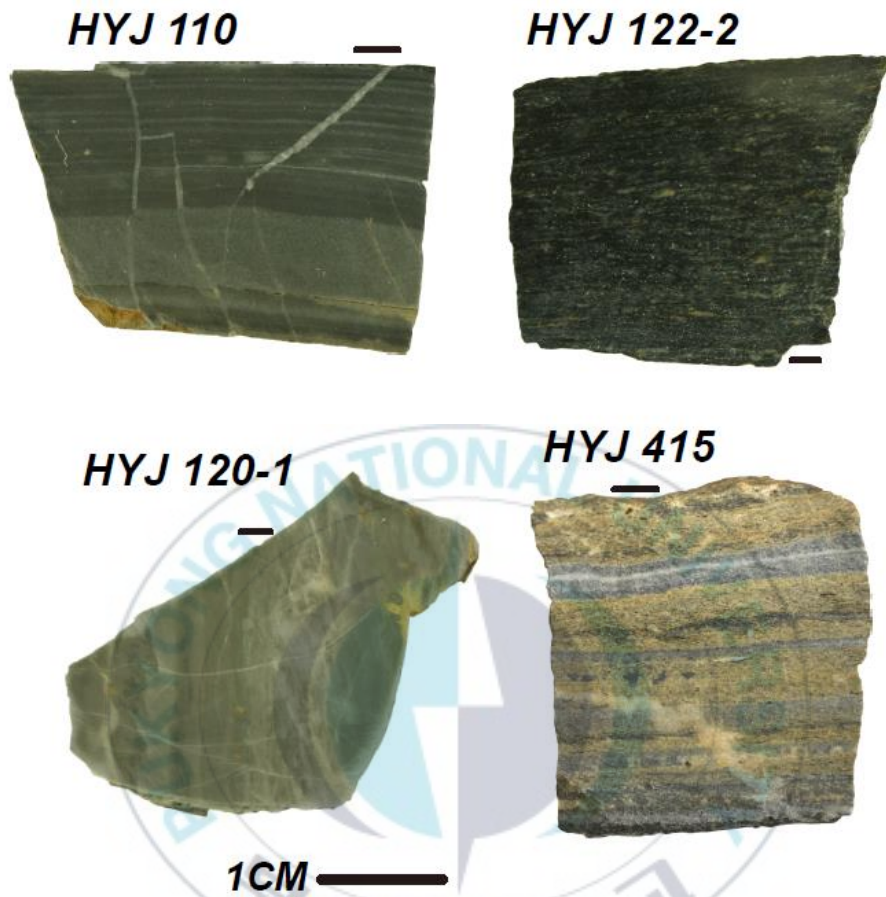


Figure 3-6. Photographs for the slab samples from the Seochangni Formation.

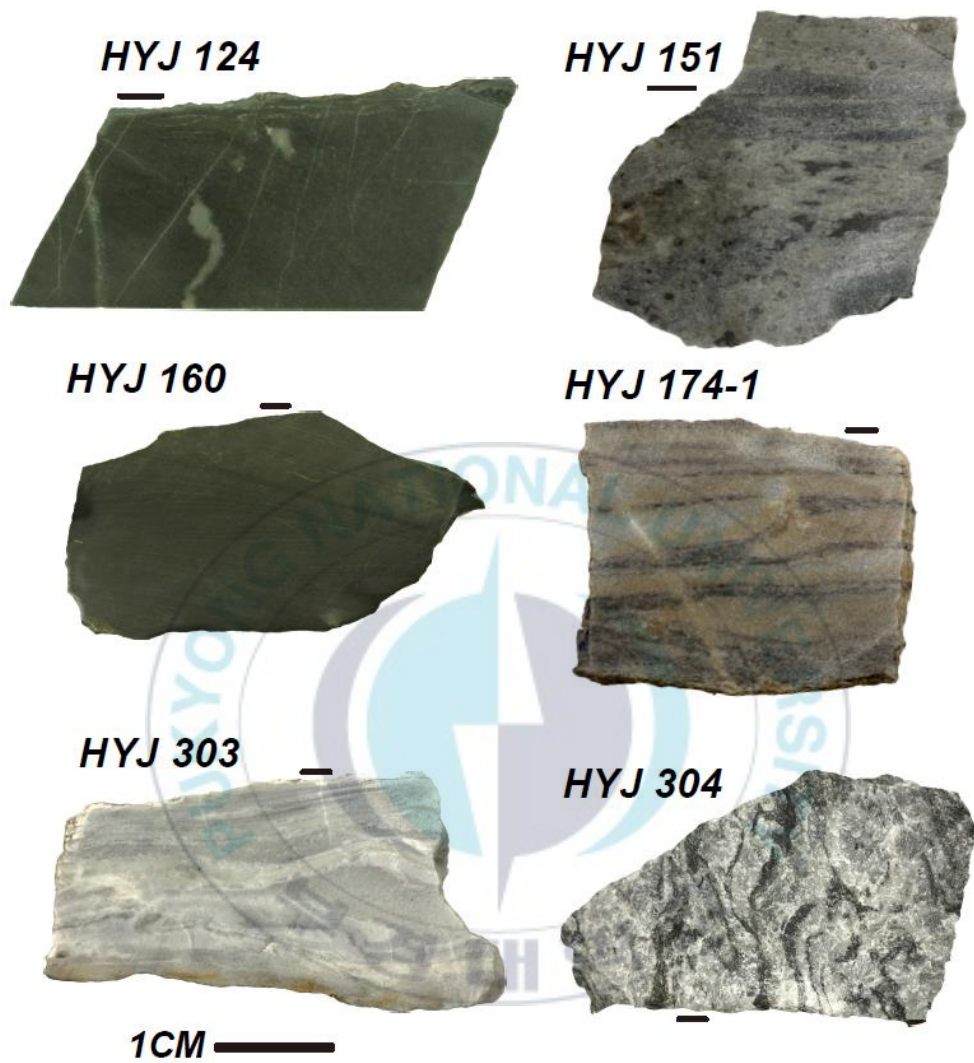


Figure 3-7. Photographs for the slab samples from the Samtaesan Formation.



Figure 3-7. (Continued)



Figure 3-8. Photographs for the slab samples from the Heungwolri Formation.



Figure 3-9. Photographs for the slab samples from the Joseon supergroup.

4. Results and Discussion

4.1 Trace element and REE plus yttrium

The rare earth element and trace element concentrations are shown in Table 3-2 and Table 3-3, respectively. The rare earth element plus yttrium concentrations in most plots are normalized to a standard shale average (Post Archean Australian Shales, PAAS of McLennan, 1989). $(Ce/Ce^*)_N$ and $(Eu/Eu^*)_N$ were calculated using the relationship shown in Figure 3-11 following the technique of Bau and Dulski (1996) and Kamber and Webb (2001), respectively.

In this study, we prefer the threshold of $\delta^{13}C$ value (-3 to 1.5‰) as the discriminative for the Paleozoic value (Table 3-4).

Rare earth elements, trace elements and calculated parameters are presented in Table 3-2 and Table 3-3, respectively and PAAS-normalized REE+Y patterns are shown in Figure 3-10.

In Figure 3-10a, Paleozoic, the Seochangni (n=1), Samtaesan (n=2) and Heungwolri Formation (n=1) presented an enrichment in HREE. The REE+Y/PAAS pattern of the Seochangni Formation displays a remarkable HREE enrichment the others display a gradual enrichment in REE+Y/PAAS values towards heavier REE.

In Figure 3-10b, no Paleozoic, the REE+Y/PAAS patterns of the Seochangni Formation (n=2) are also display enrichment in heavier REE, but much flatter than that of Figure 3-10a. On the other hand, the Heungwolri Formations (n=2) display HREE depleted REE+Y/PAAS patterns.

The overall REE+Y/PAAS patterns of carbonates sequences of the study area do not present the expected typical seawater signature such as positive lanthanum and

yttrium anomalies and negative cerium anomalies. In addition, the samples which do not belong to Paleozoic have a similar pattern to those of the Hyangsanni Dolomite considered as Neoproterozoic carbonate sequence.

Geochemical discrimination diagrams (Figure 3-11) seem to split into two groups, but it is still too soon to forejudge due to the insufficiency of data. The encouraging thing is that the geochemical data also can be parameters with carbon isotopes to discriminate whether it belongs to Paleozoic or not.



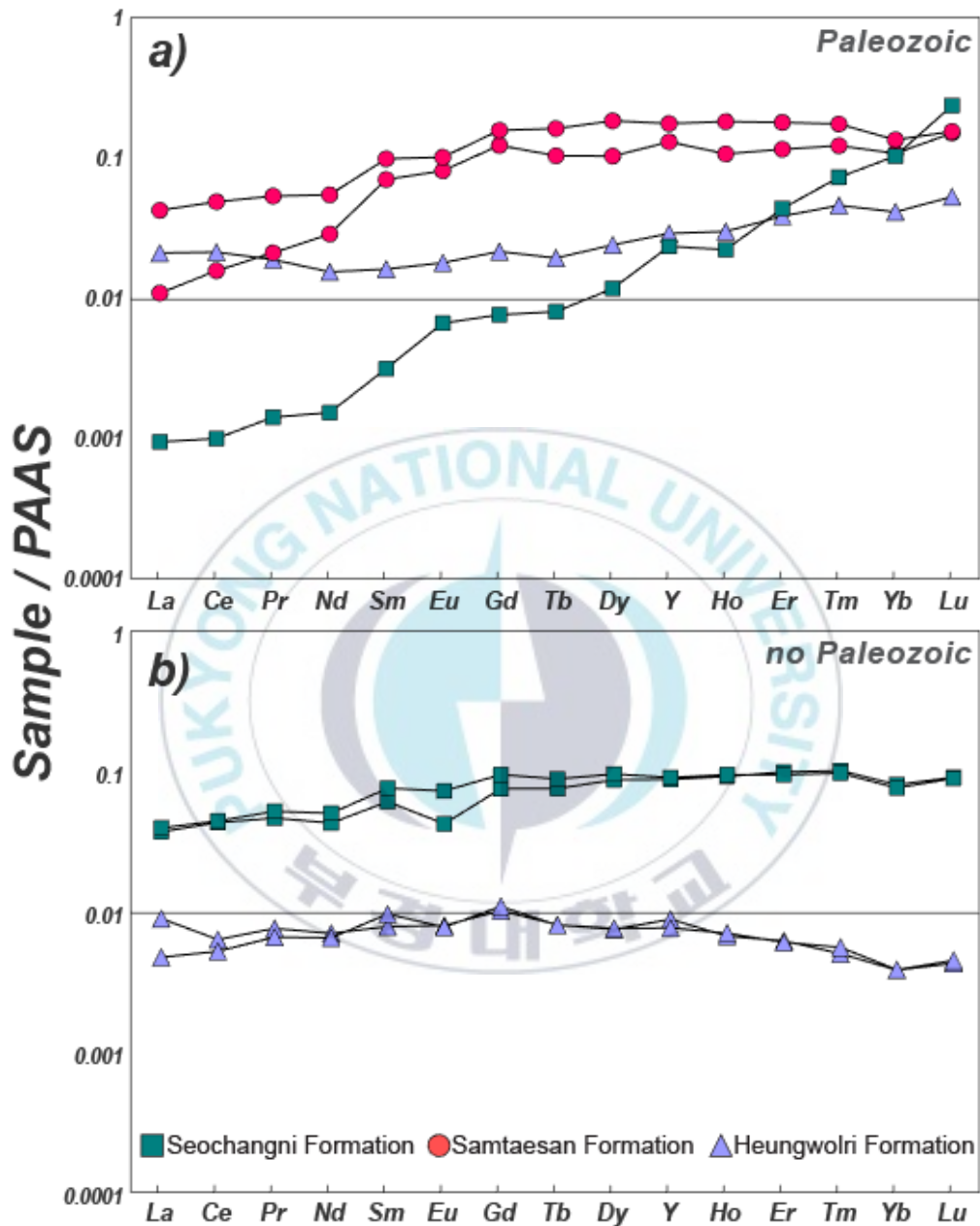


Figure 3-10. PAAS-normalized REE + Y diagrams of the Seochangni, Samtaesan and Heungwolri Formation, PAAS data are from McLennan, 1989. REE+Y/PAAS diagrams are grouped based on the $\delta^{13}\text{C}$ value. Symbols are as in Figure 3-1.

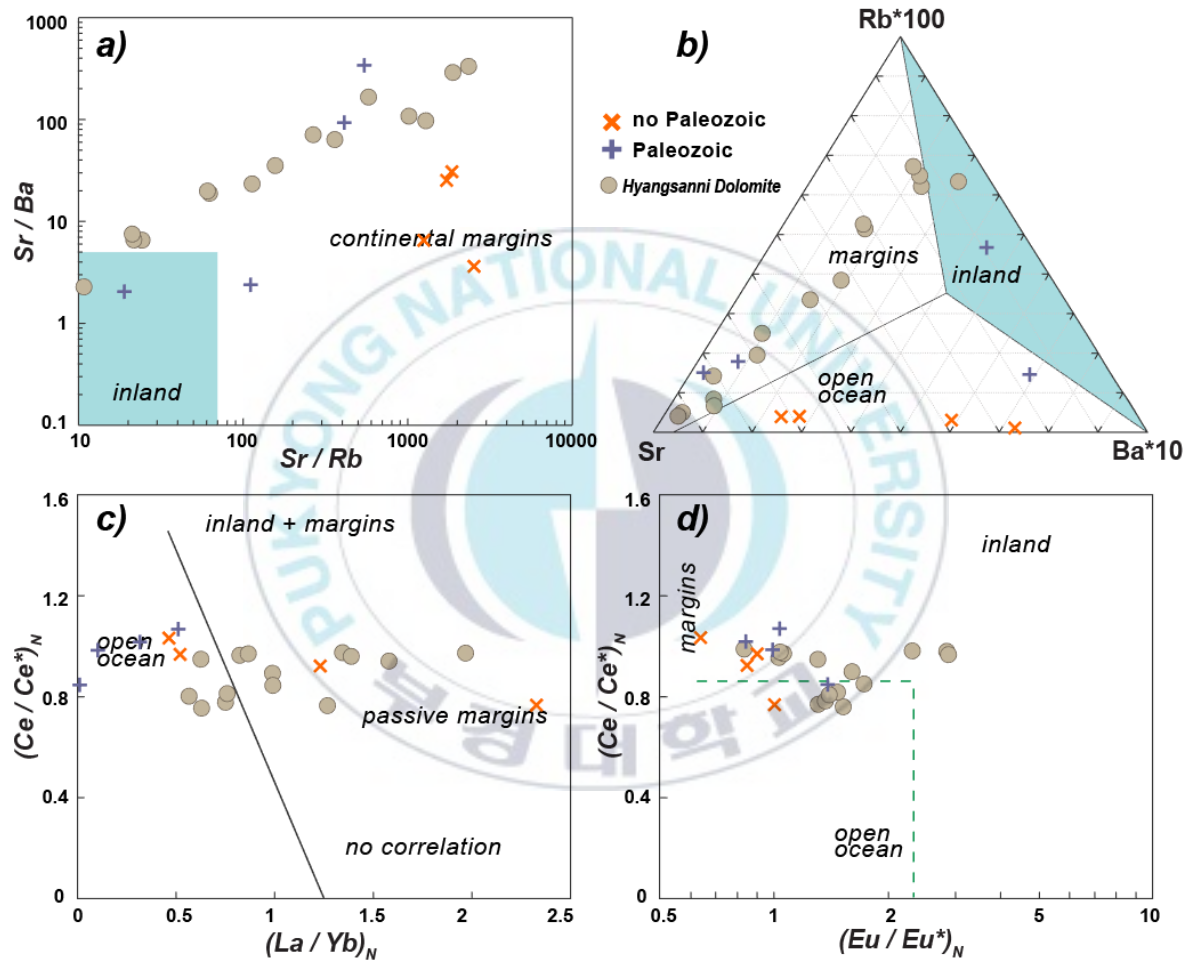


Figure 3-11. Geochemical discrimination diagrams to distinguish various depositional environments of the carbonate rocks from the Seochangni, Samtaesan and Heungwolri Formations. (a) Sr/Ba vs. Sr/Rb, (b) Rb–Sr–Ba triangular, (c) $(Ce/Ce^*)_N$ vs. $(La/Yb)_N$ and (d) $(Eu/Eu^*)_N$ vs. $(Ce/Ce^*)_N$ diagrams. Rare earth element abundances were normalized to PAAS (McLennan, 1989) and the Eu and Ce anomalies were calculated, following the equation proposed by Bau and Dulski (1996) and Kamber and Webb (2001), respectively. Hyangsanni Dolomite data with circle symbol is from Ha et al., (2021). The geochemical data also grouped based on the $\delta^{13}C$ value. The $\delta^{13}C$ values to be within the range in the carbon isotope values of the Paleozoic era are marked as cross (+) symbols and the others are symbolized by X.

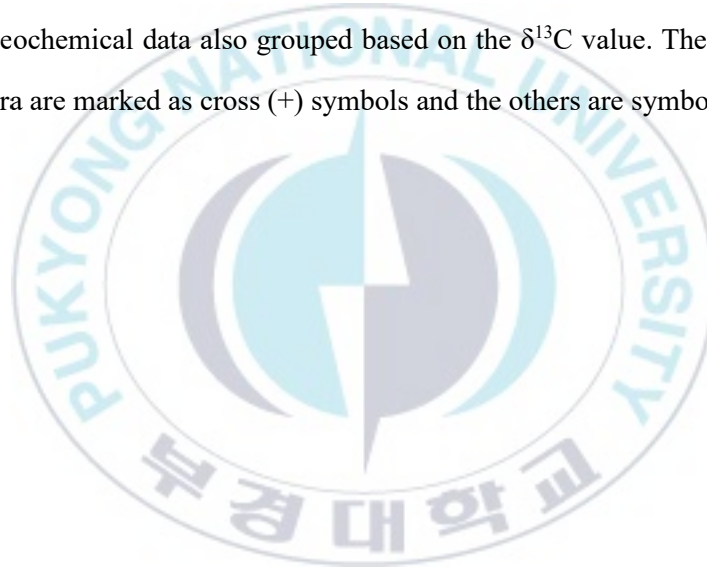


Table 3-2. Rare earth elements plus Yttrium concentrations of the Seochangni, Samtaesan and Heungwolri Formations. The data are presented in parts per million (ppm). (La/Yb)_N values are calculated by PAAS-normalized values.

Sample #	Y	La	Ce	Pr	Nd	Sm	Eu	Gd	Tb	Dy	Ho	Er	Tm	Yb	Lu	∑REE	Y/Ho	(La/Yb) _N
Seochangri Fm.																		
HYJ 110	3.28	1.97	4.76	0.57	2.01	0.47	0.063	0.49	0.08	0.56	0.126	0.39	0.057	0.31	0.054	11.92	26.0	0.46
HYJ 112-2	0.61	0.04	0.08	0.01	0.05	0.02	0.007	0.03	0.01	0.05	0.021	0.12	0.029	0.28	0.099	0.84	28.8	0.01
HYJ 120-1	3.38	2.09	4.88	0.63	2.36	0.58	0.109	0.61	0.09	0.62	0.130	0.37	0.054	0.30	0.054	12.90	26.0	0.52
Samtaesan Fm.																		
HYJ 151	3.41	0.40	1.21	0.18	0.94	0.38	0.085	0.56	0.08	0.47	0.103	0.32	0.048	0.29	0.063	5.13	33.3	0.10
HYJ 174- 2	7.58	8.03	17.73	1.88	7.00	1.39	0.309	1.52	0.23	1.27	0.276	0.79	0.100	0.64	0.092	41.26	26.5	0.31
Heungwolri Fm.																		
HYJ 24-1	0.76	0.78	1.64	0.16	0.51	0.09	0.019	0.10	0.01	0.11	0.029	0.11	0.018	0.11	0.022	0.76	26.4	0.51
HYJ 131-2	0.33	0.47	0.70	0.09	0.33	0.06	0.012	0.07	0.01	0.05	0.009	0.02	0.003	0.01	0.003	6.46	35.9	2.33
HYJ 162	0.29	0.25	0.58	0.08	0.31	0.07	0.012	0.07	0.01	0.05	0.010	0.02	0.003	0.02	0.003	0.58	29.7	1.23

Table 3-3. PAAS-normalized rare earth element parameters and trace element concentrations of the Seochangni, Samtaesan, and Heungwolri Formations. The trace elements are presented in parts per million (ppm).

Sample #	(Ce/Ce*) _N	(Pr/Pr*) _N	(Eu/Eu*) _N	Rb	Sr	Ba
Seochangri Fm.						
HYJ 110	1.03	1.08	0.64	0.0	49.4	2
HYJ 112-2	0.85	1.12	1.39	0.6	61.4	26
HYJ 120-1	0.97	1.10	0.91	0.0	99.3	28
Samtaesan Fm.						
HYJ 151	0.98	0.95	1.00	0.3	148.5	0
HYJ 174 -1	1.02	1.04	0.85	0.4	146.5	2
Heungwolri Fm.						
HYJ 24-1	1.07	1.03	1.04	1.0	19.3	10
HYJ 131-2	0.77	1.14	1.01	0.0	10.0	2
HYJ 162	0.92	1.12	0.85	0.0	15.9	1

4.2 Carbon isotope records from carbonate successions in the Chungju-Jecheon area

As seawater evolves, changes in carbon, oxygen-stable isotope, and Sr isotope values change by geological age, and using this chemostratigraphy, it is possible to estimate the age of oceanic carbonate rocks of unknown age. For carbon isotope values, relatively high values are maintained through Neoproterozoic, but there are several drop intervals (lower to around -10 ‰), and these periods are largely consistent with the global glaciations of 2-3 times (Figure. 1-1). However, in the Cambro-Ordovician of the Paleozoic era, it has a value of around 0 ‰ (Figure 4-2, about -3 to +1.5 ‰). Sr isotope composition was continuously elevated through Neoproterozoic, and most of the Neoproterozoic values were lower than those of Phanerozoic. Such an isotopic change can be usefully used to determine the geological age of carbonate rocks that are otherwise difficult to date.

In Figure 3-12, drawn for comparison, the carbon isotope composition of Cambro-Ordovician carbonates in the Taebaeksan Basin is generally in the range of -3 to 2 ‰ and generally agrees with the global values at the time. Limestones and dolomites distributed between the Geumsusan Quartzite and the Seochangni Formation have been correlated to Cambro-Ordovician Samtaesan Formation and Heungwolri Formation, respectively. However, the carbon isotope values for these carbonate rocks differ from these expectations. The distinguished $\delta^{13}\text{C}$ values of these formations are intriguing. In part, similar to carbonates in the Taebaeksan Basin, some have values that match Cambro-Ordovician values (Figure 3-1 and 3-12 and Table 3-4), but those that have distinct values from Cambro-Ordovician carbonates are more widely distributed.

Most of these have higher positive values than Cambro-Ordovician carbonates, but

some have significantly negative values. The fact that some carbonate rocks in this area have relatively high carbon isotope values is consistent with the values of Kim and Min (1996). However, Kim and Min (1996) considered these values to be within the range of changes in the carbon isotope values of the Paleozoic era because in general, high $\delta^{13}\text{C}$ value ($>1.5\text{‰}$) is referring to Neoproterozoic while Cambro-Ordovician carbonates have a $\delta^{13}\text{C}$ mean value of about 0‰ (Montañez et al., 2000), and, at that time, there were not many studies on carbonate rocks of the Neoproterozoic era. Moreover, they interpreted that unusually ^{13}C enriched carbonates in this region might be deposited in the highly evaporated sedimentary basin. However, it seems to be a misinterpretation.

While the Seochangni Formation recently recognized as the Neoproterozoic sequence has low $\delta^{13}\text{C}$ values as much as generally accepted by the $\delta^{13}\text{C}$ value of Neoproterozoic cap carbonates.

Considering the proposals that the nearby Hwanggangni Formation, a diamictite deposit, is Neoproterozoic (Reedman and Fletcher, 1976; Choi et al., 2012) and the Seochangni Formation is also Neoproterozoic (Kim et al., 2020). Geochronological information constrained by this study is also in accordance with detrital zircon U-Pb age from the Seochangni Formation (Choi, 2013; Kim et al., 2021; this study).

As stated in Chapter 2, an identifiable negative $\delta^{13}\text{C}$ values of about -6‰ indicate the characteristic of cap-carbonates. However, referring to the seawater carbon isotope evolution curve, there is a period of high variability in the early Cambrian (Figure 4-2), and at this time, the remarkable large degree of $\delta^{13}\text{C}$ variation has been examined from the significant negative value under -6‰ to a significantly higher value approaching 8‰ . However, these changes occur over a very short period.

Consequently, it cannot rule out the possibility that the carbonate rocks in the study area have been deposited in such a brief space of time. On the other hand, it is well known that the carbon isotope composition of carbonates during the entire Neoproterozoic is generally much higher than that of Cambro-Ordovician, but there are several large negative excursions, and these periods coincide with the glaciation periods. Thus, the carbonates in the study area were mainly deposited earlier than the Cambro-Ordovician carbonate rocks distributed in the Taebaeksan Basin. Namely, it is thought that the latter is more likely to be deposited in Neoproterozoic rather than Cambro-Ordovician.



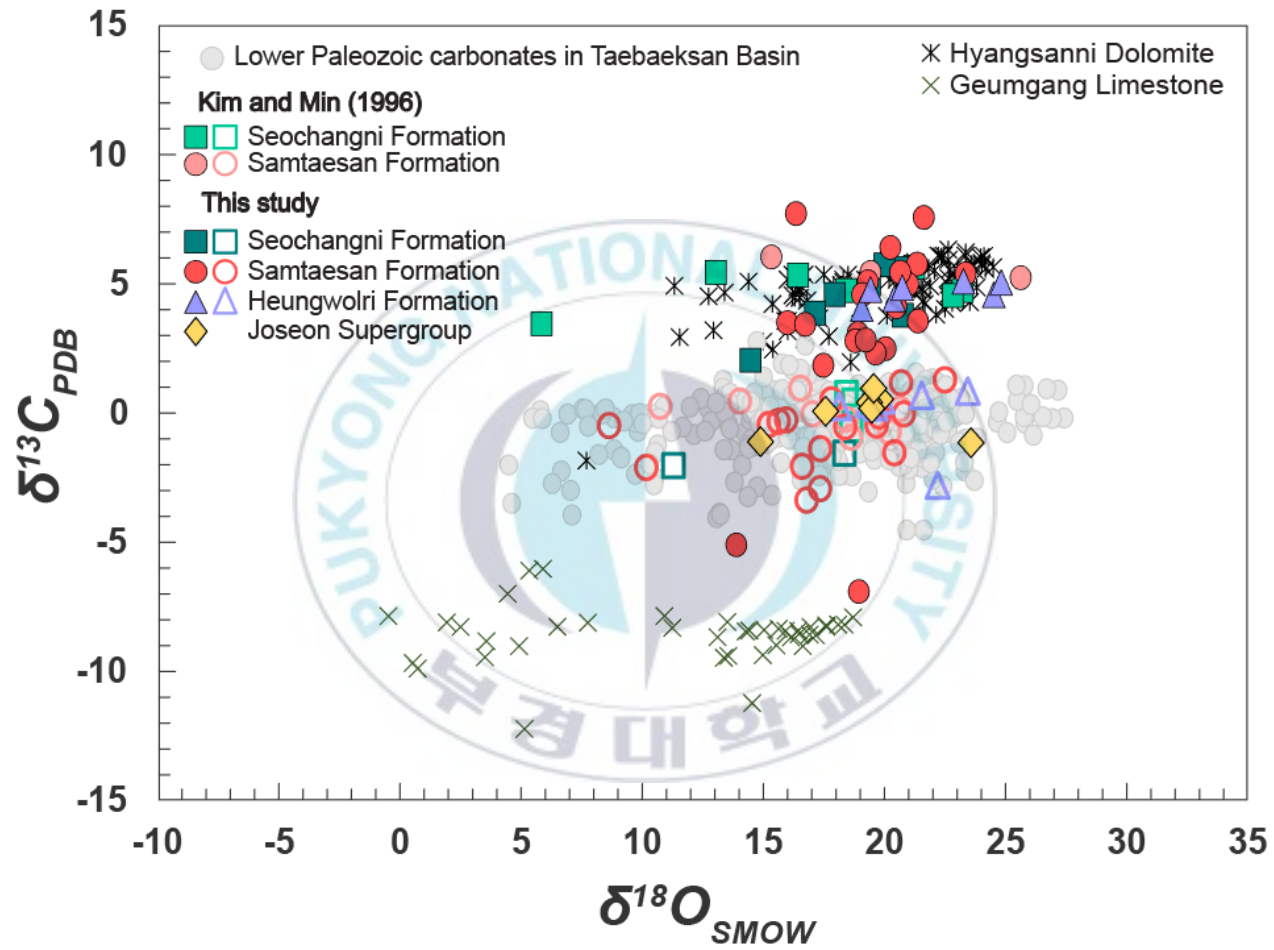


Figure 3-12. Carbon versus oxygen cross-plot for the Seochangni, Samtaesan and Heungwolri Formations and the Joseon Supergroup. Carbon and oxygen isotopic compositions analyzed from the Seochangni and Samtaesan Formations (Kim and Min, 1996) and compiled data for the Lower Paleozoic carbonate rocks in Taebaeksan Basin (Kim, 1980; Park and Woo, 1986; Lim and Woo, 1995; Yoon and Woo, 2006; Hong and Lee, 2007; Lim et al., 2015) are shown together.



4.3 Regional comparison of Carbon isotope composition

It is noteworthy that the distribution of carbonates similar to those of the Taebaeksan Basin and dissimilar carbonates are geographically distinct. Looking at this by region, it is as follows. Symbols are as in Figure 3-1.

Regions east and north of the Geumsusan Quartzite

During the study, carbonate rocks having a carbon isotope value different from that of Cambro-Ordovician were discovered, and a study was conducted to confirm their distribution. Carbon-oxygen isotope composition analysis was also performed for carbonate rocks distributed in the east and north of the Geumsusan quartzite, and as a result, it was confirmed that carbonate rocks in this area had values well in agreement with Cambro-Ordovician carbonates (Table 3-4, Fig. 3-13). In other words, it can be said that those in this area belong to the Joseon Supergroup.

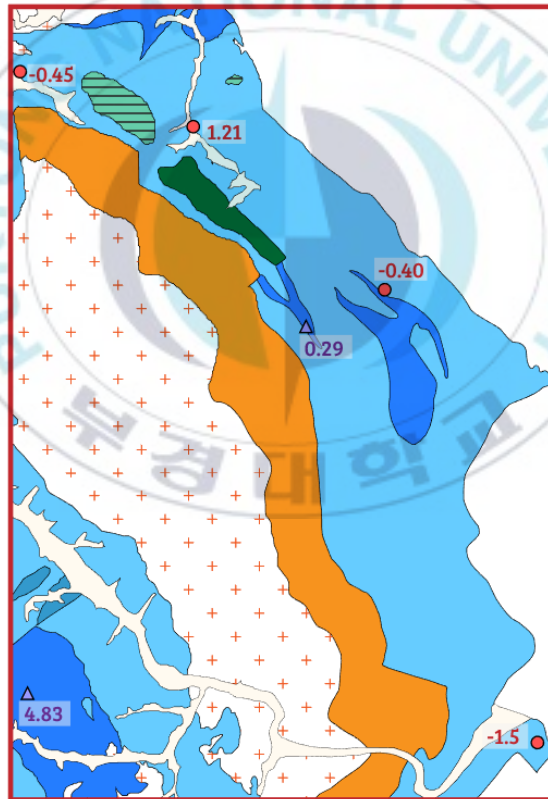
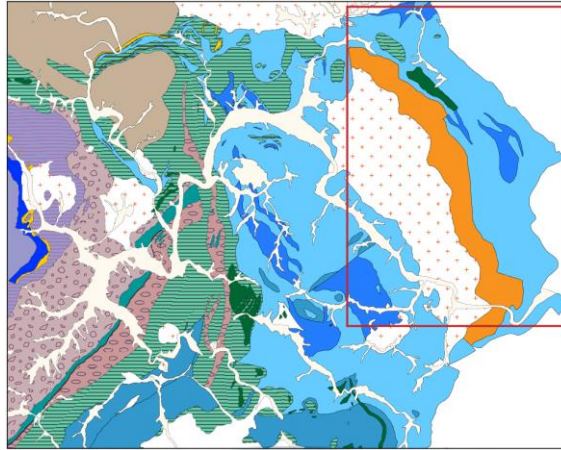


Figure 3-13. Carbon isotopic compositions for the regions east and north of the Geumsusan Quartzite

The area between Busan and Bakdallyeong gneiss complexes

In the area between the Busan gneiss complex and the Bakdallyeong gneiss complex (Figure. 3-1 and 3-14), strip-shaped limestone, quartzite, and pelitic rocks are long distributed east to west. Further east leads to the limestone north of the Geumsusan Quartzite. In the eastern part of this region, it is distributed in the form of a quartzite layer in the highlands, pelitic rocks surrounding it, and a limestone layer distributed in the outer part. The results of carbon-oxygen isotope analysis of limestones in this area show values that agree well with Cambro-Ordovician carbonates. Combining the results of this study and Kim and Min (1996) shows that limestones located close to the Bakdallyeong gneiss complex have values around 0‰ and agree with Cambro-Ordovician values. Limestones distributed further east also have a similar carbon isotope composition (Figure. 3-1 and 3-14, and Table 3-4).

However, those further south show much higher positive values and are considered to belong to other geological periods. The limestones of the north are in contact with the pelitic rocks, which are distributed around the quartzites. The U-Pb ages of detrital zircons separated from these quartzites show a distribution concentrated at about 1870 Ma, similar to the characteristics of the Jangsan Formation, the lowest layer of the Joseon Supergroup. In other words, these quartzites are believed to be correlated with the Jangsan Formation. In this case, it can be seen that the pelitic rock layers surrounding the quartzite layers will be correlated to the Myobong Formation. That is, some of the quartzite, pelitic rock, and limestone layers that were previously classified as the Seochangni Formation distributed in the southern part of the Bakdallyeong gneiss complex may be correlated with the Jangsan, Myobong, and limestone layers of the Joseon Supergroup, respectively.

Meanwhile, the southern carbonate rocks have carbon isotope values of around +5‰. These values match those of Neoproterozoic rather than Cambro-Ordovician.

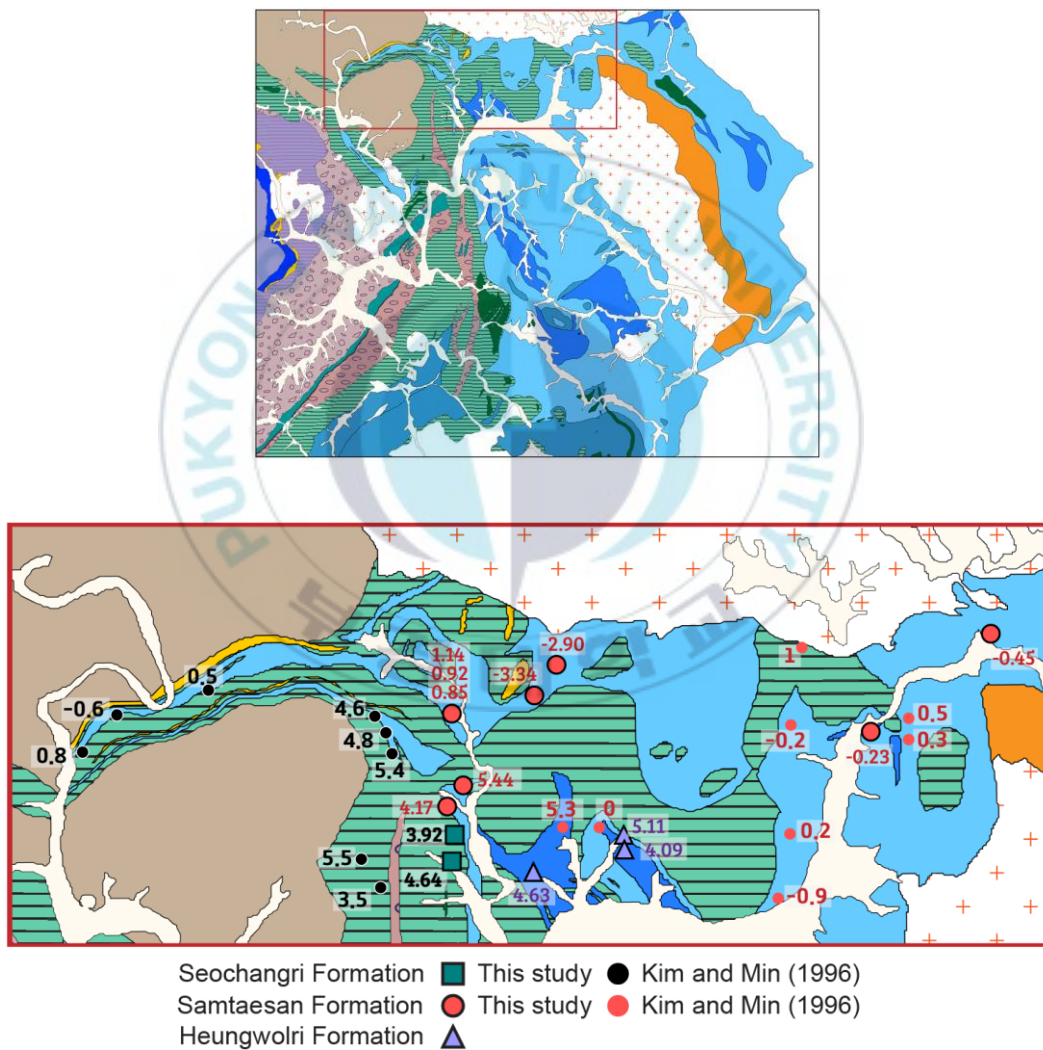
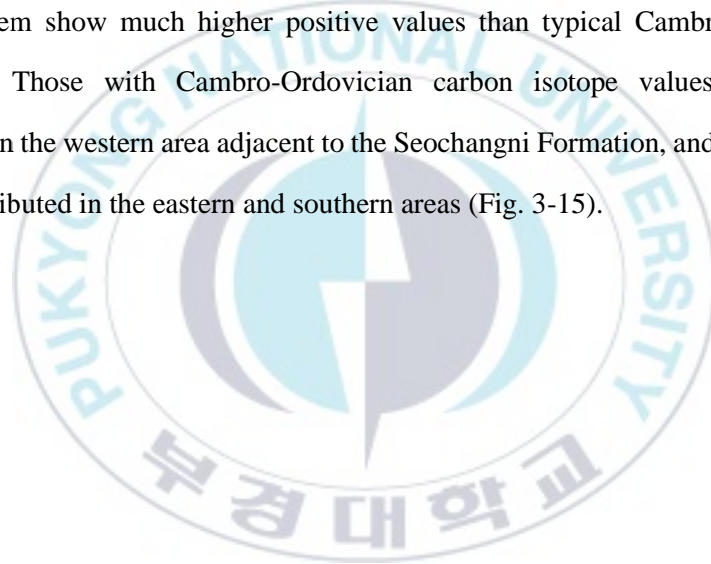


Figure 3-14. Carbon isotopic compositions for the area between Busan and Bakdallyeong gneiss complexes, including the published values (Kim and Min, 1996).

The area between the Seochangni Formation and the Geumsusan Quartzite

According to the 1:50,000-scale Hwanggangni quadrangle (Lee and Park, 1965) and Jecheon quadrangle (Kim et al., 1967), carbonate rocks distributed in this area are known to be composed of limestone, dolomite, and lime silicate rocks belonging to the Joseon Supergroup. In the Jecheon geological map, these limestone and dolomite layers were correlated to the Samtaesan Formation and the Heungwolri Formation, respectively (Kim et al., 1967). However, looking at their carbon isotope composition, many of them show much higher positive values than typical Cambro-Ordovician carbonates. Those with Cambro-Ordovician carbon isotope values are mainly distributed in the western area adjacent to the Seochangni Formation, and those that do not are distributed in the eastern and southern areas (Fig. 3-15).



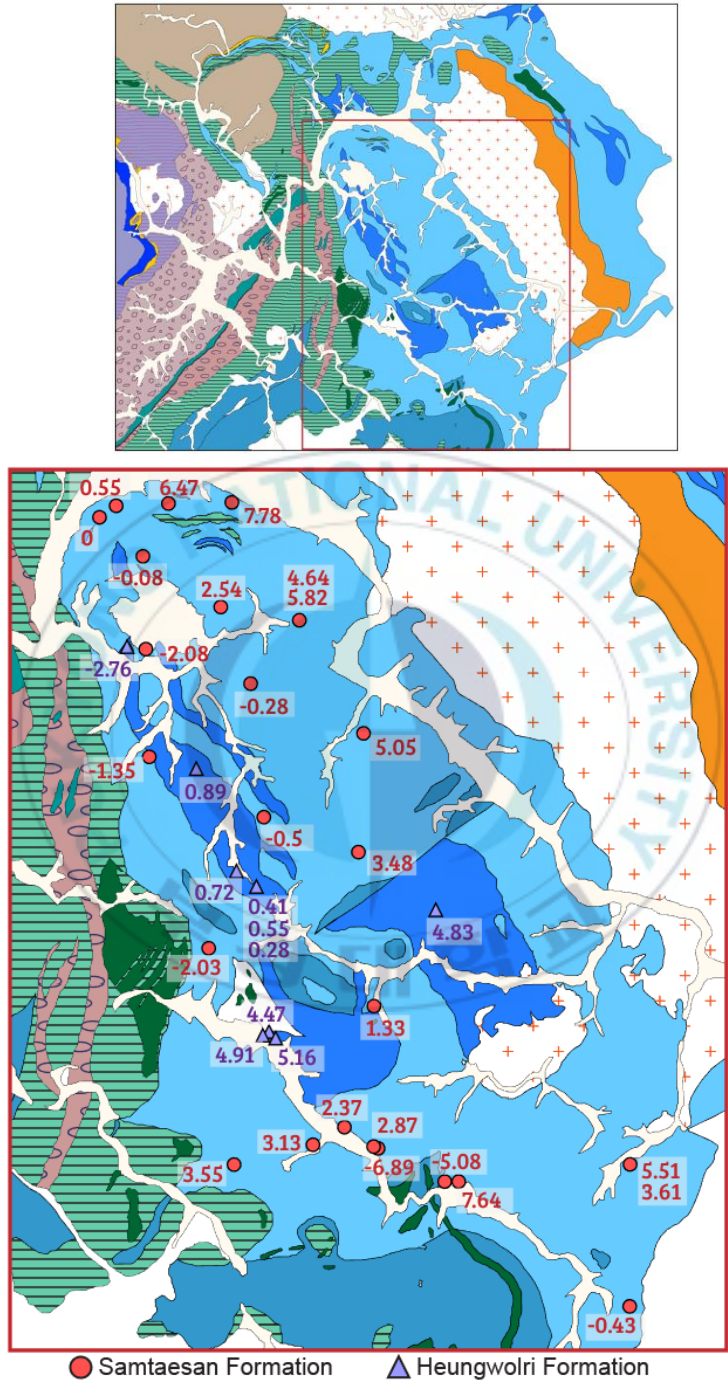


Figure 3-15. Carbon isotopic compositions for the area between the Seochangni Formation and the Geumsusan Quartzite.

The Samtaesan and the Heungwolli Formations in the area of Husan-ri

According to the Jecheon geological map, the Samtaesan Formation and the Heungwolri Formation are distributed in the Husan-ri area, surrounded by the Seochangni Formation. Analysis of these carbonate rocks showed that the carbon isotope values were around +5‰ (Figure 3-16).

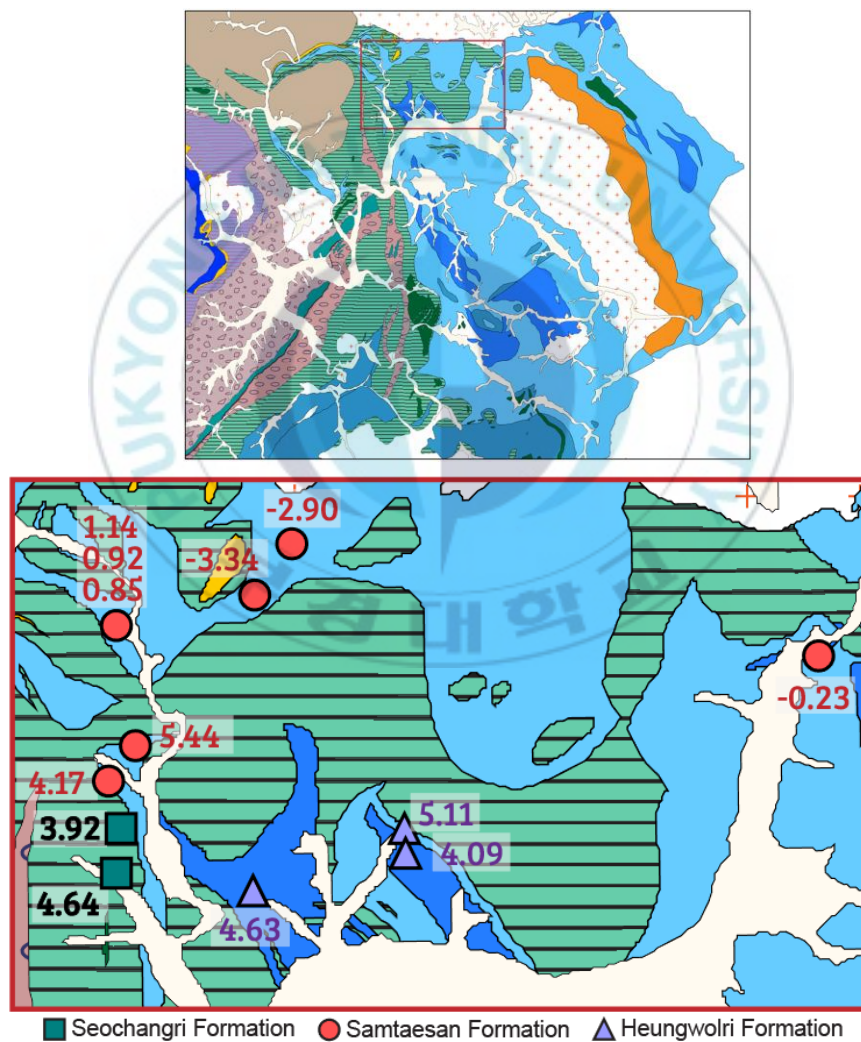


Figure 3-16. Carbon isotopic compositions for the Samtaesan and the Heungwolli Formations in the Husan-ri area.

The southwest periphery of the Busan gneiss complex

There are also two types of carbonate rocks in this area. It is distributed in a narrow belt shape among those with Neoproterozoic values (Figure 3-17).

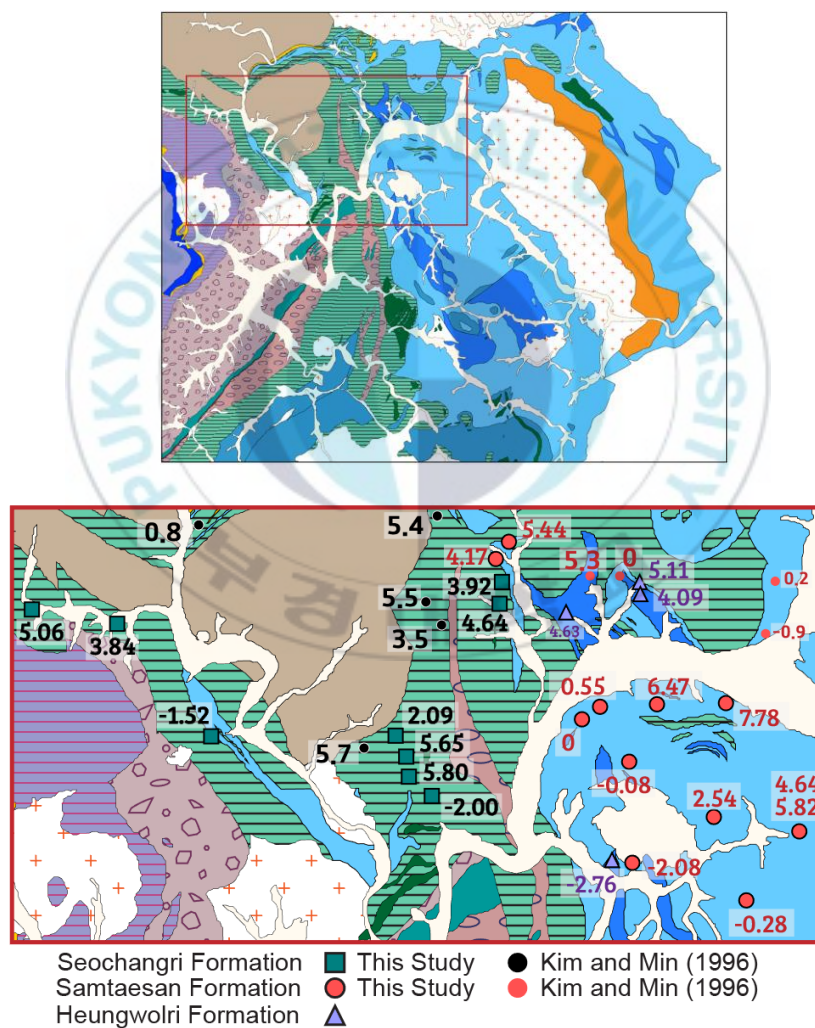


Figure 3-17. Carbon isotopic compositions for the southwest periphery of the Busan gneiss complex.

Table 3-4. Carbon and oxygen isotopic composition of the Seochangni, Samtaesan and Heunwolri Formations and Joseon Supergroup with numbers marked on the map (Fig. 3-1).

Number on the map	Sample #	Quadrangle	$\delta^{13}\text{C}$ (‰,PDB)	$\delta^{18}\text{O}$ (‰,PDB)	$\delta^{18}\text{O}$ (‰,SMOW)
Seochangri Fm.					
①	HYJ 106-1		2.09	-15.93	14.44
②	HYJ 109-1	Jecheon	5.65	-9.92	20.63
③	HYJ 110		5.80	-10.56	19.97
④	HYJ 112-2	Hwanggnagni	-2.00	-19.02	11.25
⑤	HYJ 120-1		4.64	-12.55	17.92
⑥	HYJ 122		3.92	-13.35	17.10
⑦	HYJ 410	Jecheon	5.06	-11.14	19.38
⑧	HYJ 414		-1.52	-12.16	18.32
⑨	HYJ 415		3.84	-9.82	20.74
Samtaesan Fm.					
1	HYJ 124		4.17	-10.09	20.46
2	HYJ 126-1		5.44	-7.31	23.32
3	HYJ 151	Jecheon	-2.90	-13.14	17.31
4	HYJ 153-2		-3.34	-13.68	16.76
5	HYJ 160	Hwanggnagni	-2.03	-13.86	16.57
	HYJ 174 -1		1.14	-11.03	19.49
6	HYJ 174- 2	Jecheon	0.92	-10.96	19.56
	HYJ 174- 3		0.85	-11.09	19.43
7	HYJ 303		3.55	-14.46	15.95
8	HYJ 304		3.13	-11.63	18.87
9	HYJ 305	Hwanggnagni	7.64	-8.98	21.60
10	HYJ 306		-5.08	-16.50	13.85
11	HYJ 308		-6.89	-11.58	18.92

Table 3-4 (Continued)

Number on the map	Sample #	Quadrangle	$\delta^{13}\text{C}$ (‰,PDB)	$\delta^{18}\text{O}$ (‰,PDB)	$\delta^{18}\text{O}$ (‰,SMOW)
12	HYJ 400		-1.50	-10.16	20.39
	HYJ 401-1		1.89	-13.01	17.45
13	HYJ 401-2	Danyang	2.85	-11.72	18.78
	HYJ 401-3		5.14	-11.23	19.28
14	HYJ 403		-0.50	-12.13	18.36
15	HYJ 405	Hwanggnagni	-1.35	-13.13	17.32
16	HYJ 406		7.78	-14.11	16.31
17	HYJ 407-1	Jecheon	6.47	-10.32	20.22
18	HYJ 408		0.00	-9.78	20.78
19	HYJ 409-1		4.64	-11.45	19.06
	HYJ 409-2	Hwanggnagni	5.82	-9.25	21.32
20	HYJ 419	Jecheon	-0.23	-14.50	15.91
21	HYJ 421	Yeongchun	-0.40	-15.19	15.20
22	HYJ 426		1.21	-9.89	20.66
23	HYJ 428	Jecheon	-0.45	-21.60	8.59
24	HYJ 508		1.33	-8.13	22.48
25	HYJ 517		0.55	-12.68	17.79
26	HYJ 519		-0.08	-10.77	19.76
27	HYJ 523		-2.08	-20.11	10.13
28	HYJ 524		2.54	-10.52	20.02
29	HYJ 527		-0.28	-14.80	15.60
30	HYJ 530	Hwanggnagni	5.05	-9.61	20.95
31	HYJ 532		3.48	-13.74	16.70
32	HYJ 535		-0.43	-10.87	19.65
33	HYJ 538		2.37	-10.91	19.61
34	HYJ 539		2.87	-11.31	19.20
35	HYJ 541w		3.61	-9.22	21.36
	HYJ 541b		5.51	-9.93	20.62

Table 3-4 (Continued)

Number on the map	Sample #	Quadrangle	$\delta^{13}\text{C}$ (‰,PDB)	$\delta^{18}\text{O}$ (‰,PDB)	$\delta^{18}\text{O}$ (‰,SMOW)
Heungwolri Fm.					
(1)	HYJ 23		4.47	-10.17	20.38
	HYJ 24-1		0.41	-11.22	19.29
(2)	HYJ 24-2	Hwanggnagni	0.55	-10.65	19.88
	HYJ 24-3		0.28	-10.92	19.60
(3)	HYJ 131-2		4.63	-6.18	24.49
(4)	HYJ 136	Jecheon	5.11	-5.88	24.80
(5)	HYJ 137-5		4.09	-11.47	19.04
(6)	HYJ 162		4.91	-9.85	20.71
(7)	HYJ 309		5.16	-7.39	23.24
(8)	HYJ 402	Hwanggnagni	0.72	-9.06	21.52
(9)	HYJ 404a		0.89	-7.22	23.42
(10)	HYJ 423	Yeongchun	0.29	-12.37	18.11
(11)	HYJ 520-1		-2.76	-8.43	22.17
(12)	HYJ 533	Hwanggnagni	4.83	-11.12	19.40
Lime-silicate rock					
	HYJ 22-3	Hwanggangni	-1.07	-15.53	14.85
Pungchon Ls.					
	HYJ 31-1	Changdong	0.11	-12.92	17.54
	HYJ 37-1		0.58	-10.72	19.81
	HYJ 37-2	Dangyang	0.45	-11.16	19.36
Jeongseon Ls.					
	HYJ 32-1	Changdong	0.22	-11.07	19.45
Machari Fom.					
	HYJ 33-1	Yeongwol	1.00	-10.99	19.53
Yeongheung Fm.					
	HYJ 34	Yeongwol	-1.11	-7.09	23.55

4.4 Further tectonic implications

The lower Paleozoic Joseon Supergroup has been conventionally differentiated into five types based on distinct lithologic successions and geographic distribution. Choi (1998a) proposed a revised stratigraphic nomenclature for the Joseon Supergroup: i.e the Taebaek, Yongwol, Yongtan, Pyongchang, and Mungyon groups which replace the Tuwibont-type, Yongwol-type, Chongson-type, Pyongchang-type, and Mungyong-type Joseon Supergroup, respectively. The replaced sequences had been firstly designated by Kobayashi et al. (1942).

The interpretations for the contact between the Okcheon Metamorphic Belt and Taebaeksan Basin can be categorized into three Conformity (Reedman et al., 1973; Kihm et al., 1996, 1999), Unconformity (Lee and Park, 1965; and Son, 1970), and thrust (Chough et al., 2000; Ree et al., 2001). Although the boundary area between them is a key area to better understand the tectonic evolution of the Korean Peninsula and even Northeast Asia, their contact relationship has still been pending.

As stated above, the Chungju-Jecheon area is located at the juncture of the Okcheon Metamorphic Belt and Taebaeksan Basin. According to the 1:50,000-scale Jecheon (Kim et al., 1967) and Hwanggangni (Lee and Park, 1965) quadrangles, the Samtaesan and Heungwolri Formations are the constituent upper part of the Yeongweol Group and assigned the Ordovician. Furthermore, the age-unknown Seochangni Formation covers the Joseon Supergroup unconformably but their stratigraphic relationships are still debatable and thus detailed mapping is needed as well.

The deposition timing for the metasedimentary and metavolcanic sequences of the Okcheon Metamorphic Belt has been contentious. the recent studies for the U-Pb zircon

age facilitate a better understanding of constituents of the Okcheon Metamorphic Belt. Precise depositional ages for the Okcheon Metamorphic Belt and its stratigraphy as well as its relationship with the Joseon Supergroup are poorly constrained at present. In a sense, the Chungju-Jecheon area may have a role in Paleotectonic reconstruction.

The Seochangni Formation, which consists mainly of pelitic rocks with alternating quartzose sandstones and calcareous units, is distributed in the northeastern part of the Okcheon Metamorphic Belt. The detrital zircon U-Pb ages from the Seochangni Formation displays from late Paleoproterozoic to the latest Mesoproterozoic. An intercalated limestone layer shows 0.70587 of the $^{87}\text{Sr}/^{86}\text{Sr}$ ratio. This value suggests that it was deposited at ca. 850 Ma.

The Bugnori Formation in the west is considered as composing of glaciogenic sediments, diamictite, and shows detrital zircon age distributions similar to the Seochangni Formation. The Hwanggangni Formation is also considered as making up of the diamictite, and the detrital zircon age differs from region to region. Adjacent to the Bugnori Formation, the Mesoproterozoic component is predominant, but it is dominant by ca. 750 Ma and 1870 Ma according to the distance, which suggests its deposition after ca. 750 Ma.

Ha et al. (2021) constraint on the Hyangsanni Dolomite depositional timing by applying chemostratigraphy (Figure 4-1). The Carbon, Oxygen, and Strontium isotopes were analyzed from the Hyangsanni Dolomite, located further west than the Hwanggangni Formation. The Hyangsanni Dolomite has comparatively consistent and high $\delta^{13}\text{C}(\text{PDB})$ values of about 5‰ (Figure 4-1a), and 0.7071 of minimum initial $^{87}\text{Sr}/^{86}\text{Sr}$ ratio (Figure 4-1b). Considering the isotope results, Ha et al., (2021) suggest that the depositions of the Hyangsanni Dolomite and adjacent the Hwanggangni

diamictite have an affinity with the glaciation of about 710 Ma.

Carbon isotope data from the Seochangni, Samtaesan, and Heungwolri Formations might bear on their age roughly. This study on the carbonate rocks distributed in the Chungju- Jecheon area suggests the following inference based on carbon isotopic composition.

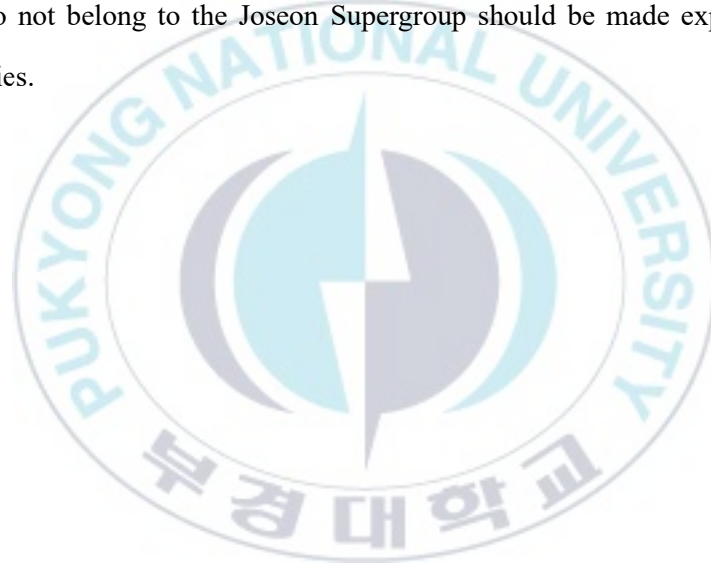
This study verifies that some of the Samtaesan and Heungwolri Formations in the Chungju-Jecheon area, which have been classified as the Joseon Supergroup, do not belong to the Joseon Supergroup. In addition, the Seochangni Formation, which was age-unknown, produced similar results which indicate both of Paleozoic and neither, to those of the Samtaesan and Heungwolri Formations. Such results raise the need for the conventional boundary between the Okcheon Metamorphic Belt and Taebaeksan Basin to be reaffirmed.

If the Okcheon Metamorphic Belt including the Hyangsanni Dolomite and Seochangni Formation correlates with the North China Craton, and the Okcheon Metamorphic Belt and Taebaeksan Basin was conformable, it means a continuous distribution from the Neoproterozoic Seochangni Formation in the Okcheon Metamorphic Belt to Paleozoic Taebaeksan Basin. On the other hand, if the carbonate rocks distributed in the juncture of the Okcheon Metamorphic Belt and Taebaeksan Basin were deposited in the early Cambrian, it is discovered the potential of sedimentary basins deposited before the Jangsan Quartzite.

The occurrence of the Neoproterozoic glaciogenic sedimentary successions and the zircon U-Pb age distribution characteristics of the northeast Okcheon Metamorphic Belt are very comparable to the southwest region of North Korea and the southern margin of North China Craton. Together with the spatial and temporal correlation of

North Korea and the North China Craton, this study provides a new view to reconstructing Paleotectonics of the Korean Peninsula, even east Asia.

In addition, in light of the $\delta^{13}\text{C}$ signal, we prefer to propose a new definition of stratigraphic classification for carbonates that occurred in the Chungju-Jecheon area. In other words, stratigraphic units having $\delta^{13}\text{C}$ values different from those of the Paleozoic would be better to denominate a new name distinguished from conventional stratigraphy. Furthermore, the precise boundary between the two types of carbonate rock that do not belong to the Joseon Supergroup should be made explicit through further studies.



5 Conclusion

Through carbon chemostratigraphy studies on carbonate rocks in the Chungju-Jecheon region, which are known to have a mixed distribution of Neoproterozoic and Paleozoic sequences through previous studies, their geological ages could be more accurately distinguished.

The depositional timing of the Seochangni Formation has been debatable, while the Samtaesan and Heunwolri Formations have conventionally been regarded as Cambro-Ordovician strata. However, the carbon values obtained in this study are quite different from our preconceptions. Some data fall well within the Cambro-Ordovician limits, but others are distributed over a wide range which sets it apart from Cambro-Ordovician values. Most of them have positive $\delta^{13}\text{C}$ values much higher than most Cambro-Ordovician (around 0‰). Furthermore, a few displays considerable negative $\delta^{13}\text{C}$ values (down to -6.9‰) than typical Cambro-Ordovician carbonates.

Taken together, this study suggests that a significant portion of the carbonate rocks, previously classified as a lower Paleozoic Joseon Supergroup, were deposited during the earliest Cambrian or Neoproterozoic. It means that Some of the Samtaesan and Heungwolri Formations distributed in the Jecheon area might have different ancestry from representative those of the Joseon Supergroup, and a new stratigraphic name may have to be given that distinguishes it from the existing one. In addition, it is also necessary to redefine the boundary between the Okcheon Metamorphic Belt and the Taebaeksan Basin. But further intensive multilateral studies are required for specifying their depositional timing.

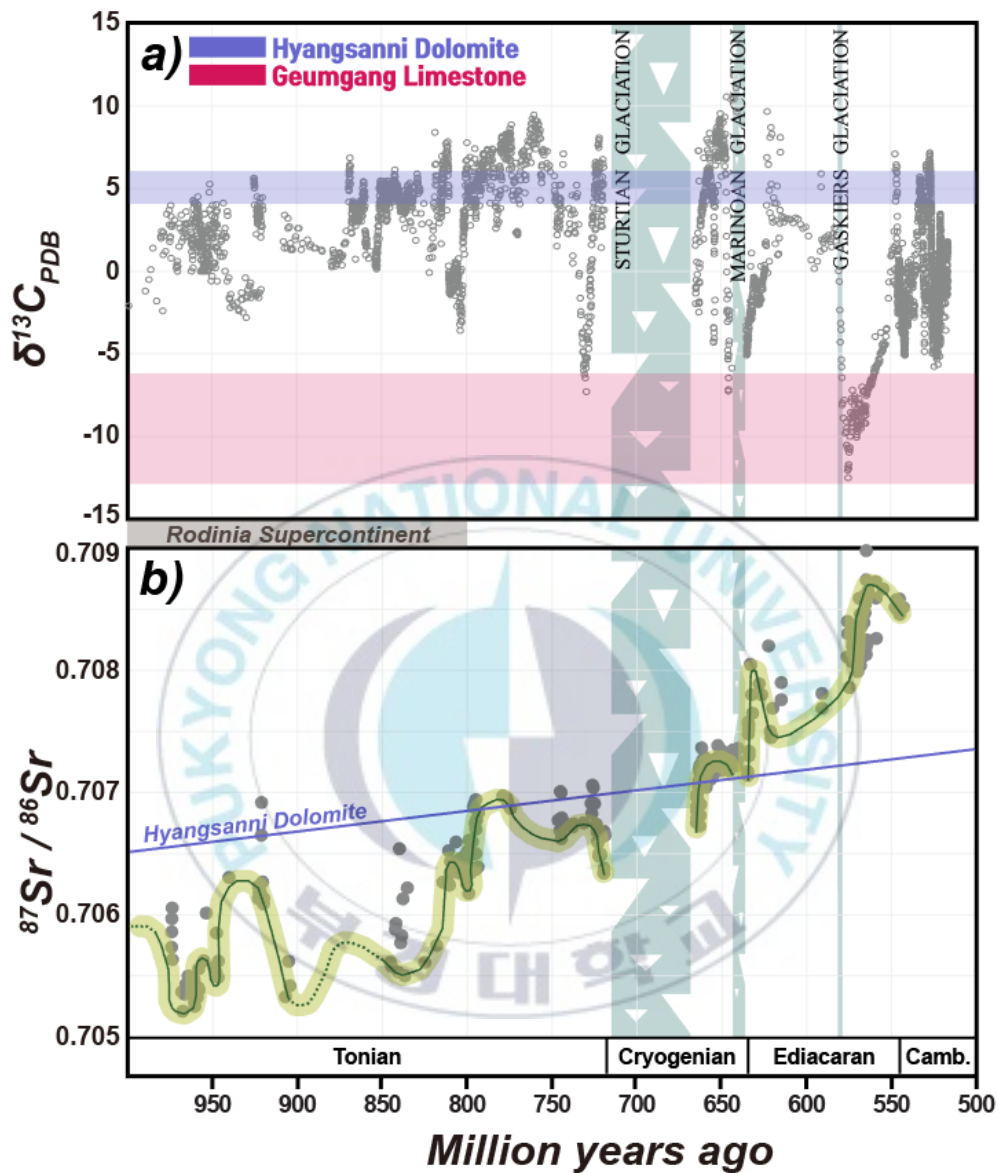


Figure 4-1. Composite a) carbon and b) strontium isotope records for the Neoproterozoic from marine carbonate rocks (modified from Zhou et al., 2020). In the top plot, the range of carbon isotope values determined in the Hyangsanni Dolomite and Geumgang Limestone are also shown as a purple-colored and pink-colored bands, respectively. The lines in the bottom plot show the corrected initial $^{87}Sr/^{86}Sr$ ratios according to the age based on its Rb/Sr ratios from the sample with the lowest present $^{87}Sr/^{86}Sr$ ratios among the analyzed values from the Hyangsanni Dolomite.

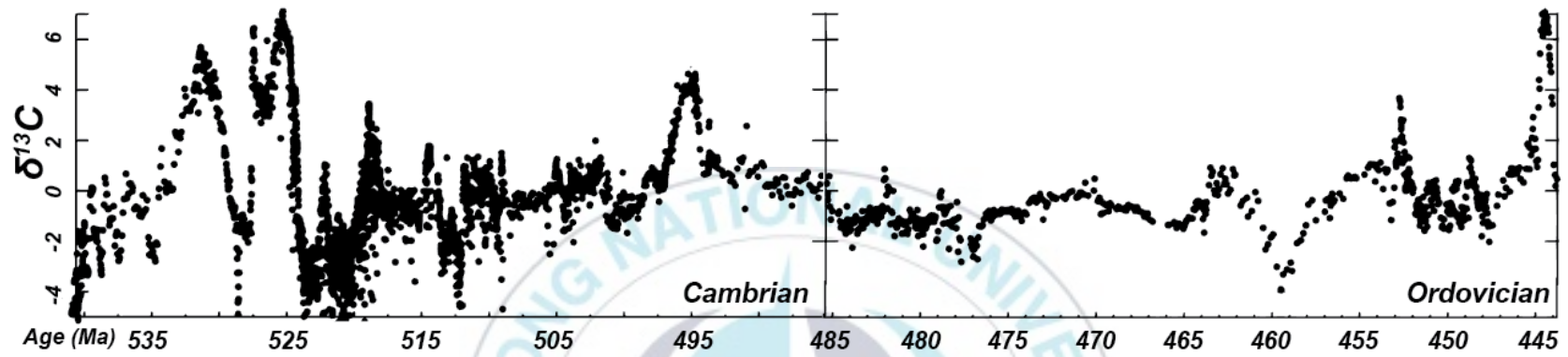


Figure 4-2. Variation of $\delta^{13}\text{C}$ through the Cambrian and Ordovician (modified from Saltzman and Thomas, 2012).

SUMMARY AND CONCLUDING REMARKS

Integrating geochemical data with available reference data and stratigraphic correlation among periphery strata leads to the following inferences.

Its distinctly negative carbon isotope values (lower than -12) and direct contact with the diamictite layer thought to have been deposited during glaciation suggests that the Geumgang Limestone is most likely a cover carbonate layer deposited after Neoproterozoic glaciation.

Based on carbon isotope values, we suggest that much of the carbonate rocks distributed west of the Geumsusan Quartzite are Neoproterozoic sequences (or very early Cambrian). Therefore, it is necessary to redefine the boundary between the Okcheon Metamorphic Belt and Taebaeksan Basin.

Information on the carbonates from this study manifests that the Neoproterozoic glaciation event was present in South Korea. Therefore, it can be another clue to untangling the Neoproterozoic tectonic connection between North and South China Cratons and Korean Peninsula. The redefinition of boundary between the Okcheon metamorphic belt and the Taebaeksan Basin will help understand the evolution of the integrated basin combining the Okcheon Metamorphic Belt and the Taebaeksan Basin from the Neoproterozoic to the Cambro-Ordovician and its correlation with the Pyeongnam Basin in North Korea.

REFERENCES

- Aharon, P. (2005). Redox stratification and anoxia of the early Precambrian oceans: implications for carbon isotope excursions and oxidation events. *Precambrian Research*, 137(3-4), 207-222.
- Baker, A. J., & Fallick, A. E. (1989). Evidence from Lewisian limestones for isotopically heavy carbon in two-thousand-million-year-old sea water. *Nature*, 337(6205), 352-354.
- Baker, A. J., & Fallick, A. E. (1989). Heavy carbon in two-billion-year-old marbles from Lofoten-Vesterålen, Norway: Implications for the Precambrian carbon cycle. *Geochimica et Cosmochimica Acta*, 53(5), 1111-1115.
- Bau, M. (1999). Scavenging of dissolved yttrium and rare earths by precipitating iron oxyhydroxide: experimental evidence for Ce oxidation, Y-Ho fractionation, and lanthanide tetrad effect. *Geochimica et Cosmochimica Acta*, 63(1), 67-77.
- Bau, M., & Dulski, P. (1996). Distribution of yttrium and rare-earth elements in the Penge and Kuruman iron-formations, Transvaal Supergroup, South Africa. *Precambrian Research* 79, 37-55.
- Baumgartner, L. P., & Valley, J. W. (2001). Stable isotope transport and contact metamorphic fluid flow. *Reviews in Mineralogy and Geochemistry*, 43(1), 415-467.
- Bolhar, R., & Van Kranendonk, M. J. (2007). A non-marine depositional setting for the northern Fortescue Group, Pilbara Craton, inferred from trace element geochemistry of stromatolitic carbonates. *Precambrian Research*, 155(3-4), 229-250.
- Brasier, M. D., Shields, G., Kuleshov, V. N., & Zhegallo, E. A. (1996). Integrated chemo- and biostratigraphic calibration of early animal evolution: Neoproterozoic–early Cambrian of southwest Mongolia. *Geological Magazine*, 133(4), 445-485.
- Filho, S., Paula-Santos, G.M., & Dias-Brito, D. (2018). Carbonate REE Y signatures from the restricted early marine phase of South Atlantic Ocean (late Aptian–Albian): The influence of early anoxic diagenesis on shale-normalized REE Y patterns of ancient carbonate rocks. *Palaeogeography, Palaeoclimatology, Palaeoecology* 500, 69-83.

- Chen, X., Kuang, H., Liu, Y., Wang, Y., Yang, Z., Vandyk, T.M., Le Heron, D.P., Wang, S., Geng, Y., & Bai, H. (2020). Subglacial bedforms and landscapes formed by an ice sheet of Ediacaran-Cambrian age in west Henan, North China. *Precambrian Research* 344, 105727.
- Cheong, C. H. (1969). Stratigraphy and paleontology of the Samcheog Coalfield, Gangweondo, Korea (I). *Journal of the Geological Society of Korea*, 5(1), 13-55. (in Korean with English abstract)
- Cheong, C., Jeong, G.Y., Kim, H., Choi, M., Lee, S., & Cho, M. (2003). Early Permian peak metamorphism recorded in U–Pb system of black slates from the Ogcheon metamorphic belt, South Korea, and its tectonic implication. *Chemical Geology* 193, 81-92.
- Cheong, C. H., Lee, D. Y., Ryu, Y. S., & Kang, K. W., (1979). Explanatory text of the geological map of Yeongwol Sheet, Sheet 6826-II, Scale 1:50,000. Geological Survey of Korea.
- Cheong, C. S., Kee, W. S., Jeong, Y. J., & Jeong, G. Y. (2006). Multiple deformations along the Honam shear zone in southwestern Korea constrained by Rb–Sr dating of synkinematic fabrics: implications for the Mesozoic tectonic evolution of northeastern Asia. *Lithos*, 87(3-4), 289-299.
- Cheong, W., Cho, M., Yi, K., Lee, M. S., & Kim, Y. (2016). Jurassic (~170Ma) Zircon U-Pb Age of a “Granite Boulder” in the Geumgang Limestone, Ogcheon Metamorphic Belt, Korea : Reinterpretation of its Origin 25, 29-37.
- Cho, D. L., Suzuki, K., Adachi, M., & Chwae, U. (1996). A preliminary CHIME age determination of monazite from metamorphic and granitic rocks in the Gyeonggi massif, Korea. *Journal of Earth and Planetary Sciences, Nagoya University*, 43, 49-65.
- Cho, M., Kim, H., Lee, Y., Horie, K., & Hidaka, H. (2008). The oldest (ca. 2.51 Ga) rock in South Korea: U-Pb zircon age of a tonalitic migmatite, Daeijak Island, western Gyeonggi massif. *Geosciences Journal*, 12(1), 1-6.
- Cho, M., Kim, T., & Kim, H. (2004). SHRIMP U-Pb zircon Age of a Felsic Meta-tuff in the Ogcheon Metamorphic Belt, Korea: Neoproterozoic (ca. 750 Ma) Volcanism, *Journal of the Petrological Society of Korea* 13, 119-125. (in Korean with English abstract)
- Cho, M., Cheong, W., Ernst, W.G., Yi, K., & Kim, J. (2013). SHRIMP U-Pb ages of detrital zircons in metasedimentary rocks of the central Ogcheon fold-thrust belt, Korea: Evidence for tectonic assembly of Paleozoic sedimentary protoliths. *Journal of Asian Earth Sciences* 63, 234-249.

- Cho, M., Lee, Y., Kim, T., Cheong, W., Kim, Y., & Lee, S.R. (2017). Tectonic evolution of Precambrian basement massifs and an adjoining fold-and-thrust belt (Gyeonggi Marginal Belt), Korea: An overview. *Geosciences Journal* 21, 845-865.
- Choi, D. K. (1998). The Yongwol Group (Cambrian-Ordovician) redefined: a proposal for the stratigraphic nomenclature of the Choson Supergroup. *Geosciences Journal*, 2(4), 220-234.
- Choi, D.K. (2019). Evolution of the Taebaeksan Basin, Korea: I, early Paleozoic sedimentation in an epeiric sea and break-up of the Sino-Korean Craton from Gondwana. *Island Arc* 28, e12275.
- Choi, D.K., & Chough, S.K. (2005). The Cambrian-Ordovician stratigraphy of the Taebaeksan Basin, Korea: a review. *Geosciences Journal* 9, 187-214.
- Choi, D. K., Lee, J. G., Kim, D. H., Lee, S. B., Park, T. Y., & Hong, P. S. (2014). Early Paleozoic trilobite biostratigraphy of the Joseon Supergroup, Taebaeksan Basin, Korea: A synthesis. *Journal of the Geological Society*, 106-106.
- Choi, D. K., Lee, J. G., LEE, S. B., PARK, T. Y. S., & Hong, P. S. (2016). Trilobite biostratigraphy of the lower Paleozoic (Cambrian–Ordovician) Joseon Supergroup, Taebaeksan Basin, Korea. *Acta Geologica Sinica-English Edition*, 90(6), 1976-1999.
- Choi, D. K., & Park, T. Y. S. (2017). Recent advances of trilobite research in Korea: Taxonomy, biostratigraphy, paleogeography, and ontogeny and phylogeny. *Geosciences Journal*, 21(6), 891-911.
- Choi, D.K., Woo, J., & Park, T. (2012). The Okcheon Supergroup in the Lake Chungju area, Korea: Neoproterozoic volcanic and glaciogenic sedimentary successions in a rift basin. *Geosciences Journal* 16, 229-252.
- Choi, J., E. (2013). SHRIMP U-Pb zircon ages of the Suchangri formation in Okcheon. MSc Thesis, Pukyong National University, Busan, Korea.
- Choi, S. J., Kim, D. Y., Cho, D. L., & Kim, Y. B. (2015). Detrital zircon U-Pb ages of the metapelite on the southwestern part of the Ogcheon Belt and its stratigraphical implication. *The Journal of the Petrological Society of Korea*, 24(1), 55-63. (in Korean with English abstract)
- Chough, S. K., Kim, H., Woo, J., & Lee, H. S. (2006). Tectonic implications of quartzite-shale and phyllite beds in the Seochangri Formation (Okcheon Group), Bonghwajae section, mid-Korea. *Geosciences Journal*, 10(4), 403-421.

- Chough, S., Kwon, S., Ree, J., & Choi, D. (2000). Tectonic and sedimentary evolution of the Korean peninsula: a review and new view. *Earth-Science Reviews* 52, 175-235.
- Cluzel, D., Cadet, J. P., & Lapierre, H. (1990). Geodynamics of the Ogcheon belt (South Korea). *Tectonophysics*, 183(1-4), 41-56.
- Cluzel, D. (1992). Late Paleozoic to early Mesozoic geodynamic evolution of the Circum-Pacific orogenic belt in South Korea and Southwest Japan. *Earth and Planetary Science Letters* 108, 289-305.
- Cluzel, D., Jolivet, L., & Cadet, J. P. (1991). Early middle Paleozoic intraplate orogeny in the Ogcheon belt (South Korea): a new insight on the Paleozoic buildup of East Asia. *Tectonics*, 10(6), 1130-1151.
- Corsetti, F.A., & Grotzinger, J.P. (2005). Origin and significance of tube structures in Neoproterozoic post-glacial cap carbonates: example from Noonday Dolomite, Death Valley, United States. *Palaios* 20, 348-362.
- Corsetti, F.A., & Lorentz, N.J. (2006). On Neoproterozoic cap carbonates as chronostratigraphic markers, in: Anonymous, *Neoproterozoic geobiology and paleobiology*. Springer, pp. 273-294.
- Corsetti, F. A., Stewart, J. H., & Hagadorn, J. W. (2007). Neoproterozoic diamictite-cap carbonate succession and $\delta^{13}\text{C}$ chemostratigraphy from eastern Sonora, Mexico. *Chemical Geology*, 237(1-2), 129-142.
- Cox, G.M., Halverson, G.P., Stevenson, R.K., Vokaty, M., Poirier, A., Kunzmann, M., Li, Z., Denyszyn, S.W., Strauss, J.V., & Macdonald, F.A. (2016). Continental flood basalt weathering as a trigger for Neoproterozoic Snowball Earth. *Earth and Planetary Science Letters* 446, 89-99.
- Craig, H. (1953). The geochemistry of the stable carbon isotopes. *Geochimica et cosmochimica acta*, 3(2-3), 53-92.
- Derry, L. A., & Jacobsen, S. B. (1990). The chemical evolution of Precambrian seawater: evidence from REEs in banded iron formations. *Geochimica et Cosmochimica Acta*, 54(11), 2965-2977.
- Du, Q., Qin, Z., Wang, J., Wang, Z., Deng, Q., & Yang, F. (2020). The Cryogenian Nanhuan System (South China) during the interglacial-glacial transition: geochemistry, sedimentary provenance, and tectonic setting. *International Geology Review*, 1-19.

- Elderfield, H., & Greaves, M.J. (1982). The rare earth elements in seawater. *Nature* 296, 214.
- Ernst, W. G., & Liou, J. G. (1995). Contrasting plate-tectonic styles of the Qinling-Dabie-Sulu and Franciscan metamorphic belts. *Geology*, 23(4), 353-356.
- Fairchild, I.J., & Kennedy, M.J. (2007). Neoproterozoic glaciation in the Earth System. *Journal of the Geological Society* 164, 895-921.
- Fairchild, I.J., Spiro, B., Herrington, P.M., & Song, T. (2000). Controls on Sr and C isotope compositions of Neoproterozoic Sr-rich limestones of East Greenland and North China.
- Fölling, P. G., & Frimmel, H. E. (2002). Chemostratigraphic correlation of carbonate successions in the Gariep and Saldania Belts, Namibia and South Africa. *Basin Research*, 14(1), 69-88.
- Font, E., Nédélec, A., Trindade, R., Macouin, M., & Charrière, A. (2006). Chemostratigraphy of the Neoproterozoic Mirassol d'Oeste cap dolostones (Mato Grosso, Brazil): an alternative model for Marinoan cap dolostone formation. *Earth and Planetary Science Letters* 250, 89-103.
- Friend, C.R., Nutman, A.P., Bennett, V.C., & Norman, M. (2008). Seawater-like trace element signatures (REE Y) of Eoarchean chemical sedimentary rocks from southern West Greenland, and their corruption during high-grade metamorphism. *Contributions to Mineralogy and Petrology* 155, 229-246.
- Frimmel, H.E. (2010). On the reliability of stable carbon isotopes for Neoproterozoic chemostratigraphic correlation. *Precambrian Research* 182, 239-253.
- Geological Investigation Corps of Taebaeksan Region (1962) Report on the geology and mineral resources of the Taebaeksan Region. Geological Society of Korea, Seoul, 89 p. (in
- Grotzinger, J.P., Fike, D.A., & Fischer, W.W. (2011). Enigmatic origin of the largest-known carbon isotope excursion in Earth's history. *Nature Geoscience* 4, 285-292.
- Guacaneme, C., Babinski, M., Paula-Santos, G.M.d., & Pedrosa-Soares, A.C. (2017). C, O, and Sr isotopic variations in Neoproterozoic-Cambrian carbonate rocks from Sete Lagoas Formation (Bambuí Group), in the Southern São Francisco Basin, Brazil. *Brazilian Journal of Geology* 47, 521-543.
- Ha, Y., Satish-Kumar, M., Park, K. H., Song, Y. S., & Liu, S. (2021). Carbon, oxygen and strontium isotope geochemistry of the late Neoproterozoic carbonate

- platform deposit Hyangsanni Dolomite of the Okcheon metamorphic belt, Korea. *Lithos*, 396, 106219.
- Halverson, G.P., Dudás, F.Ö., Maloof, A.C., & Bowring, S.A. (2007). Evolution of the $^{87}\text{Sr}/^{86}\text{Sr}$ composition of Neoproterozoic seawater. *Palaeogeography, Palaeoclimatology, Palaeoecology* 256, 103-129.
- Halverson, G.P., Hoffman, P.F., Schrag, D.P., Maloof, A.C., & Rice, A.H.N. (2005). Toward a Neoproterozoic composite carbon-isotope record. *GSA Bulletin* 117, 1181-1207.
- Halverson, G.P., Maloof, A.C., & Hoffman, P.F. (2004). The Marinoan glaciation (Neoproterozoic) in northeast Svalbard. *Basin Research* 16, 297-324.
- Halverson, G.P., Porter, S.M., & Gibson, T.M. (2018). Dating the late Proterozoic stratigraphic record. *Emerging topics in life sciences* 2, 137-147.
- Halverson, G.P., & Shields-Zhou, G. (2011). Chemostratigraphy and the Neoproterozoic glaciations. *Geological Society, London, Memoirs* 36, 51-66.
- Halverson, G.P., Wade, B.P., Hurtgen, M.T., & Barovich, K.M. (2010). Neoproterozoic chemostratigraphy. *Precambrian Research* 182, 337-350.
- Halverson, G.P., Hoffman, P.F., Schrag, D.P., & Kaufman, A.J. (2002). A major perturbation of the carbon cycle before the Ghaub glaciation (Neoproterozoic) in Namibia: Prelude to snowball Earth?. *Geochemistry, Geophysics, Geosystems* 3, 1-24.
- Higgins, J. A., Blättler, C. L., Lundstrom, E. A., Santiago-Ramos, D. P., Akhtar, A. A., Ahm, A. C., & Swart, P. K. (2018). Mineralogy, early marine diagenesis, and the chemistry of shallow-water carbonate sediments. *Geochimica et Cosmochimica Acta*, 220, 512-534.
- Hoffman, P.F., Kaufman, A.J., Halverson, G.P., & Schrag, D.P. (1998). A Neoproterozoic snowball earth. *Science (New York, N.Y.)* 281, 1342-1346.
- Hohl, S.V., Becker, H., Jiang, S., Ling, H., Guo, Q., & Struck, U. (2017). Geochemistry of Ediacaran cap dolostones across the Yangtze Platform, South China: implications for diagenetic modification and seawater chemistry in the aftermath of the Marinoan glaciation. *Journal of the Geological Society* 174, 893-912.
- Hong, S.H., Hwang, S. G., & Cho, D. L. (1995). Explanatory text of the geological map of Changdong Sheet, Scale 1:50,000. Geological Survey of Korea.

- Hong, S.K., & Lee, Y.I. (2007). Geological age of the Jeongseon Formation, Joseon Supergroup (lower Paleozoic): a perspective from carbon isotope stratigraphy. *Geosciences Journal* 11, 1.
- Hood, A., Planavsky, N. J., Wallace, M. W., & Wang, X. (2018). The effects of diagenesis on geochemical paleoredox proxies in sedimentary carbonates. *Geochimica et Cosmochimica Acta*, 232, 265-287.
- Hu, B., Zhai, M., Li, T., Li, Z., Peng, P., Guo, J., & Kusky, T.M. (2012). Mesoproterozoic magmatic events in the eastern North China Craton and their tectonic implications: Geochronological evidence from detrital zircons in the Shandong Peninsula and North Korea. *Gondwana Research* 22, 828-842.
- Huang, J., Chu, X., Chang, H., & Feng, L. (2009). Trace element and rare earth element of cap carbonate in Ediacaran Doushantuo Formation in Yangtze Gorges. *Chinese Science Bulletin* 54, 3295-3302.
- Hudson, J. D., & Anderson, T. F. (1989). Ocean temperatures and isotopic compositions through time. *Earth and Environmental Science Transactions of the Royal Society of Edinburgh*, 80(3-4), 183-192.
- Jacobsen, S.B., & Kaufman, A.J. (1999). The Sr, C and O isotopic evolution of Neoproterozoic seawater. *Chemical Geology* 161, 37-57.
- Jacques, L., Ogle, N., Moussa, I., Kalin, R., Vignaud, P., Brunet, M., & Bocherens, H. (2008). Implications of diagenesis for the isotopic analysis of Upper Miocene large mammalian herbivore tooth enamel from Chad. *Palaeogeography, Palaeoclimatology, Palaeoecology*, 266(3-4), 200-210.
- James, N.P., Narbonne, G.M., & Kyser, T.K. (2001). Late Neoproterozoic cap carbonates: Mackenzie Mountains, northwestern Canada: precipitation and global glacial meltdown. *Canadian Journal of Earth Sciences* 38, 1229-1262.
- Jiang, G., Kaufman, A.J., Christie-Blick, N., Zhang, S., & Wu, H. (2007). Carbon isotope variability across the Ediacaran Yangtze platform in South China: implications for a large surface-to-deep ocean $\delta^{13}\text{C}$ gradient. *Earth and Planetary Science Letters* 261, 303-320.
- Jiang, G., Kennedy, M.J., & Christie-Blick, N. (2003). Stable isotopic evidence for methane seeps in Neoproterozoic postglacial cap carbonates. *Nature* 426, 822.
- Jones, C. E., & Jenkyns, H. C. (2001). Seawater strontium isotopes, oceanic anoxic events, and seafloor hydrothermal activity in the Jurassic and Cretaceous. *American Journal of Science*, 301(2), 112-149.

- Kaufman, A.J., Hayes, J., Knoll, A.H., & Germs, G.J. (1991). Isotopic compositions of carbonates and organic carbon from upper Proterozoic successions in Namibia: stratigraphic variation and the effects of diagenesis and metamorphism. *Precambrian Research* 49, 301-327.
- Kaufman, A. J., Jacobsen, S. B., & Knoll, A. H. (1993). The Vendian record of Sr and C isotopic variations in seawater: implications for tectonics and paleoclimate. *Earth and Planetary Science Letters*, 120(3-4), 409-430.
- Kaufman, A.J., & Knoll, A.H. (1995). Neoproterozoic variations in the C-isotopic composition of seawater: stratigraphic and biogeochemical implications. *Precambrian Research* 73, 27-49.
- Kaufman, A. J., Knoll, A. H., & Narbonne, G. M. (1997). Isotopes, ice ages, and terminal Proterozoic earth history. *Proceedings of the National Academy of Sciences*, 94(13), 6600-6605.
- Kaufman, A. J., Sial, A. N., Frimmel, H. E., & Misi, A. (2009). Neoproterozoic to Cambrian palaeoclimatic events in southwestern Gondwana. *Developments in Precambrian Geology*, 16, 369-388.
- Kang, J. H. (1994). Geological structure and tectonics of the Ogcheon zone in the Chungju-Jangseonri area, South Korea. *Journal of Science (Hiroshima University) C*, 10, 11-23.
- Kang, J., Lee, D., Noh, S., Jeong, J., & Koh, S. (2017). Geology and constituent rocks of the Chungju-Goesan area in the northwestern part of Ogcheon metamorphic zone, Korea: Considering on the history of igneous activities accompanying formation and evolution processes of the Ogcheon rift basin. *Journal of the geological society of korea* 53, 51-77. (in Korean with English abstract)
- Kamber, B. S., Greig, A., & Collerson, K. D. (2005). A new estimate for the composition of weathered young upper continental crust from alluvial sediments, Queensland, Australia. *Geochimica et Cosmochimica Acta*, 69(4), 1041-1058.
- Kamber, B. S., & Webb, G. E. (2001). The geochemistry of late Archaean microbial carbonate: implications for ocean chemistry and continental erosion history. *Geochimica et Cosmochimica Acta*, 65(15), 2509-2525.
- Kee, W., Kim, S.W., Kwon, S., Santosh, M., Ko, K., & Jeong, Y. (2019). Early Neoproterozoic (ca. 913–895 Ma) arc magmatism along the central–western Korean Peninsula: Implications for the amalgamation of Rodinia supercontinent. *Precambrian Research* 335, 105498.

- Kennedy, M. J. (1996). Stratigraphy, sedimentology, and isotopic geochemistry of Australian Neoproterozoic postglacial cap dolostones; deglaciation, $\delta^{13}\text{C}$ excursions, and carbonate precipitation. *Journal of sedimentary Research*, 66(6), 1050-1064.
- Kennedy, M.J., & Christie-Blick, N. (2011). Condensation origin for Neoproterozoic cap carbonates during deglaciation. *Geology* 39, 319-322.
- Kennedy, M.J., Christie-Blick, N., & Prave, A.R. (2001). Carbon isotopic composition of Neoproterozoic glacial carbonates as a test of paleoceanographic models for snowball Earth phenomena. *Geology* 29, 1135-1138.
- Kennedy, M.J., Runnegar, B., Prave, A.R., Hoffmann, K., & Arthur, M.A. (1998). Two or four Neoproterozoic glaciations?. *Geology* 26, 1059-1063.
- Kihm, Y. H., Kim, J. H., & Lee, J. U. (1999). Geological structures of the Choseon and Ogcheon Supergroups in the Deoksan-Cheongpung area, Jecheon-gun, Chungcheongbuk-do. Korea. *Journal of the Geological Society of Korea*, 35, 233-252. (in Korean with English abstract)
- Kihm, Y., H., Kim, J., H., & Koh, H., J. (1996). Geology of the Deogsan-myeon area, Jecheon-gun, Chungcheongbuk-do, Korea: contact between the Choseon and Ogcheon supergroups 32, 483-499. (in Korean with English abstract)
- Kim, D.H., Chang, T.W., Kim, W.Y., & Hwang, J.H., (1978). Geologicmap of Korea, Okcheon Sheet (1:50,000). Korea Research Institute of Geoscience and Mineral Resources.
- Kim, D.H., & Choi, D.K. (2000). Lithostratigraphy and biostratigraphy of the Mungok Formation (Lower Ordovician), Youngwol, Korea. *Geosciences Journal*, 4(4), 301-311.
- Kim, H. S. (1971). Metamorphic facies and regional metamorphism of Ogcheon metamorphic belt. *Geological Society of Korea* 3, 7(4), 221-256. (in Korean with English abstract)
- Kim, J.,N., Han., R.,Y., Zhao, L., Li., Q.,L., & Kim, S.,S (2016). Study on the petrographic and SIMS zircon U-Pb geochronological characteristics of the magmatic rocks associated with the Jongju and Cholsan REE deposits in northern Korean Peninsula. (in Chinese with English abstract)
- Kim, K.,H. (1980). Carbon and Oxygen Isotope Studies of the Paleozoic Limestones from the Taebaegsan Region, South Korea 13, 21-27. (in Korean with English abstract)

- Kim, K.W., & Lee, H.K. (1965). Geological Report of the Chungju Sheet (1:50,000). Geological Survey of Korea, 35p. (in Korean)
- Kim, K.W., Park, B.S., & Lee, H.K., (1967). Explanatory text of the geological map of Jecheon Sheet, Sheet 6825-III, Scale 1:50,000. Geological Survey of Korea, 46p.
- Kim, M.G., & Lee, Y.I., (2018). The Pyeongan Supergroup (upper Paleozoic–Lower Triassic) in the Okcheon Belt, Korea: A review of stratigraphy and detrital zircon provenance, and its implications for the tectonic setting of the eastern Sino-Korean Block. *Earth-Science Reviews* 185, 1170-1186.
- Kim, M. J., Park, K. H., Yi, K., & Koh, S. M. (2013). Timing of metamorphism of the metavolcanics within the Gyemyeongsan Formation. *The Journal of the Petrological Society of Korea*, 22(4), 291-298. (in Korean with English abstract)
- Kim, M. J., Ha, Y., Choi, J. E., Park, K. H., Song, Y. S., & Liu, S. (2021). U-Pb ages and Hf isotopic compositions of detrital zircons from the Seochangni Formation of the northeastern Okcheon Metamorphic Belt: Implications to the crustal evolution of the Sino-Korean craton since Paleoproterozoic. *Lithos*, 106340.
- Kim, N., Cheong, C. S., Park, K. H., Kim, J., & Song, Y. S. (2012). Crustal evolution of northeastern Yeongnam Massif, Korea, revealed by SHRIMP U–Pb zircon geochronology and geochemistry. *Gondwana Research*, 21(4), 865-875.
- Kim, O. J. (1968). Stratigraphy and tectonics of Okcheon System in the area between Chungju and Munkyeong. *Economic and Environmental Geology*, 1(1), 35-46. (in Korean with English abstract)
- Kim, O.J., Lee, H.Y., Lee, D.S., & Yun, S. (1973). The Stratigraphy and Geologic Structure of the Great Limestone Series in South Korea. *Journal of the Korean Institute of Mining Geology*, 6(2), 81-114. (in Korean with English abstract)
- Kim, O. J., Min, K. D., & Kim, K. H. (1986). Geology and Mineral Resources of the Okchŏn Zone-The Boundary between the Okchŏn and Chosŏn Systems in the South of Jechŏn, and the Geology in its Vicinity. *Economic and Environmental Geology*, 19(3), 225-230. (in Korean with English abstract)
- Kim, S.W., Cho, D., Lee, S., Kwon, S., Park, S., Santosh, M., & Kee, W. (2018). Mesoproterozoic magmatic suites from the central-western Korean Peninsula: Imprints of Columbia disruption in East Asia. *Precambrian Research* 306, 155-173.
- Kim, S.W., Kee, W.S., Santosh, M., Cho, D., Hong, P.S., Ko, K., Lee, B.C., Byun, U.H., & Jang, Y. (2020). Tracing the Precambrian tectonic history of East Asia

from Neoproterozoic sedimentation and magmatism in the Korean Peninsula. *Earth-Science Reviews*, 103311.

- Kim, S.W., Kee, W., Lee, S.R., Santosh, M., & Kwon, S. (2013b). Neoproterozoic plutonic rocks from the western Gyeonggi massif, South Korea: implications for the amalgamation and break-up of the Rodinia supercontinent. *Precambrian Research* 227, 349-367.
- Kim, S.W., Kwon, S., Koh, H.J., Yi, K., Jeong, Y., & Santosh, M., (2011). Geotectonic framework of Permo–Triassic magmatism within the Korean Peninsula. *Gondwana Research*. 20, 865–889.
- Kim, S. W., Kwon, S., Santosh, M., Cho, D. L., Kee, W. S., Lee, S. B., & Jeong, Y. J. (2019). Detrital zircon U-Pb and Hf isotope characteristics of the Early Neoproterozoic successions in the central-western Korean Peninsula: Implication for the Precambrian tectonic history of East Asia. *Precambrian Research*, 322, 24-41.
- Kim, S.W., Oh, C.W., Ryu, I., Williams, I., Sajeev, K., Santosh, M., & Rajesh, V. (2006). Neoproterozoic bimodal volcanism in the Okcheon Belt, South Korea, and its comparison with the Nanhua Rift, South China: implications for rifting in Rodinia. *The Journal of geology* 114, 717-733.
- Kim, S.W., Park, S., Jang, Y., Kwon, S., Kim, S.J., & Santosh, M. (2017). Tracking Paleozoic evolution of the South Korean Peninsula from detrital zircon records: Implications for the tectonic history of East Asia. *Gondwana Research* 50, 195-215.
- Kim, S. W., Williams, I. S., Kwon, S., & Oh, C. W. (2008). SHRIMP zircon geochronology, and geochemical characteristics of metaplutonic rocks from the south-western Gyeonggi Block, Korea: Implications for Paleoproterozoic to Mesozoic tectonic links between the Korean Peninsula and eastern China. *Precambrian Research*, 162(3-4), 475-497.
- Ryu, I. C., & Kim, T. H. (2009). Stratigraphy and geological structure of the northwestern Okcheon metamorphic belt near the Chungju area. *Economic and Environmental Geology*, 42(1), 9-25. (in Korean with English abstract)
- Kirschvink, J.L. (1992). Late Proterozoic low-latitude global glaciation: the snowball Earth.
- Knauth, L.P., & Kennedy, M.J. (2009). The late Precambrian greening of the Earth. *Nature* 460, 728-732.

- Knoll, A. H., & Walter, M. R. (1992). Latest Proterozoic stratigraphy and Earth history. *Nature*, 356(6371), 673-678.
- Kobayashi, T. (1966). The Cambro-Ordovician formations and faunas of South Korea. Part X. stratigraphy of Chosen Group in Korea and South Manchuria and its relation to the Cambro-Ordovician formations of other areas. Sect. A. The Chose Group of South Korea. *Journal of the Faculty of Science, University of Tokyo, Section II*, 16, 1-84.
- Kobayashi, T., Yosimura, I., Iwaya, Y., & Hukasawa, T. (1942). 115. The Yokusen Geosyncline in the Chosen Period Brief Notes on the Geologic History of the Yokusen Orogenic Zone, 1. *Proceedings of the Imperial Academy*, 18(9), 579-584.
- Koh, S. M., Kim, J. H., & Park, K. H. (2005). Neoproterozoic A-type volcanic activity within the Okcheon Metamorphic Belt. *The Journal of the Petrological Society of Korea*, 14(3), 157-168. (in Korean with English abstract)
- Kuznetsov, A. B., Gorokhov, I. M., Melezhik, V. A., Mel'nikov, N. N., Konstantinova, G. V., & Turchenko, T. L. (2012). Strontium isotope composition of the lower proterozoic carbonate concretions: The Zaonega Formation, Southeast Karelia. *Lithology and Mineral Resources*, 47(4), 319-333.
- Kroopnick, P. M. (1985). The distribution of ^{13}C of ΣCO_2 in the world oceans. *Deep Sea Research Part A. Oceanographic Research Papers*, 32(1), 57-84.
- Kwon, S.-T., Sajeev, K., Mitra, G., Park, Y., Kim, S.W., & Ryu, I. (2009). Evidence for Permo-Triassic collision in far east Asia: the Korean collisional orogen. *Earth and Planetary Science Letters* 279, 340-349.
- Kwon, Y. K., Chough, S. K., Choi, D. K., & Lee, D. J. (2006). Sequence stratigraphy of the Taebaek Group (Cambrian–Ordovician), mideast Korea. *Sedimentary Geology*, 192(1-2), 19-55.
- Kwon, Y. K., Kwon, Y. J., Yeo, J. M., & Lee, C. Y. (2019). Basin Evolution of the Taebaeksan Basin during the Early Paleozoic. *Economic and Environmental Geology*, 52(5), 427-448. (in Korean with English abstract)
- Lawrence, M.G., Greig, A., Collerson, K.D., & Kamber, B.S. (2006a). Rare earth element and yttrium variability in South East Queensland waterways. *Aquatic Geochemistry* 12, 39-72.
- Lawrence, M.G., & Kamber, B.S. (2006b). The behaviour of the rare earth elements during estuarine mixing-revisited. *Marine Chemistry* 100, 147-161.

- Le Heron, D.P., Eyles, N., & Busfield, M.E. (2020). The Laurentian Neoproterozoic Glacial Interval: reappraising the extent and timing of glaciation. *Austrian Journal of Earth Sciences* 113, 59-70.
- Le Heron, D.P., Vandyk, T.M., Kuang, H., Liu, Y., Chen, X., Wang, Y., Yang, Z., Scharfenberg, L., Davies, B., & Shields, G. (2019). Bird's-eye view of an Ediacaran subglacial landscape. *Geology* 47, 705-709.
- Le Heron, D.P., Vandyk, T.M., Wu, G., & Li, M. (2018). New perspectives on the Luoquan Glaciation (Ediacaran-Cambrian) of North China. *The Depositional Record* 4, 274-292.
- Lee, C.H., & Kim, J.H., 1972, Geologic map of Korea, Goesan Sheet (1:50,000). Geological Survey of Korea (in Korean).
- Lee, H., M., (2013). Geochemical and isotopic characteristics of the Pirrit Hills granite in West Antarctica (Ph.D. Thesis). Kongju National University, Chungcheongnamdo, Korea.
- Lee, J.G. (1995). Late Cambrian Trilobites from the Machari Formation, Yeongweol, Korea: (Ph.D. Thesis). Seoul National University, Seoul, Korea.
- Lee, B. Y., Oh, C. W., Lee, S. H., Seo, J., & Yi, K. (2020). Ages and tectonic settings of the Neoproterozoic igneous rocks in the Gyeonggi Massif of the southern Korean Peninsula and the correlation with the Neoproterozoic igneous rocks in China. *Lithos*, 370, 105625.
- Lee, C. H., Lee, M. S., & Park, B., S., (1980). Explanatory notice of the 1:50,000 geologic map of Korea, Miweon sheet. Korea Research Institute of Geoscience and Mineral Resource, Seoul. 29p. (in Korean with English summary)
- Lee, H., G., Yu, E. G., & Hong, S. H., (1971). Explanatory notice of the 1:50,000 geologic map of Korea, Yongyuri sheet. Korea Research Institute of Geoscience and Mineral Resource, Seoul. 29p. (in Korean with English summary)
- Lee, H.S., & Chough, S.K. (2006). Sequence stratigraphy of Pyeongan Supergroup (Carboniferous-Permian), Taebaek area, mideast Korea. *Geosciences Journal* 10, 369.
- Lee, M. S., Yeo, J. P., Lee, J. I., Jwa, Y. J., Yoshida, S., & Lee, H. Y. (1998). Glaciogenic diamictite of Ogcheon System and its geologic age, and paleogeography of Korean Peninsula in Late Paleozoic. *Journal of the Geological Society of Korea*, 34, 343-370. (in Korean with English abstract)

- Lee, K. S., Chang, H. W., & Park, K. H. (1998). Neoproterozoic bimodal volcanism in the central Ogcheon belt, Korea: age and tectonic implication. *Precambrian Research*, 89(1-2), 47-57.
- Lee, K., Chang, H., & Park, K. (1998). Neoproterozoic bimodal volcanism in the central Ogcheon belt, Korea: age and tectonic implication. *Precambrian Research* 89, 47-57.
- Lee, M.S., & Park, B.S. (1965) Explanatory text of the geological map of Hwanggangni Sheet, Sheet 6825-III, Scale 1:50,000. Geological Survey of Korea, 43p.
- Lee, M., Yeo, J., Lee, J., Jwa, Y., Yoshida, S., & Lee, H. (1998). Glaciogenic diamictite of Ogcheon System and its geologic age, and paleogeography of Korean Peninsula in Late Paleozoic. *Journal of the Geological Society of Korea* 34, 343-370.
- Lee, W.K. (1983) Sedimentary Petrological Study on the Heungwolri Formation. *Journal of the Geological Society of Korea*, 19, 190-202.
- Li, L., Yun, H., & Zhang, X. (2018). Precambrian-Cambrian transition in the southern margin of North China.
- Li, Z., Evans, D.A., & Halverson, G.P. (2013). Neoproterozoic glaciations in a revised global palaeogeography from the breakup of Rodinia to the assembly of Gondwanaland. *Sedimentary Geology* 294, 219-232.
- Li, Z. X., Zhang, L., & Powell, C. M. (1996). Positions of the East Asian cratons in the Neoproterozoic supercontinent Rodinia. *Australian Journal of Earth Sciences*, 43(6), 593-604.
- Ling, H., Chen, X., Li, D., Wang, D., Shields-Zhou, G.A., & Zhu, M. (2013). Cerium anomaly variations in Ediacaran–earliest Cambrian carbonates from the Yangtze Gorges area, South China: implications for oxygenation of coeval shallow seawater. *Precambrian Research* 225, 110-127.
- Lim, J. N., Chung, G. S., Park, T. Y. S., & Lee, K. S. (2015). Lithofacies and stable carbon isotope stratigraphy of the Cambrian Sesong Formation in the Taebaeksan Basin, Korea. *Journal of the Korean earth science society*, 36(7), 617-631. (in Korean with English abstract)
- Lim, S. B., Chun, H. Y., Kim, Y. B., Kim, B. C., & Cho, D. L. (2005). Geologic ages, stratigraphy and geological structures of the metasedimentary strata in Bibong similar to Yeonmu area, NW Okcheon belt, Korea. *Journal of the Geological Society of Korea*, 41(3), 335-368. (in Korean with English abstract)

- Lim, S.-B., Chun, H.-Y., Kim, Y.B., Kim, B.C., & Song, K.-Y. (2006). Stratigraphy and geological ages of the metasedimentary strata in Jinsan~Boksu area, Chungcheongnam-do, NW Okcheon belt. *Journal of the Geological Society of Korea*, 42, 149-174. (in Korean with English abstract)
- Lim, S.-B., Chun, H.-Y., Kim, Y.B., Lee, S.R., & Kee, W.-S. (2007). Geological ages and stratigraphy of the metasedimentary strata in Hoenam~Miwon area, NW Okcheon belt. *Journal of the Geological Society of Korea*, 43, 125-150. (in Korean with English abstract)
- Lim, S. W., & Woo, K. S. (1995). The origin of the dolomite of the Pungchon Formation near Taebaeg City, Kangwondo, Korea. *The Korean Journal of Petroleum Geology*, 3(1), 28-39. (in Korean with English abstract)
- Liu, S., Zhang, J., Li, Q., Zhang, L., Wang, W., & Yang, P. (2012). Geochemistry and U–Pb zircon ages of metamorphic volcanic rocks of the Paleoproterozoic Lüliang Complex and constraints on the evolution of the Trans-North China Orogen, North China Craton. *Precambrian Research*, 222, 173-190.
- Macdonald, F.A., Jones, D.S., & Schrag, D.P. (2009). Stratigraphic and tectonic implications of a newly discovered glacial diamictite–cap carbonate couplet in southwestern Mongolia. *Geology* 37, 123-126.
- Macdonald, F. A., Smith, E. F., Strauss, J. V., Cox, G. M., Halverson, G. P., Roots, C. F., & Relf, C. (2010). Neoproterozoic and early Paleozoic correlations in the western Ogilvie Mountains, Yukon. *Yukon Exploration and Geology*, 161-182.
- McLennan, S.M. (1989) Rare Earth Elements in Sedimentary Rocks. Influence of Provenance and Sedimentary Processes. *Reviews in Mineralogy*, 21, 169-200.
- McLennan, S.M., Nance, W.B., & Taylor, S.R., (1980). Rare earth element-thorium correlations in sedimentary rocks, and the composition of the continental crust. *Geochim. Cosmochim. Acta*, 44: 833-1840.
- McArthur, J. M., Howarth, R. J., & Shields, G. A. (2012). Strontium isotope stratigraphy. *The geologic time scale*, 1, 127-144.
- McFadden, K.A., Huang, J., Chu, X., Jiang, G., Kaufman, A.J., Zhou, C., Yuan, X., & Xiao, S. (2008). Pulsed oxidation and biological evolution in the Ediacaran Doushantuo Formation. *Proceedings of the National Academy of Sciences of the United States of America* 105, 3197-3202.
- McKenzie, J.A. (1981). Holocene dolomitization of calcium carbonate sediments from the coastal sabkhas of Abu Dhabi, UAE: a stable isotope study. *The Journal of geology* 89, 185-198.

- Meert, J.G., & Torsvik, T.H. (2004). Paleomagnetic constraints on Neoproterozoic 'Snowball Earth' continental reconstructions. The extreme Proterozoic: geology, geochemistry, and climate. AGU Geophysical Monograph Series 146, 5-11.
- Melezhik, V., Bingen, B., Fallick, A., Gorokhov, I., Kuznetsov, A., Sandstad, J., Solli, A., Bjerkgård, T., Henderson, I., & Boyd, R. (2008). Isotope chemostratigraphy of marbles in northeastern Mozambique: apparent depositional ages and tectonostratigraphic implications. *Precambrian Research* 162, 540-558.
- Melezhik, V. A., Gorokhov, I. M., Fallick, A. E., & Gjelle, S. (2001). Strontium and carbon isotope geochemistry applied to dating of carbonate sedimentation: an example from high-grade rocks of the Norwegian Caledonides. *Precambrian Research*, 108(3-4), 267-292.
- Melezhik, V. A., Gorokhov, I. M., Kuznetsov, A. B., & Fallick, A. E. (2001). Chemostratigraphy of Neoproterozoic carbonates: implications for 'blind dating'. *Terra Nova*, 13(1), 1-11.
- Melezhik, V., Roberts, D., Fallick, A., Gorokhov, I., & Kusnetzov, A. (2005). Geochemical preservation potential of high-grade calcite marble versus dolomite marble: implication for isotope chemostratigraphy. *Chemical Geology* 216, 203-224.
- Meng, E., Liu, F. L., Liu, P. H., Liu, C. H., Yang, H., Wang, F., & Cai, J. (2014). Petrogenesis and tectonic significance of Paleoproterozoic meta-mafic rocks from central Liaodong Peninsula, northeast China: evidence from zircon U-Pb dating and in situ Lu-Hf isotopes, and whole-rock geochemistry. *Precambrian Research*, 247, 92-109.
- Meyer, E. E., Quicksall, A. N., Landis, J. D., Link, P. K., & Bostick, B. C. (2012). Trace and rare earth elemental investigation of a Sturtian cap carbonate, Pocatello, Idaho: evidence for ocean redox conditions before and during carbonate deposition. *Precambrian Research*, 192, 89-106.
- Min, K., & Cho, M. (1998). Metamorphic evolution of the northwestern Ogcheon metamorphic belt, South Korea. *Lithos* 43, 31-51.
- Miyazaki, T., & Shuto, K. (1998). Sr and Nd isotope ratios of twelve GSJ rock reference samples. *Geochemical Journal* 32, 345-350.
- Mohanty, S.P., Barik, A., Sarangi, S., & Sarkar, A. (2015). Carbon and oxygen isotope systematics of a Paleoproterozoic cap-carbonate sequence from the Sausar Group, Central India. *Palaeogeography, Palaeoclimatology, Palaeoecology* 417, 195-209.

- Montañez, I.P., Osleger, D.A., Banner, J.L., Mack, L.E., & Musgrove, M. (2000). Evolution of the Sr and C isotope composition of Cambrian oceans. *GSA today* 10, 1-7.
- Myrow, P. M., & Kaufman, A. J. (1999). A newly discovered cap carbonate above Varanger-age glacial deposits in Newfoundland, Canada. *Journal of Sedimentary Research*, 69(3), 784-793.
- Neo, N., Takazawa, E., & Shuto, K. (2006). Quantitative analysis of trace elements in basaltic and peridotitic rocks by quadruple inductively-coupled plasma mass spectrometry. Report of Grant-in-Aid for Scientific Research (C), (16540413), 79-94.
- Nogueira, A.C., Riccomini, C., Sial, A.N., Moura, C.A.V., & Fairchild, T.R. (2003). Soft-sediment deformation at the base of the Neoproterozoic Puga cap carbonate (southwestern Amazon craton, Brazil): Confirmation of rapid icehouse to greenhouse transition in snowball Earth. *Geology* 31, 613-616.
- Nogueira, A.C., Riccomini, C., Sial, A.N., Moura, C.A., Trindade, R.I., & Fairchild, T.R. (2007). Carbon and strontium isotope fluctuations and paleoceanographic changes in the late Neoproterozoic Araras carbonate platform, southern Amazon craton, Brazil. *Chemical Geology* 237, 168-190.
- Nozaki, Y., Zhang, J., & Amakawa, H. (1997). The fractionation between Y and Ho in the marine environment. *Earth and Planetary Science Letters* 148, 329-340.
- Oh, C.W., Choi, S.-G., Seo, J., Rajesh, V.J., Lee, J.H., Zhai, M., & Peng, P., (2009). The tectonic evolution of the Gogunsan Islands in the southwestern margin of the Gyeonggi Massif and its implication for the Neoproterozoic tectonic evolution relating to the Rodinia in the Northeast Asia. *Gondwana Research*. 16, 272-284.
- Oh, C. W., Lee, B. C., Yi, S. B., & Ryu, H. I. (2019). Correlation of Paleoproterozoic igneous and metamorphic events of the Korean Peninsula and China; Its implication to the tectonics of Northeast Asia. *Precambrian Research*, 326, 344-362.
- Oh, C.W. (2006). A new concept on tectonic correlation between Korea, China and Japan: histories from the late Proterozoic to Cretaceous. *Gondwana Research* 9, 47-61.
- Oh, C.W., & Kusky, T. (2007). The Late Permian to Triassic Hongseong-Odesan collision belt in South Korea, and its tectonic correlation with China and Japan. *International Geology Review* 49, 636-657.

- Otsuji, N. (2013). Late-Tonian to early-Cryogenian apparent depositional ages for metacarbonate rocks from the Sør Rondane Mountains, East Antarctica, 413.
- Park, B. K., & Woo, K. S. (1986). Carbon and oxygen isotope composition of the Middle Cambrian Pungchon Limestone Formation. Korea. Journal of the Geological Society of Korea, 22, 40-52. (in Korean with English abstract)
- Park, B. S., & Yeo, S. C. (1971). Explanatory text of the geological map of Moggye sheet. Geological Survey of Korea, 40. (in Korean)
- Park, K., Choi, D.K., & Kim, J.H. (1994). The Mungog Formation (Lower Ordovician) in the northern part of Yeongweol area: lithostratigraphic subdivision and trilobite faunal assemblages. Journal of the Geological Society of Korea, 30(2), 168-181. (in Korean with English abstract)
- Park, S., Kim, S.W., Kwon, S., Santosh, M., Ko, K., & Kee, W. (2017). Nature of Late Mesoproterozoic to Early Neoproterozoic magmatism in the western Gyeonggi massif, Korean Peninsula and its tectonic significance. Gondwana Research 47, 291-307.
- Park, K. H. (2011). SHRIMP U-Pb ages of detrital zircons in the Daehyangsan Quartzite of the Okcheon Metamorphic Belt. Journal of the Geological Society of Korea, 47, 423-431. (in Korean with English abstract)
- Peng, P., Zhai, M., Li, Q., Wu, F., Hou, Q., Li, Z., Li, T., & Zhang, Y. (2011). Neoproterozoic (~ 900 Ma) Sariwon sills in North Korea: Geochronology, geochemistry and implications for the evolution of the south-eastern margin of the North China Craton. Gondwana Research 20, 243-254.
- Pokrovsky, B., Chumakov, N., Melezhik, V., & Bujakaite, M. (2010). Geochemical properties of Neoproterozoic “cap dolomites” in the Patom paleobasin and problem of their genesis. Lithology and Mineral Resources 45, 577-592.
- Ramkumar, M. (2015). Toward standardization of terminologies and recognition of chemostratigraphy as a formal stratigraphic method. In *Chemostratigraphy* (pp. 1-21). Elsevier.
- Ree, J. H., Cho, M., Kwon, S. T., & Nakamura, E. (1996). Possible eastward extension of Chinese collision belt in South Korea: the Imjingang belt. *Geology*, 24(12), 1071-1074.
- Ree, J.-H., Kwon, S.-H., Park, Y., Kwon, S.-T., & Park, S.-H. (2001). Pre-tectonic and post-tectonic emplacements of the granitoids in the south central Okchon belt, South Korea: Implications for the timing of the strike-slip shearing and thrusting. *Tectonics*, 20, 850–867.

- Reedman, A. J., Fletcher, C. J. N., Evans, R. B., Workman, D. R., Yoon, K. S., Rhyu, H. S., ... & Park, J. N. (1973). Geology of the Hwanggangri mining district, Republic of Korea. Anglo-Korean Mineral Exploration Group, 119p.
- Reedman, A. J., & Fletcher, C. J. N. (1976). Tillites of the Ogcheon Group and their stratigraphic significance. *Journal of the Geological Society of Korea*, 12(3), 107-112.
- Riccomini, C., Nogueira, A.C., & Sial, A.N. (2007). Carbon and oxygen isotope geochemistry of Ediacaran outer platform carbonates, Paraguay Belt, central Brazil. *Anais da academia Brasileira de Ciências* 79, 519-527.
- Rooney, A.D., Strauss, J.V., Brandon, A.D., & Macdonald, F.A. (2015) A Cryogenian chronology: two long-lasting synchronous Neoproterozoic glaciations. *Geology* 43, 459–462
- Ryu, Y., & Ahn, J. (2016). A test for Snowball Earth hypothesis in Korean peninsula by analyzing stable carbon isotopes of carbonates from the Okcheon Supergroup. *Journal of the geological society of korea* 52, 829-845. (in Korean with English abstract)
- Saltzman, M., & Thomas, E. (2012). Carbon isotope stratigraphy. *The geologic time scale* 1, 207-232.
- Sansjofre, P., Ader, M., Trindade, R., Elie, M., Lyons, J., Cartigny, P., & Nogueira, A. (2011). A carbon isotope challenge to the snowball Earth. *Nature* 478, 93-96.
- Sawaki, Y., Ohno, T., Tahata, M., Komiya, T., Hirata, T., Maruyama, S., Windley, B.F., Han, J., Shu, D., & Li, Y. (2010). The Ediacaran radiogenic Sr isotope excursion in the Doushantuo Formation in the three Gorges area, South China. *Precambrian Research* 176, 46-64.
- Schrag, D.P., Berner, R.A., Hoffman, P.F., & Halverson, G.P. (2002). On the initiation of a snowball Earth. *Geochemistry, Geophysics, Geosystems* 3, 1-21.
- Sherrell, R. M., Field, M. P., & Ravizza, G. (1999). Uptake and fractionation of rare earth elements on hydrothermal plume particles at 9 45' N, East Pacific Rise. *Geochimica et Cosmochimica Acta*, 63(11-12), 1709-1722.
- Shen, B., Xiao, S., Kaufman, A.J., Bao, H., Zhou, C., & Wang, H. (2008). Stratification and mixing of a post-glacial Neoproterozoic ocean: evidence from carbon and sulfur isotopes in a cap dolostone from northwest China. *Earth and Planetary Science Letters* 265, 209-228.

- Shen, B., Xiao, S., Zhou, C., Kaufman, A.J., & Yuan, X. (2010). Carbon and sulfur isotope chemostratigraphy of the Neoproterozoic Quanji Group of the Chaidam Basin, NW China: Basin stratification in the aftermath of an Ediacaran glaciation postdating the Shuram event?. *Precambrian Research* 177, 241-252.
- Shen, Y., Zhang, T., & Chu, X. (2005). C-isotopic stratification in a Neoproterozoic postglacial ocean. *Precambrian Research* 137, 243-251.
- Shields, G.A. (2005). Neoproterozoic cap carbonates: a critical appraisal of existing models and the plumeworld hypothesis. *Terra Nova* 17, 299-310.
- Shields, G.A. (2007). A normalised seawater strontium isotope curve: possible implications for Neoproterozoic-Cambrian weathering rates and the further oxygenation of the Earth. *EEarth* 2, 35-42.
- Shields, G.A., & Veizer, J. (2002). *Precambrian marine carbonate isotope database: Version 1.1.*
- Shin, W. J., Choi, S. H., Ryu, J. S., Song, B. Y., Song, J. H., Park, S., & Min, J. S. (2018). Discrimination of the geographic origin of pork using multi-isotopes and statistical analysis. *Rapid Communications in Mass Spectrometry*, 32(21), 1843-1850.
- Sial, A. N., Campos, M. S., Gaucher, C., Frei, R., Ferreira, V. P., Nascimento, R. C., & Rodler, A. (2015). Algoma-type Neoproterozoic BIFs and related marbles in the Seridó Belt (NE Brazil): REE, C, O, Cr and Sr isotope evidence. *Journal of South American Earth Sciences*, 61, 33-52.
- Slack, J. F., Grenne, T., Bekker, A., Rouxel, O. J., & Lindberg, P. A. (2007). Suboxic deep seawater in the late Paleoproterozoic: evidence from hematitic chert and iron formation related to seafloor-hydrothermal sulfide deposits, central Arizona, USA. *Earth and Planetary Science Letters*, 255(1-2), 243-256.
- Son, J. W., & Choi, D. K. (2005). Revision of the upper Cambrian trilobite biostratigraphy of the Sesong and Hwajeol formations, Taebaek group, Korea. *Journal of Paleontological society of Korea*, 21(2), 195. (in Korean with English abstract)
- Son, J.W., Kim, D.H., & Choi, D.K. (2001). Stratigraphy of the Cambro-Ordovician Strata in the Mt. Samtae area, Danyang, Korea. *Journal of the Paleontological Society of Korea*, 17, 23-34. (in Korean with English abstract)
- Suzuki, K., Dunkley, D., Adachi, M., & Chwae, U. (2006). Discovery of a c. 370 Ma granitic gneiss clast from the Hwanggangri pebble-bearing phyllite in the Okcheon metamorphic belt, Korea. *Gondwana Research*, 9(1-2), 85-94.

- Tahata, M., Ueno, Y., Ishikawa, T., Sawaki, Y., Murakami, K., Han, J., Shu, D., Li, Y., Guo, J., & Yoshida, N. (2013). Carbon and oxygen isotope chemostratigraphies of the Yangtze platform, South China: decoding temperature and environmental changes through the Ediacaran. *Gondwana Research* 23, 333-353.
- Takahashi, T., Hirahara, Y., Miyazaki, T., Vaglarov, B. S., Chang, Q., Kimura, J. I., & Tatsumi, Y. (2009). Precise determination of Sr isotope ratios in igneous rock samples and application to micro-analysis of plagioclase phenocrysts. JAMSTEC Report of Research and Development, 2009, 59-64.
- Tam, P. Y., Zhao, G., Zhou, X., Sun, M., Guo, J., Li, S., & He, Y. (2012). Metamorphic P-T path and implications of high-pressure pelitic granulites from the Jiaobei massif in the Jiao-Liao-Ji Belt, North China Craton. *Gondwana Research*, 22(1), 104-117.
- Tang, H., Chen, Y., Santosh, M., Zhong, H., Wu, G., & Lai, Y. (2013). C-O isotope geochemistry of the Dashiqiao magnesite belt, North China Craton: implications for the Great Oxidation Event and ore genesis. *Geological Journal* 48, 467-483.
- Valley, J. W. (2001). Stable isotope thermometry at high temperatures. *Reviews in mineralogy and geochemistry*, 43(1), 365-413.
- Veizer, J., Ala, D., Azmy, K., Bruckschen, P., Buhl, D., Bruhn, F., Carden, G.A., Diener, A., Ebner, S., & Godderis, Y. (1999). $^{87}\text{Sr}/^{86}\text{Sr}$, $\delta^{13}\text{C}$ and $\delta^{18}\text{O}$ evolution of Phanerozoic seawater. *Chemical Geology* 161, 59-88.
- Veizer, J., Godderis, Y., & Francois, L. M. (2000). Evidence for decoupling of atmospheric CO_2 and global climate during the Phanerozoic eon. *Nature*, 408(6813), 698-701.
- Wada, H., & Suzuki, K. (1983). Carbon isotopic thermometry calibrated by dolomite-calcite solvus temperatures. *Geochimica et Cosmochimica Acta*, 47(4), 697-706.
- Wang, G., Wang, J., Wang, Z., Chen, C., & Yang, J. (2017). Carbon isotope gradient of the Ediacaran cap carbonate in the Shennongjia area and its implications for ocean stratification and palaeogeography. *Journal of Earth Science* 28, 187-195.
- Wang, P., Du, Y., Yu, W., Algeo, T.J., Zhou, Q., Xu, Y., Qi, L., Yuan, L., & Pan, W. (2020). The chemical index of alteration (CIA) as a proxy for climate change during glacial-interglacial transitions in Earth history. *Earth-Science Reviews* 201, 103032.

- Wissert, M., Kern, M., Radbruch, L., Graf, G., Mütter, M., & Voltz, R. (2008). Case Management in palliative care in Germany: Presenting author Lukas Radbruch. *Palliative Medicine*, 22.
- Won, C. G., & Lee, H.Y., (1967), Explanatory text of the geological map of Danyeong Sheet, Sheet 6824-I, Scale 1:50,000. Geological Survey of Korea.
- Wu, F. Y., Han, R. H., Yang, J. H., Wilde, S. A., Zhai, M. G., & Park, S. C. (2007). Initial constraints on the timing of granitic magmatism in North Korea using U–Pb zircon geochronology. *Chemical Geology*, 238(3-4), 232-248.
- Wu, F. Y., Yang, J. H., Wilde, S. A., Liu, X. M., Guo, J. H., & Zhai, M. G. (2007). Detrital zircon U–Pb and Hf isotopic constraints on the crustal evolution of North Korea. *Precambrian Research*, 159(3-4), 155-177.
- Yang, J., Lyons, T.W., Zeng, Z., Odigie, K.O., Bates, S., & Hu, L. (2019). Geochemical constraints on the origin of Neoproterozoic cap carbonate in the Helan Mountains, North China: Implications for mid-late Ediacaran glaciation?. *Precambrian Research* 331, 105361.
- Yi, J. M., Kim, K. H., Tanaka, T., & Kawabe, L. (2000). REE and Sr isotopic compositions of carbonate pebbles in the phyllitic rocks of the Hwanggangni Formation, Okcheon zone. *Journal of the Geological Society of Korea*, 36, 257-278. (in Korean with English abstract)
- Yin, A., Nie, S. (1993). An indentation model for the North and South China collision and the development of the Tan-Lu and Honam fault systems, eastern Asia. *Tectonics* 12, 801-813.
- Yosimura, I. (1940) Geology of the Neietsu District, Kogendo, Tyosen. *Journal of the Geological Society of Japan* 40, 112-122.
- Yoon, K. H., & Woo, K. S. (2006). Textural and geochemical characteristics of crystalline limestone (high-purity, limestone) in the Daegi Formation. Korea. *Journal of the geological society of Korea*, 42, 561-576. (in Korean with English abstract)
- Young, G.M. (2013). Precambrian supercontinents, glaciations, atmospheric oxygenation, metazoan evolution and an impact that may have changed the second half of Earth history. *Geoscience Frontiers* 4, 247-261.
- Yu, W.C., Algeo, T.J., Du, Y.S., Zhou, Q., Wang, P., Xu, Y., Yuan, L.J., & Pan, W., (2017). Newly discovered Sturtian cap carbonate in the Nanhua Basin, South China. *Precambrian Res.* 293, 112–130.

- Zhai, M., Zhang, X., Zhang, Y., Wu, F., Peng, P., Li, Q., Li, Z., Guo, J., Li, T., Zhao, L., Zhou, L., & Zhu, X. (2019). The geology of North Korea: An overview. *Earth-Science Reviews* 194, 57-96.
- Zhang, S., Jiang, G., Zhang, J., Song, B., Kennedy, M. J., & Christie-Blick, N. (2005). U-Pb sensitive high-resolution ion microprobe ages from the Doushantuo Formation in south China: Constraints on late Neoproterozoic glaciations. *Geology*, 33(6), 473-476.
- Zhao, G., & Cawood, P. A. (2012). Precambrian geology of China. *Precambrian Research*, 222, 13-54.
- Zhao, G., Cao, L., Wilde, S. A., Sun, M., Choe, W. J., & Li, S. (2006). Implications based on the first SHRIMP U-Pb zircon dating on Precambrian granitoid rocks in North Korea. *Earth and Planetary Science Letters*, 251(3-4), 365-379.
- Zhao, G., Cawood, P.A., Li, S., Wilde, S.A., Sun, M., Zhang, J., He, Y., & Yin, C. (2012). Amalgamation of the North China Craton: key issues and discussion. *Precambrian Research* 222, 55-76.
- Zhao, G., Sun, M., Wilde, S. A., & Li, S. (2003). Assembly, accretion and breakup of the Paleo-Mesoproterozoic Columbia Supercontinent: records in the North China Craton. *Gondwana Research*, 6(3), 417-434.
- Zhou, G., Luo, T., Zhou, M., Xing, L., & Gan, T. (2017). A ubiquitous hydrothermal episode recorded in the sheet-crack cements of a Marinoan cap dolostone of South China: implication for the origin of the extremely ^{13}C -depleted calcite cement. *Journal of Asian Earth Sciences*, 134, 63-71.
- Zhou, Y., von Strandmann, Philip AE Pogge, Zhu, M., Ling, H., Manning, C., Li, D., He, T., & Shields, G.A. (2020). Reconstructing Tonian seawater $^{87}\text{Sr}/^{86}\text{Sr}$ using calcite microspar. *Geology* 48, 462-467.

옥천변성대 탄산염 암석의 탄소, 산소 및 스트론튬 지구화학

하 영 지

부경대학교 대학원 지구환경시스템과학부 지구환경과학 전공

요 약

옥천 변성대 내에는 넓은 범위에 걸쳐 시대미상의 탄산염암이 분포하고 있다. 이 탄산염암체에 적용할 수 있는 적합한 절대연대측정법이 거의 없기 때문에 아직까지 이들의 정확한 생성시기가 밝혀지지 않고 있다. 본 논문은 이러한 시대미상 탄산염암에 화학층서법을 적용하여 보다 정밀하게 이들의 생성시기를 밝혀내고자 하였다.

제 1 장에서는 이 논문의 주제에 대하여 개괄적으로 설명하였다. 특히 신원생대 탄산염 퇴적층을 연구하는데 있어서 탄소 동위원소 자료의 중요성과 한계점을 논의하였다.

제 2 장은 옥천-보은 및 충주 지역에서 소위 금강 석회암으로 통칭되는 탄산염암에 대한 연구로 이 층이 빙하기 이후 퇴적된 덮개탄산염인지 여부에 대하여 논의하였다. 결론적으로 금강 석회암은 일관되게 낮은 $\delta^{13}\text{C}$ 값 (-12.25%~-6.05%)을 보이며, 이는 전형적인 덮개탄산염암의 $\delta^{13}\text{C}$ 값에 해당한다. 따라서, 신원생대 빙하기 사건 동안 옥천 변성대 일부가 퇴적되었다는 기존 가설을 뒷받침하는 결과이다.

제 3 장에서는 충주-제천 지역에 분포하는 서창리층, 삼태산층, 그리고 홍월리층에 대해 다루었다. 삼태산층과 홍월리층은 그간 태백산 분지의 하부고생대 지층으로 여겨져 왔다. 하지만 이 암석들에 대한 탄소 동위원소 분석결과는 전통적인 믿음과 다른 결과를 보여준다. 이들 층들에서 얻어진 $\delta^{13}\text{C}$ 값은

캠브리아기-오르도비스기의 평균값인 약 0% 보다 뚜렷이 구분되는 1.5% 이상의 높은 값을 보이는 것이 많으며, 이는 캠브리아기 초기 혹은 그보다 더 오래된 신원생대를 의미한다. 따라서 충주-제천 지역에 분포하는 과거에 삼태산층과 홍월리층으로 명명되었던 탄산염 암석들 중에는 고생대의 암석들뿐만 아니라 신원생대 암체가 혼합되어 있는 것으로 해석된다.

종합하여, 본 연구는 옥천 변성대에 신원생대 빙하기와 관련된 퇴적층이 존재함을 밝혔다. 또한 금수산규암층 서부에 분포하는 탄산염 암석들과 태백산 분지 내 삼태산층과 홍월리층으로 기재된 층들의 상당부분은 신원생대층임을 밝혀내었다. 따라서 옥천변성대와 태백산분지의 경계를 다시 확정할 필요성을 제기한다.

주요어: 신원생대 후기, 고생대 초기, 옥천변성대, 태백산분지, 탄산염암, 화학층서

